Aging in Wild and Laboratory Yeast: Nutrient Sensing, Telomeres, and the Nucleolus

Elizabeth Xin-Yan Kwan

A dissertation

submitted in partial fulfillment of the

requirements for the degree of

Doctor of Philosophy

University of Washington

2012

Reading Committee:

Antonio Bedalov, Chair

Bonita Brewer

Catherine Peichel

Program Authorized to Offer Degree:

Molecular and Cellular Biology

ABSTRACT

Aging and longevity are considered to be highly complex genetic traits. In order to gain insight into aging as a polygenic trait, we employed an outbred *Saccharomyces cerevisiae* model, generated by crossing a vineyard strain (RM11-1a) and a laboratory strain (S288c), to identify quantitative trait loci that control chronological lifespan, replicative lifespan, and telomere length. Among the major loci that regulate chronological lifespan in this cross, one genetic linkage was found to be congruent with a previously mapped locus that controls telomere length variation. We found that a single nucleotide polymorphism in *BUL2*, encoding a component of an ubiquitin ligase complex involved in trafficking of amino acid permeases, controls chronological lifespan and telomere length as well as amino acid uptake. Cellular amino acid availability changes conferred by the *BUL2* polymorphism alter telomere length by modulating activity of a transcription factor Gln3. Among the *GLN3* transcriptional targets relevant to this phenotype, we identified Wtm1, whose upregulation promotes nuclear retention of ribonucleotide reductase (RNR) components and inhibits the assembly of the RNR enzyme complex during S-phase. Inhibition of RNR is one of the mechanisms by which Gln3 modulates telomere length. Thus, identification of a polymorphism in *BUL2* in this outbred yeast population revealed a previously unknown link between cellular amino acid availability, chronological lifespan and telomere length control.

A genome scan for loci that control replicative lifespan identified the rDNA as a major quantitative trait locus, accounting for 45% of the genetic variation in lifespan. Despite its large size, rDNA is inherited as a single genetic locus due to the virtual absence of meiotic recombination. The lifespan extension conferred by the vineyard rDNA was

independent of Sir2 and Fob1, proteins known to be involved in rDNA metabolism and replicative lifespan. Among the rDNA sequence differences between the two strains, we identified a polymorphism in the rDNA origin of replication in the vineyard strain, which leads to a marked decrease in origin activation in plasmid maintenance assays as compared to the laboratory sequence, is responsible for lifespan extension. We also found that vineyard rDNA has markedly reduced size compared to laboratory rDNA and that strains carrying vineyard rDNA have increased capacity for replication initiation at weak origins both in the genome and on plasmids. Our results suggest that rDNA origin activation alters DNA replication dynamics which modulates replicative lifespan.

TABLE OF CONTENTS

LIST OF FIGURES

LIST OF TABLES

INTRODUCTION

The process of aging is difficult to define. The effects of age are seen in cosmetic characteristics like gray hairs and wrinkles, but also manifest in more serious and less visible attributes, such as the increased risk for diseases like arteriosclerosis, osteoporosis, Alzheimer's disease, and cancer. One could say that the defining universal features of the aging process are the encroachment of functional decline and the increasing mortality rate as one grows older. The onset of aging phenotypes, however, is not the same for all individuals. Different people age at different rates, have different susceptibility to age-related diseases, and have different lifespans. What allows for the variation in the onset of age-related changes? Recent studies have suggested that a combination of factors, both environmental and genetic, can contribute to our rates of aging and our longevity.

Diet is one environmental factor that has a dramatic impact on aging phenotypes and longevity. First reported in 1935, mice whose calorie intake was reduced by 30% lived approximately 50% longer than their well-fed counterparts [1]. The aging benefits from a restriction of diet, referred to as "calorie restriction" or "dietary restriction," was further recapitulated in studies of longevity of worms, flies, yeast, and even Rhesus monkeys, suggesting the presence of a universal mediator of aging [2,3,4,5,6]. Use of these model organisms identified that changes in conserved genetic pathways underlying growth and metabolism can similarly alter longevity. Mouse, *Drosophila melanogaster,* and *Caenorhabditis elegans* mutants deficient in IGF-1 (insulin/insulin-like growth factor) signaling are significantly longer lived and retain youthful phenotypes longer [7,8,9,10]. Inhibition of the conserved nutrient-signaling TOR pathway by the drug rapamycin also

increases mouse longevity [11]. Though these studies have begun to dissect the processes involved in the conversion of caloric intake into increased lifespan, the exact mechanism meting out the longevity benefit remains elusive. If we can uncover which functions driven by calorie restriction affect lifespan, we may better understand the processes underlying organismal aging.

Aging has been also studied at a cellular level. Cultured fibroblasts can undergo a finite number of divisions before senescence. This mitotic arrest is thought to be imposed by the erosion of telomeres, repetitive regions capping linear chromosome ends, with each round of cell division. Telomeres consist of a highly repetitive sequence and are considered a sort of cellular clock, marking each division with the gradual shortening due to the intrinsic DNA replication problem with lagging strand synthesis [12,13,14]. When telomeres decrease to a certain length, cells cease division and senesce or otherwise undergo crisis as unprotected chromosomal ends are recognized as DNA damage, usually resulting in cell death. Reactivation of telomerase expression, the ribonucleotide reverse transcriptase that extends telomeres, can increase the replicative potential of cultured fibroblasts, but has also been associated with the development of neoplasia/cancer. While most somatic cells (muscle cells, neurons, etc.) in an organism exist in a post-mitotic state, telomere maintenance remains relevant for actively replicating cells, such as blood and epithelium, and has been associated with overall organismal aging. Indeed, epidemiological studies have found a strong correlation between leukocyte telomere length and rate of mortality: people with longer telomeres generally had longer lifespans than those whose telomeres were shorter [15].

The unicellular yeast *Saccharomyces cerevisiae* has emerged as a powerful model system for determining genetic factors that affect cellular aging and longevity. The asymmetric cell division in *S. cerevisiae* fortuitously creates an aging "mother" lineage as well as a renewed "daughter" lineage, allowing for two distinct forms of aging to be studied in *S. cerevisiae*: replicative aging and chronological aging. Replicative lifespan is defined by the number of daughter cells that are generated by a budding mother cell. Chronological lifespan is a survival time of a yeast population in stationary phase [16]. These two types of aging in yeast have been thought to have their counterparts in humans as the aging of dividing stem cells (replicative aging) and the aging of non-dividing cells such as neurons or muscle cells (chronological aging). Comprehensive studies have been carried out to understand the effect of every single nonessential gene on both replicative and chronological aging [17,18,19,20]. Many genes identified as promoting longevity are found in pathways that regulate yeast growth and metabolism, such as the yeast Akt/PKB homolog Sch9, ribosomal subunits, and TOR complexes, while genes that decrease lifespan are found in pathways which autophagy and stress. Similar screens have been performed to identify processes which affect telomere biology. While *S. cerevisiae* has active telomerase expression, strains in which genes encoding telomerase components have been deleted senesce 40-60 cell divisions after the loss of telomerase activity [21], similar to human fibroblasts in culture. Screens for gene deletions that either alter telomere length or senescence in the absence of telomerase have identified over 200 genes involved in telomere maintenance [22,23,24]. Interestingly, while many genes identified directly interact with telomeres, a substantial fraction is from seemingly unrelated processes such as vesicle

transport, transcription, and ribosome biogenesis. Currents studies are still ongoing in order to understand the mechanisms behind these many regulators of longevity and telomere maintenance.

The enormous genetic diversity found in outbred populations such as humans, however, may limit the applicability of single gene changes discovered in inbred laboratory organisms to aging in humans. While mutations in single genes have been implicated in progeroid syndromes, such as the WRN RecQ helicase variant linked to the development of Werner Syndrome [25,26], the importance of genetics in determining human longevity and human rates of aging is not limited to a single gene changes. The genetic diversity within the human population stems from scores of polymorphisms scattered across the genome. Rates of aging are highly variable and suggest that the interplay of many polymorphic genes affects aging within a single person. People with similar genetic backgrounds age at more similar rates, as documented in twin studies which showed higher longevity concordance in monozygotic than dizygotic twins [27]. We were interested in addressing the following questions: How do multiple polymorphisms integrate to contribute to the overall process of aging? Are the effects of individual polymorphisms channeled through the same circuits as those identified using single gene mutations in model organisms? Or are there aging mediators whose effects can be appreciated only in an outbred setting?

To address the role of genetic diversity in aging, I decided to take advantage of genetic variation within *S. cerevisiae* by examining longevity in an outbred yeast model. The laboratory strain S288c and the RM11-1a vineyard strain, isolated from a California

Zinfandel winery, are both isolates of the *S. cerevisiae* species and are 0.5% divergent across their genomes, which is approximately half of the genetic divergence identified between human and chimpanzee species. The laboratory strain (BY) and the vineyard strain (RM) were crossed to generate a library of 122 outbred "segregant" strains, which were then genotyped at 2,956 polymorphic markers across the genome for laboratory or vineyard strain inheritance (Figure 1.1) [28]. This outbred model allowed me to map the natural polymorphisms that control aging-related phenotypes in yeast and assess their genetic complexity. In the following work, I describe the findings of two separate ventures: one that focuses on chronological aging and one that focuses on replicative lifespan. In my first project, I identified a polymorphism in a gene that regulates amino acid import in both chronological aging and telomere length. This finding enabled me to link cellular nutrient availability with telomere maintenance and chronological lifespan. My second project identified the rDNA locus as the major regulator of replicative lifespan in our outbred yeast model. Characterization of this enigmatic region led to the discovery that control of initiation of rDNA replication may present a key regulator of replicative lifespan.

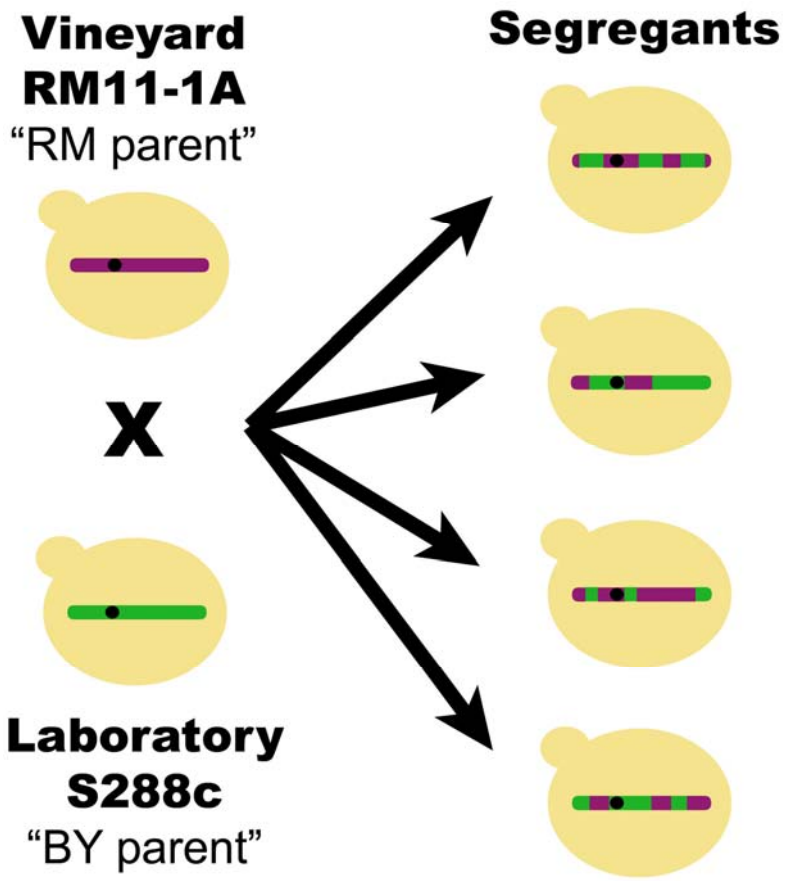

Figure 1.1. Schematic of the cross between S288c and RM11-a strains used to generate the outbred segregant collection.

CHAPTER 2

Natural polymorphism in *BUL2* links cellular amino acid availability with chronological aging and telomere maintenance in yeast [29]

INTRODUCTION

The observation that dietary restriction promotes longevity in organisms ranging from yeast to primates raises the expectation that molecular mechanisms mediating this lifespan extension may also be shared among species. In support of the idea that related genetic circuitry controls aging in different species are the findings that genetic or pharmacological modulations of the conserved nutrient responsive pathways, such as target of rapamycin (TOR) [30] or insulin-like-growth factor (IGF-1) [31], increase lifespan in a wide range of species including mammals. The budding yeast *S. cerevisiae* has become a popular model for studying the genetic and molecular basis for variation in lifespan. Two different forms of aging have been studied in yeast. Replicative lifespan (RLS) is defined by the number of daughter cells that are generated by a budding mother cell whereas chronological lifespan (CLS) is defined as the ability of yeast cells to survive in stationary phase as judged by the their capability to reenter the cell cycle after nutrients are reintroduced [32]. The two types of aging in yeast are thought to have their counterparts in mammals as the aging of dividing stem cells or the aging of non-dividing cells such as neurons or muscle cells, respectively. In addition to replicative and chronological aging, mutant yeast cells dividing in the absence of telomerase components exhibit loss of viability [21] similarly to replicative senescence of human fibroblasts in culture [33].

Recent epidemiological studies of human populations demonstrated a correlation between reduced leukocyte telomere length and overall mortality [15], suggesting a link between telomere maintenance and organismal aging. Furthermore, life stress has been shown to influence leukocyte telomere length [34], establishing a role for environmental stress in telomere stability. Little is known about how these processes connect, though twin studies suggest that both telomere length regulation and longevity in humans have a strong genetic component [27,35].

Most of what we have learned about telomere maintenance mechanisms and the genetics of aging comes from model organisms where the effects of the single gene changes can be examined independently from other genetic alterations. However, because natural populations are genetically diverse, differences in aging and telomere maintenance are more likely to result from the integration of effects of polymorphisms at multiple loci. In order to gain insight into telomere maintenance in genetically diverse populations, we have previously employed an outbred yeast model consisting of 122 haploid progeny derived by a cross of vineyard RM11-1a (RM) and laboratory S288c yeast (BY) [28]. Parental strains differ at 0.5% of their nucleotides and the progeny have been genotyped at >3000 markers, allowing for quantitative trait locus (QTL) mapping. In a previous telomere length study, we identified several loci that control telomere variation in this cross [23].

In this study, we used the same outbred model to explore chronological aging as a complex trait. During the course of these studies, we found that one of the loci that controls chronological lifespan is identical to a major locus found to control telomere length,

suggesting a previously unrecognized link between the two yeast aging-related phenotypes. This was an intriguing finding because changes in telomere length are linked to DNA replication, while chronological aging occurs in non-dividing cells. Furthermore, the two phenotypes were regulated in opposite directions by this locus: strains that inherited the vineyard allele had shorter telomeres and longer lifespans. We found that a single amino acid substitution in Bul2, a component of an ubiquitin ligase complex which polyubiquitylates amino acid permeases and regulates their presence at the cell membrane, controls cellular amino acid availability and is responsible for the variation in both telomere length and CLS. We also elucidated a pathway by which decreased cellular amino acid uptake conferred by the BUL2 polymorphism and the consequent inhibition of nutrient-responsive TOR1 signaling lead to reduced telomere length.

RESULTS

Regulation of chronological lifespan is a dynamic process controlled by many loci

To determine chronological lifespan of the 122 haploid progeny (segregants) from the RM/BY cross, strains were grown in YPD medium in 96-well plates to stationary phase, where cells maintain metabolic activity but cease mitotic division. Chronological lifespan (CLS) studies are often done in synthetic media, where yeast lifespans can be analyzed in a few weeks [16]. Because of the observation that the use of synthetic medium in CLS studies exposes cells to lifespan-limiting acidification [36], we decided to carry out segregant CLS analysis in YPD where acidification of the media during culture outgrowth is not a problem. After intervals of approximately 30 days, we harvested 1 μL of each stationary phase culture, spotted culture dilutions on YPD plates, and determined viability of cultures as the ratio of

microcolonies after 24 hours of growth to the total cell number plated. We found excellent correlation (R=0.98) between the cell viability determined using our microcolony method and the viability measured using colony forming ability (Figure 2.9). The vast majority of cultures were found to be fully viable after the initial interval of 5 days in stationary phase (Figure 2.1A). Further along in stationary phase, segregant culture viabilities decreased to an average of 70% after 31 days (range 30-91%), 35% after 59 days (range 11-62%) and 20% after 100 days (range 0.5-40%). The observed viability distributions of the chronologically aged segregant strains displayed several interesting features. First, the variation in viability between segregants was continuous, suggesting that multiple genetic loci control survival among the segregants. Second, we observed that the parental strains' phenotypes are in the middle of the range. Such transgressive segregation, in which the segregant progeny exhibit more extreme phenotypes than either parental strain, suggests the presence of compensatory genetic loci within both the RM and BY parental backgrounds. Finally, the rank of the segregant viabilities was not static, as illustrated by the changing order of the parental strains over time, which suggests that different genes are responsible for early and late viabilities.

We used genome-wide linkage analysis to identify the loci (QTL) responsible for the variation in chronological lifespan. Each segregant strain has been characterized for BY or RM inheritance at 2,956 polymorphic markers across the genome [11]. Using genome-wide linkage analysis, phenotype distributions can be compared between segregants that inherit the BY or RM sequence at each locus. A significant difference between the two distributions establishes a linkage between the trait of interest and the genomic sequence near the tested polymorphic marker. We found that stationary phase survival is linked to several genetic

loci, consistent with the observed continuous range in viability (Figure 2.1B-D, Table 2.2). We also noticed that the strength of linkage of the mapped loci changes with time. The chromosome 13 linkage, for instance, has LOD scores >3.5 at 31 and 59 days, yet it has no role in controlling viability after 100 days in culture. On the other hand, the chromosome 14 linkage had the opposite temporal pattern: not significant at day 31 yet has LOD scores >3.5 at day 59 and 100. The alteration of the relative importance of different loci at different time points suggests that cells depend on different cellular processes during early and late stages of chronological lifespan.

Chronological lifespan, telomere length and cellular permease activity are linked to the same polymorphism in *BUL2*

Comparison between the genome scan for loci that control chronological lifespan and our previous analysis for loci that control telomere length (Figure 2.1E) revealed that the strongest linkage for chronological lifespan at day 31 (chromosome 13 locus) is congruent with a previously identified locus that controls telomere length [23]. The segregant strains that inherited the RM allele of chromosome 13 locus had longer CLS (65% vs. 56 % viability at 30 days) and shorter telomeres (261 bp vs. 286 bp) compared to strains which inherited the BY allele of the locus. In order to determine whether other mutants with short or long telomeres exhibit either reciprocal effects or alterations in CLS in general, we examined a panel of deletion mutants known to have telomere length alterations and found no correlation between telomere length changes and CLS (Figure 2.10). Likewise, a more general comparison of CLS and telomere length, using data from the recent global CLS study [20] and our previous telomere length screen [23], did not reveal any correlation between

telomere length and CLS (Figure 2.10). While we found no general correlation between telomere length and CLS, the striking overlap of genetic linkage between telomere length and chronological aging in this cross led us to hypothesize that these two traits are both controlled by a common polymorphism and that identifying the responsible gene may reveal an unexpected link between telomere maintenance and chronological aging.

Among the polymorphisms in the mapped region, we identified one in the coding region of BUL2, a gene encoding a component of the Rsp5p E3-ubiquitin ligase complex involved in amino acid permease sorting. During growth in the presence of rich nitrogen sources, high affinity amino acid permeases, such as the general amino acid permease *GAP1* and the proline transporter *PUT4*, are polyubiquitylated by a complex consisting of Bul1, Bul2 and Rps5, which specifies vacuolar-targeting of permeases for degradation [37,38]. Cellular amino acid permease activity can be monitored using the toxic proline analogue ADCB, which is transported across the cell membrane via nitrogen-regulated PUT4 and *GAP1* [39]. We found that the parental RM and BY strains exhibit a striking difference in ADCB sensitivity when grown with a rich nitrogen source (Figure 2.2A). Consistent with higher permease activity and amino acid intake relative to the RM strain, the BY strain was not able to grow at concentrations of ADCB that were non-toxic to the RM strain. Genome-wide linkage analysis of ADCB sensitivity in the segregants demonstrates that the *BUL2*-containing locus underlies the parental differences in permease activity (Figure 2.2B). The BY strain carries a single Leu883Phe substitution relative to the RM version of Bul2, which is conserved among many fungal homologs (Figure 2.2C) and all but three of the sequenced *S. cerevisiae* strains (F883L is present in S288c and the two baking isolates YS2 and YS9)

[40]. Engineering the RM allele of *BUL2* into the BY strain restored ADCB resistance, whereas substitution of the BY *BUL2* allele into the RM strain resulted in ADCB sensitivity (Figure 2.2D). These findings indicate that the BY *BUL2* Phe883Leu polymorphism confers a loss of Bul2 function, similar to that of a *bul2Δ* mutant, and increases permease activity and amino acid uptake.

We next evaluated whether the same *BUL2* polymorphism that controls cellular permease activity also mediates chronological lifespan and telomere length variation. The replacement of *BUL2* in the BY parental strain with the RM allele led to an increase in chronological lifespan (from 55% to 65% viable cells at 30 days in YPD medium), which was similar in magnitude to the increase in chronological lifespan conferred by the RM *BUL2* allele in the segregants (Figure 2.3A,B). Conversely, the replacement of the RM *BUL2* allele with the BY *BUL2* allele in the RM parental strain decreased chronological lifespan (67% vs. 62%) after 30 days. We next examined the effect of *BUL2* alleles on the time-dependant viability curves in both laboratory and vineyard background using the synthetic media that is commonly used for CLS studies. (In order to minimize the viability reduction due to media acidification, we used buffered SC medium [36]). Consistent with previous reports, we observed that CLS is shortened in SC medium compared to YPD, however, restoration of *BUL2* function using RM *BUL2* allele in the laboratory strain extended chronological life span even more robustly than we have observed in YPD (Figure 2.3C). *BUL2* replacement in the vineyard strain with the hypomorphic *BUL2BY* allele shortened CLS and deletion of *BUL2* led to further reduction in CLS (Figure 2.3D), which parallels the effect of *BUL2* allele replacement and *BUL2* deletion on cellular permease activity in the

vineyard strain, judged by increased ADCB sensitivity in the *BUL2BY* alleles and *BUL2* deletion (Figure 2.2D). The effects of *BUL2* allele replacement on CLS results were also confirmed using standard colony formation metrics [16]. These findings demonstrate that the BUL2 polymorphism controls variation of chronological lifespan in the RM/BY cross.

The average telomere length in the segregants that contain the BY allele of *BUL2* was 286 bp, which is 25 bp longer than the telomere length average of segregants that contain the RM allele (261 bp) (Figure 2.4A). Therefore, if *BUL2* is the responsible polymorphism for telomere length alteration, then the BUL2 allele replacement in the RM parental strain is expected to create a 25bp increase in telomere length, while the allele replacement in the BY strain would have a modest telomere length reduction. We found that allele replacement of *BUL2* in both parental strains led to alterations in telomere length as predicted by the segregant analysis: telomeres were found to be longer in the RM strains with *BUL2* replaced by the BY allele and telomeres were shorter in the BY strains containing the RM *BUL2* allele replacement (Figure 2.4B). As expected from the segregant analysis, the effect of allele replacement was modest, but also consistent and reproducible, as shown by analysis of several independent strains. Deletion of *BUL2* lengthened telomeres in the RM background, but had no effect in the BY background (Figure 2.4C). These results demonstrate that the leucine residue substitution present in the BY parent creates loss of Bul2 function, leading to higher activity of amino acid permeases on cell membranes, reduced chronological lifespan, and increased telomere length.

Telomere length alterations by Bul2 polymorphisms is mediated by Gln3

Reduced availability of cellular nitrogen and amino acids conferred by the restoration of Bul2 function is expected to reduce the activity of the nutrient sensitive *TOR1* kinase. Since the region containing the *BUL2* locus had been previously identified as a regulatory hotspot that controls abundance of many transcripts in this cross [41], we evaluated whether these transcriptional alterations could be mediated by alterations in *TOR1* activity. Consistent with this possibility, we found that the set of genes overexpressed in strains containing *BUL2RM* significantly overlaps with genes that were found to be overexpressed in response to amino acid deprivation (P=1.1x10^{-8}) and rapamycin (P=1.2x10^{-3}) (Figure 2.5A, Table 2.3) [21], known inhibitors of *TOR1* activity [42,43]. Because reduction of *TOR1* signaling has been shown to extend chronological lifespan [19,44], the viability gain in chronological aging assays conferred by the restoration of Bul2 function can be explained by reduced activity of the nutrient responsive TOR pathway. Could the same gene network be mediating telomere length alterations conferred by *BUL2* function?

To investigate this possibility, we re-examined data from our previous genome-wide telomere length screen [23], focusing on deletion mutants of genes in the nitrogen signaling circuit. We reasoned that such mutants would likely affect telomere length through the same mechanism as *BUL2*, thus we might gain insight into *BUL2's* mechanism of action on telomere length from known modes of action through these other nitrogen-signaling mutants. Among the mutants in genes involved in nitrogen signaling, we found that cells lacking *TOR1* have modest reduction in telomere length and that cells lacking *URE2* have strikingly short telomeres (Figure 2.5B). In rich nitrogen environments, Ure2 binds to the transcriptional activator Gln3 and inactivates it through cytoplasmic sequestration [45,46].

Upon encountering nitrogen-limiting environments, Gln3 is released from its complex with Ure2 and translocates to the nucleus to upregulate nitrogen catabolite responses [47]. The short telomere phenotype in *ure2Δ* mutants is mediated by Gln3, as we found that the deletion of GLN3 restored the short telomere lengths in *ure2Δ* cells back to wildtype lengths (Figure 2.5C).

We hypothesized that the reduced nitrogen availability occurring in cells with functional Bul2 (i.e. the RM allele) leads to increased Gln3 transcriptional activity and shorter telomeres. In order to evaluate whether transcriptional alterations previously mapped to the region containing the *BUL2* locus [41] could be mediated by Gln3, we compared the set of genes that are upregulated by the RM *BUL2* allele with the genes that are upregulated in response to *URE2* deletion. Of the 19 transcripts that are significantly upregulated in strains with the RM *BUL2* allele, 10 transcripts were found to be overexpressed in our transcript array analysis of *ure2Δ* cells (of which there were 208 transcripts), including known direct Gln3 targets such as *BAT2* and DIP5 (Figure 2.5A, Table 2.4) (P=8.5 x 10^{-11}) [48]. These findings, along with previous reports which link loss of Bul2 to decreased Gln3 nuclear localization [49], support a model in which restoration of Bul2 function leads to decreased cellular nitrogen availability, thereby promoting Gln3 transcriptional activity and reduction of telomere length.

Could Bul2's effect on telomere length be mediated by Gln3? To address this question, we examined the effect of the BUL2 allele replacement in cells lacking *GLN3*. We found that neither did the RM BUL2 allele in the BY *gln3Δ* strain shorten telomeres, nor did

the BY allele replacement increase telomere length in the RM *gln3Δ* strain (Figure 2.5D). The requirement of Gln3 for *BUL2* allele-induced telomere alterations supports the idea that *BUL2* telomere length changes are mediated by modulation of Gln3 transcriptional activity. These findings, along with previous reports which link loss of Bul2 to decreased Gln3 nuclear localization [49], support a model in which restoration of Bul2 function leads to decreased cellular nitrogen availability, thereby promoting Gln3 transcriptional activity and reduction of telomere length.

Gln3 modulates nuclear-cytoplasmic shuffling of ribonucleotide reductase components

In order to determine the relationship of the telomere maintenance defect caused by the deletion of *URE2* to other pathways that participate in telomere maintenance, we compared telomere lengths of *ure2Δ* single mutants and double mutants that were *ure2Δ* and deficient in either DNA damage signaling (*tel1Δ)*, telomerase (*tlc1Δ*), or telomere-capping (y*ku70Δ*) functions. The *ure2Δ* cells showed synthetic telomere length phenotypes with the y*ku70Δ, tel1Δ,* and *tlc1Δ* mutants (Figure 2.11), suggesting that Ure2's effect on telomere maintenance acts independently from pathways involved in telomere extension, telomere-capping, and *TEL1*-mediated DNA damage signaling.

Our previous study of telomere maintenance genes identified a significant subset of mutants involved in nucleotide biosynthesis as having altered telomere length [23]. For instance, loss of the ribonucleotide reductase large subunit *RNR1* results in telomere shortening on par with loss of *YKU70* or *TEL1*. Since nitrogen availability dictates growth, we speculated that mimicry of nitrogen starvation created by increased nuclear Gln3 would

induce cells to conserve nitrogen and restrict nucleotide synthesis, and this in turn would cause shortening of telomeres. We first examined transcript levels in *ure2Δ* cells, anticipating reductions in nucleotide biosynthesis gene expression, but found only modest decreases in *RNR1* and other nucleotide genes unlikely to account for the magnitude of telomere shortening in *ure2Δ* mutants. However, among the upregulated genes in *ure2Δ* cells, we found a strong increase in expression of Wtm1, an inhibitor of ribonucleotide reductase. Wtm1 protein levels were found to be almost 5-fold higher in *ure2Δ* cells compared to wildtype (Figure 2.6A). In addition, allele replacement with *BUL2RM* in the BY background gave rise to a 50% increase in Wtm1, while in the vineyards strain the replacement of *BUL2* with the hypomorphic *BUL2BY* and *BUL2* deletion decreased the Wtm1 protein level by 40% and 80% respectively (Figure 2.6A).

The ribonucleotide reductase complex assembles during S-phase and consists of large Rnr1 subunits and the two small subunits Rnr2 and Rnr4. Unlike Rnr1, which is always cytoplasmic, Rnr2 and Rnr4 are localized in the nucleus during G1 and translocate to the cytoplasm during S-phase [50]. This process is controlled by Dif1, which promotes nuclear import, and Wtm1, which anchors the small subunits Rnr2 and Rnr4 in the nucleus [51,52]. Based on our observation that Wtm1 expression increases in *ure2Δ* cells, we hypothesized that *ure2Δ* cells have increased nuclear retention of the small subunits Rnr2 and Rnr4. As previously observed, we found that Rnr4-GFP is nuclear during G1 and cytoplasmic during S-phase in wildtype cells (Figure 2.6B,C). While Rnr4-GFP is appropriately nuclear in *ure2Δ* cells during G1, 56% of *ure2Δ* cells retain Rnr4-GFP in the nucleus during S-phase. We determined that this aberrant nuclear Rnr4 localization in *ure2Δ* is dependent on Wtm1 since

ure2Δwtm1Δ double mutants have completely restored cytoplasmic localization of Rnr4-GFP. Rescue by *WTM1* deletion is not merely due to loss of nuclear Rnr4 localization: more than 50% of *wtm1Δ* cells still maintain nuclear localization of Rnr4-GFP in G1 (Figure 2.6C). Examination of strains with different BUL2 alleles revealed that alteration of Bul2 function has a small but reproducible effect on S-phase Rnr4-GFP localization (Figure 2.6D). Both RM *BUL2BY* and RM *bul2Δ* strains had 2.6% of S-phase cells with nuclear Rnr4-GFP, which is a significant decrease from the 5.6% seen in the RM wildtype strain. The fraction of cells with nuclear Rnr4-GFP increases from 8.0% in BY wildtype to 10.3% in the BY strain with the RM allele of BUL2 and decreases to 5.6% of S-phase cells in the BY *bul2Δ* strain. These results suggest that cells with decreased TOR signaling, such as in *ure2Δ* mutants and cells with *BUL2RM*, form fewer ribonucleotide reductase complexes during S-phase due to increased Wtm1 expression.

We then investigated whether deletion of *WTM1* would rescue the *ure2Δ* telomere length shortening. Telomere length comparison of *ure2Δ* and *ure2Δwtm1Δ* mutants reveals that deletion of *WTM1* partially rescues telomere shortening due to loss of *URE2* (Figure 2.7A). Along the same lines, we found that deletion of the Rnr1 inhibitor *SML1* [53] also abrogates the *ure2Δ* short telomere length defect (Figure 2.7B). These findings support our hypothesis that the shortened telomeres in *ure2Δ* cells are due, at least in part, to limitation of ribonucleotide reductase activity.

DISCUSSION

Examination of quantitative trait loci that regulate chronological aging and telomere length in the progeny from a cross between the laboratory strain S288c and a vineyard strain, RM11-1a, led to identification of a polymorphism in *BUL2* which alters trafficking of amino acid permeases and cellular amino acid import. Loss of Bul2 function, conferred by the laboratory allele of the gene, initiates a cascade of events outlined in Figure 2.8 that centers on TOR, a nutrient-responsive protein kinase previously implicated in CLS control. Our study defines a novel downstream role for TOR signaling in the regulation DNA replication and telomere maintenance through Gln3-mediated assembly of ribonucleotide reductase during S-phase.

Amino acids are powerful activators of TOR signaling not only in yeast, but also in multicellular eukaryotes. For *Drosophila melanogaster* larvae, amino acid deprivation inhibits TOR activity and leads to growth inhibition and reduced body size [54]. Similarly, *Caenorhabditis elegans* lacking the intestinal amino acid transporter pep-2 also have reduced body size [55]. Increasing evidence suggests that reduced intake of amino acids, which consequently reduces TOR activity, may be a key component of life-extending dietary interventions. Lifespan extension granted by dietary restriction in *D. melanogaster* was abolished by re-addition of amino acids [56]. Additionally, dietary reduction of a single essential amino acid, either tryptophan or methionine, was sufficient to confer lifespan extension in both mice and rats [57,58,59]. While dietary restriction studies in *S. cerevisiae* typically involve glucose restriction, our finding that restoration of Bul2 function and resulting reduction of cellular amino acid import extends CLS supports the idea that amino acid-mediated regulation of TOR signaling controls longevity.

While several of the upstream molecular events that control TOR activity, such as growth factors and energy status, are understood in great detail [60], we only have rudimentary knowledge of how cells sense amino acid sufficiency and transmit this signal to TOR. TOR forms two separate complexes: the rapamycin-sensitive TOR complex 1 (TORC1), which regulates growth, ribosome biogenesis, translation and lifespan, and the rapamycin-insensitive TOR complex 2 (TORC2) involved in actin cytoskeleton organization and cell wall integrity [61]. Recent studies in mammalian cells have identified several components that are required for TOR activation by amino acids, including Rag GTPase heterodimers involved in the recruitment of TORC1 complex to the lysosomal membrane compartment [62]. In addition to their roles as activators of TOR, the *S. cerevisiae* Rag GTPase orthologs Gtr1 and Gtr2 [43] are also implicated in the retrieval of Gap1 and other high affinity amino acid permeases from the vacuolar trafficking pathway [63], thus promoting their localization to the plasma membrane. Because the retrieval of Gap1 from the vacuolar targeting pathway is regulated by amino acid availability (discussed below), these findings raise the possibility that the related amino acid-responsive pathway that controls TOR also controls recycling of high affinity transporters to the cell membrane.

In contrast to the majority of the 23 amino acid permeases in yeast, which are constitutively expressed and import specific amino-acids with low affinity, high affinity permeases such as the general amino acid permease Gap1 and proline permease Put4 are highly expressed only during nitrogen limitation [37,64,65]. Gap1 and its related class of permeases have a high capacity for amino acid transport and are thought to scavenge amino

acids for use as a source of nitrogen. Intracellular sorting is one of the mechanisms by which the quality of available nitrogen controls the presence of high affinity permeases at the cell membrane: during growth with a good nitrogen source such as ammonium, glutamate and glutamine, Gap1 is sorted to the vacuole for degradation [37]. When cellular nitrogen and amino acids levels are low, Gap1 is sorted to the plasma membrane. A complex consisting of Rps5, Bul1 and Bul2 ubiquitylates Gap1 and specifies its sorting to the multivesicular endosome. From the endosome, Gap1 can be targeted either to the vacuole or trafficked to the plasma membrane depending of the amino acid availability [66]. The amino acid-regulated step in this process appears to be Gap1 retrieval from the endosome rather than Gap1 ubiquitylation. Nevertheless, ubiquitylation is a prerequisite for controlling Gap1 localization because in its absence, Gap1 never reaches the endosome and is constitutively targeted to the plasma membrane. Therefore, loss of Bul2 function, such as in cells with the BY allele of *BUL2*, results in non-discriminatory import of amino acids and greater intracellular amino acid and nitrogen availability. Our finding that the common laboratory strain S288c carries a loss-of-function mutation in *BUL2*, subsequently leading to indiscriminant amino acid uptake, is important for future studies that exploit yeast as a model for amino acid sufficiency and TOR signaling. Specifically, such studies should include strains with wild-type *BUL2*; for example, they could employ the allele substitution strains described here. The mutation in *BUL2* adds to the list of genetic alterations in the standard laboratory strain that are not representative of other members of the species such as loss of function changes in *AMN1* [67] and *MKT1* [68].

Similar to the control of Gap1, mammalian growth factor receptors are also regulated by ubiquitin-mediated trafficking. While yeast cells detect cellular resources directly through their import via permeases, multicellular organisms rely on growth factors such as IGF-1, which also stimulates TOR activity through Akt-Tsc-Rheb signaling, to coordinate nutrient availability with growth [30]. Cell surface localization of the IGF-1 receptor (IGF-1R) has been shown to depend on ubiquitylation by Nedd4, a homolog of the catalytic Rsp5 subunit of the Rsp5/Bul1/Bul2 ubiquitin ligase [69]. It is intriguing that *Nedd4*$^{-/+}$ mice have reduced IGF-1 receptors on the cell surface and phenotypes consistent with reduced IGF-1 signaling, including decreased body size [70], raising the possibility that they may share increased longevity with other IGF-1-related dwarf mice.

Reduced amino acid import in cells with functional Bul2 inhibits TORC1 activity, consistent with our observation of increased activity of TOR-inhibited transcription factor *GLN3* in cells containing the RM *BUL2* allele compared with cells which have the BY allele of *BUL2*. (In favorable nitrogen conditions, high TORC1 activity sequesters Gln3 in the cytoplasm.) Reduced TOR activity has been previously shown to extend both chronological and replicative lifespan in yeast [18,19,44]. Because reduced TOR activity extends lifespan also in higher eukaryotes [11,71,72], there is great interest in understanding the downstream events that mediate this effect.

Several mechanisms by which nutrients and TOR inhibition promotes CLS in yeast have been proposed, including reduced accumulation of acetate and/or acidification of culture media [36], promotion of respiration and autophagy [73,74], and increased activity of

stationary phase and stress-responsive transcription factors [44]. CLS experiments are often carried out in synthetic media which is complicated by significant media acidification due to release of organic acids during fermentation (the initial media pH of 4.2 decreases to < 3 after cells reach stationary phase). A combination of acidic pH and high concentration of acetate in the media has been linked to reduction of cell viability [36]. Because our chronological aging assays are performed in rich media (YPD), which has an initial pH of 6.0 that reduces only to 5.8 after cells reach stationary phase, or buffered synthetic media, acetate toxicity is an unlikely mechanism for CLS modulation in our study.

A study by Bonawitz *et al.* linked reduction in TOR activity to increased cellular respiratory capacity [73]. While translation is generally inhibited by reduced TOR activity, Bonawitz *et al.* found that translation of mitochondrial proteins was enhanced and led to increased respiration during growth in glucose. Respiration becomes increasingly important for maintaining energy supplies and viability as cells transition from fermentative growth to stationary phase. The importance of respiration during the stationary phase transition is supported by the findings of two recent genome-wide studies that identified respiratory deficient mutants among those with the shortest CLS [20,74]. In the same studies, mutants defective in autophagy, another process stimulated by TOR inhibition, were also found to have short CLS. These observations suggest that autophagy and respiration constitute important mediators by which reduced TOR activity promotes CLS.

The inhibition of TOR that occurs in cells during the post-diauxic shift and preparation for stationary phase also elicits specific transcriptional responses that are

essential for maintaining viability during quiescence [44]. One target of TOR is the Rim15 protein kinase that translates nutrient limitation signals from TOR, as well as Ras/PKA and Sch9, into upregulation of cellular responses necessary for survival in stationary phase [75]. Similarly to Gln3, Rim15 is phosphorylated by the nutrient-sensing kinases and retained in the cytoplasm, but upon nutrient deprivation, dephosphorylated Rim15 translocates to the nucleus to activate transcription factors Gis1 and Msn2/4, which upregulate genes necessary for post-diauxic shift [76] and stress response respectively [77,78]. Deletion of either *RIM15* or its target transcription factors shortens CLS and abolishes benefits conferred by caloric restriction or mutations in Tor/Ras/Sch9 that mimic calorie restriction [44]. Since Rim15 and Gln3 are both directly regulated by TOR through cytoplasmic sequestration, we predicted that Gln3, like Rim15, would be essential for proper stationary phase transition and survival. In support of this idea, we have found that deletion of *GLN3* in the vineyard strain dramatically shortens CLS (Figure 2.12) and that alteration of Bul2 function did not affect CLS in *gln3Δ* mutants. However, consistent with previous reports [19,44], we found that deletion of *GLN3* in the laboratory strain increased CLS. The paradoxical increase in CLS in response to *GLN3* deletion in the laboratory strain is in opposition to the CLS detriment conferred by the loss of function of other transcription factors such as Msn2/4 or Gis1 which are, similarly to Gln3, upregulated during starvation. Furthermore, the opposing effect of *GLN3* deletion in the laboratory and vineyard strains makes it difficult to determine the precise role of *GLN3* as a mediator of CLS alterations in the cascade of events initiated by the *BUL2* polymorphism.

Serving as a central link between nutrient availability and growth, TORC1 regulates many cellular processes including ribosome biogenesis, protein translation, autophagy and respiration [30]. During the examination of how telomere maintenance is affected by amino acid import, we discovered that ribonucleotide reductase (RNR) complex assembly during S-phase is modulated by the TOR-responsive transcription factor Gln3, defining a novel downstream role for TOR in DNA replication. We found that increased Gln3 activity, conferred by the deletion of *URE2*, upregulates Wtm1, which, in turn, promotes nuclear retention of the small *RNR4* subunit in the nucleus. Deletion of *WTM1* restores cytoplasmic localization of the small subunits and partially rescues the telomere length defect of *ure2Δ* cells. TORC1 inhibition by rapamycin was previously associated with genotoxic stress sensitivity and inability to maintain high Rnr1 and Rnr3 levels in response to DNA damage [79]. Using telomere length as a phenotype, we have uncovered a role of TORC1-responsive transcription factor *GLN3* in modulation of RNR assembly during S-phase in response to cellular amino acid availability. TOR-mediated control of DNA replication adds further to TORC1's role in coordinating nutrient availability, growth and cell division.

What is the relevance of our observation to mammalian and human aging? Both dietary restriction and inhibition of TOR activity have been linked to lifespan extension in mice [1,11]. At the same time, epidemiological studies in humans have found an association between longevity and long telomeres [27,35]. Because our study demonstrates that dietary restriction and consequent reduction in TOR activity lead to reduction of telomere length, it will be important to determine whether reduced signaling in response to dietary restriction

through this highly conserved nutrient and growth related pathway also reduces telomere length in mammals.

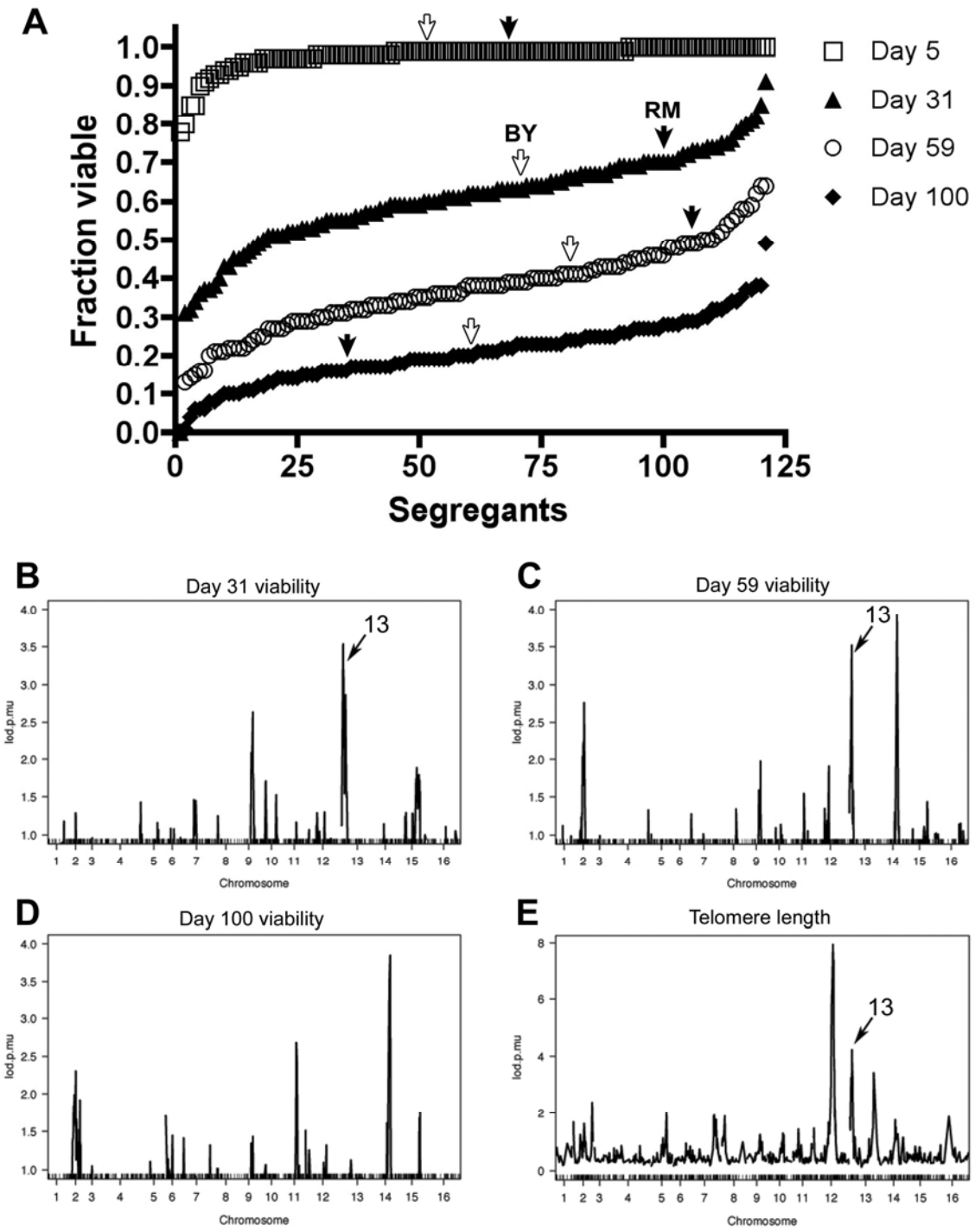

Figure 2.1: Genomic linkage of chronological lifespan in *S. cerevisiae* segregants. (A) Stationary phase viabilities of the segregants and parental strains (denoted by arrow) at different time points. Genome-wide linkage scans for viability after (B) 30 days, (C) 59 days, (D) 100 days and for (E) telomere length. Linkage to locus in common for telomere length and chronological lifespan on chromosome 13 is denoted by arrow.

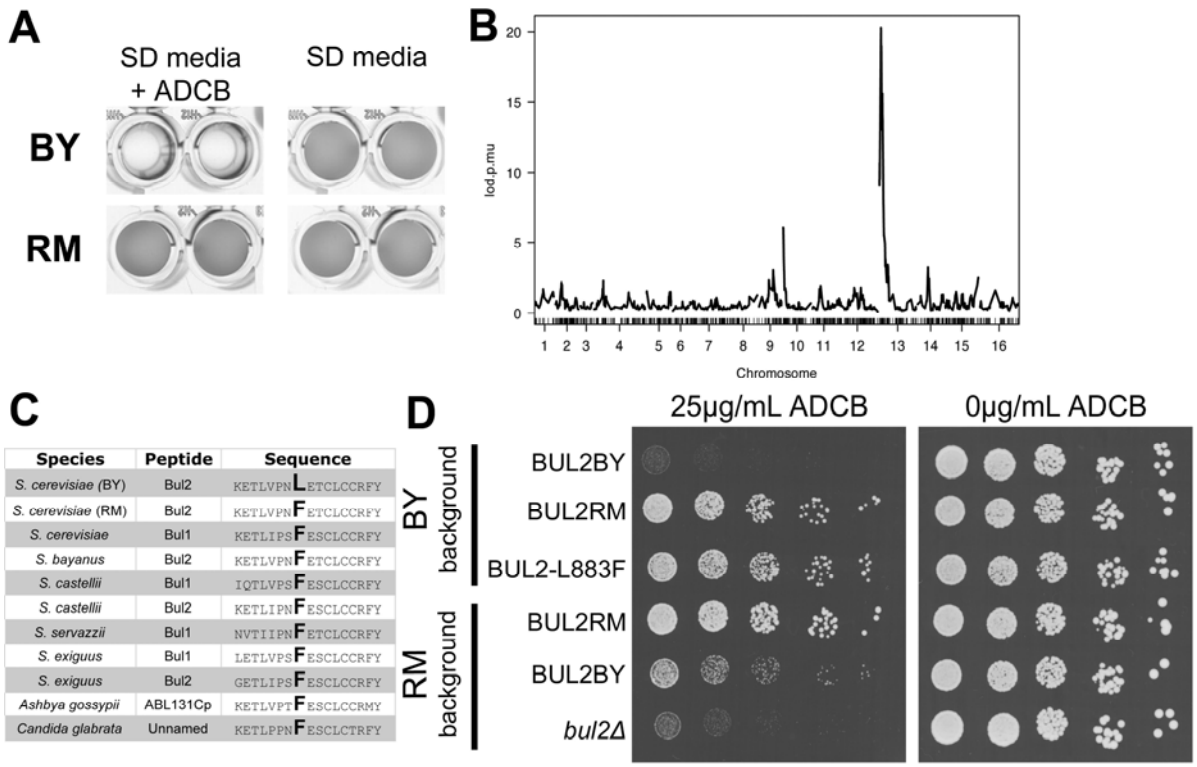

Figure 2.2. Chromosome 13 locus contains a loss of function polymorphism in *BUL2*.
(A) The RM and BY parental strains show differential growth in media containing the toxic proline analog ADCB. (B) QTL mapping reveals that segregant sensitivity to ADCB is strongly linked to the same locus on chromosome 13 that controls chronological lifespan. (C) Alignment of amino acid sequences from Bul2 homologs identifies a leucine substitution of a conserved phenylalanine residue at position 883 conferred by the BY allele of *BUL2* (T2647C). (D) Full *BUL2* RM allele replacement and single nucleotide point mutation encoding the *BUL2 L883F* substitution both confer ADCB resistance in the BY strain background. *BUL2BY* allele replacement or deletion of *BUL2* decreases growth of RM strains in media containing ADCB.

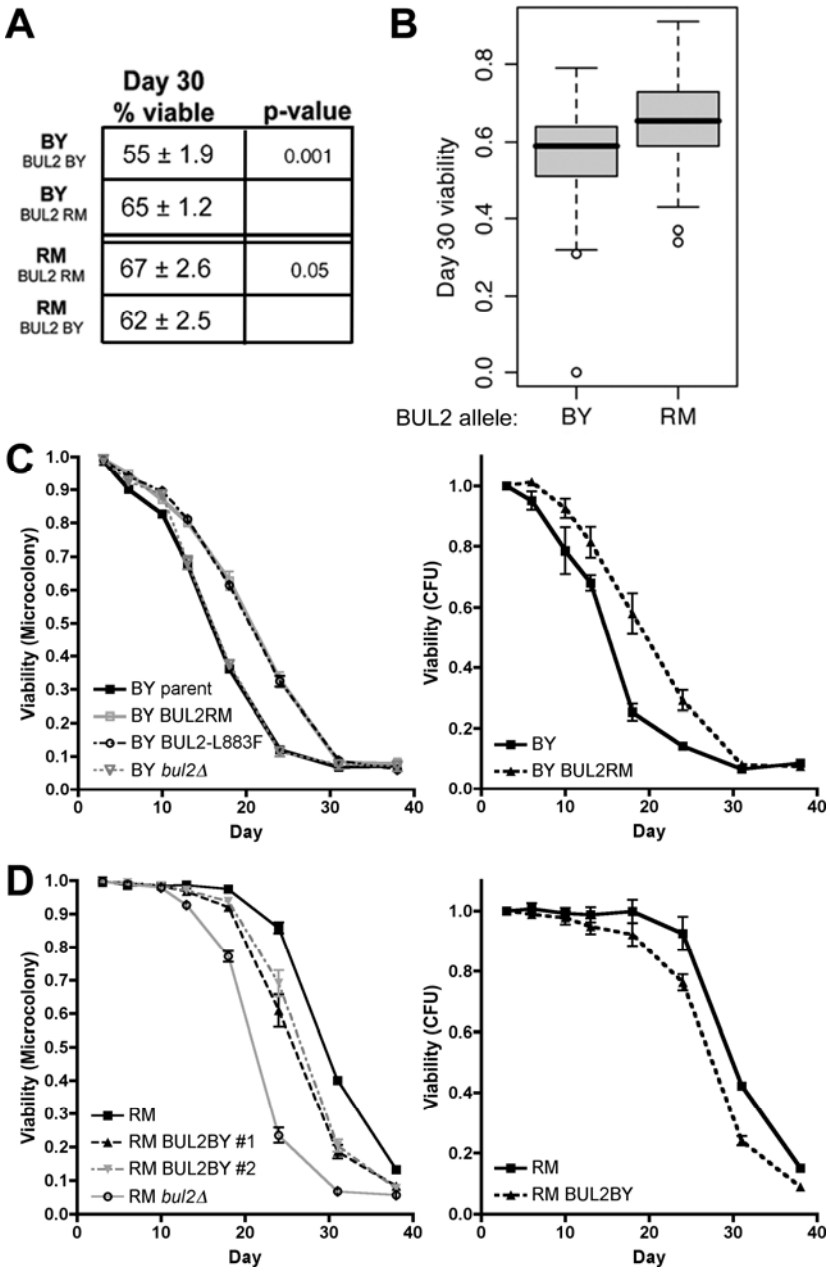

Figure 2.3. Bul2 function mediates chronological lifespan. (A) Viability of the parental and *BUL2* allele replacement strains after 30 days in stationary phase in YPD. (B) Viabilities of segregants after 30 days in stationary phase, separated on basis of BUL2 inheritance. Mean viability for segregant populations with *BUL2BY* and *BUL2RM* are 56% and 65% respectively (P=6.1x10^{-5}). (C) The *BUL2RM* allele replacement significantly extended longevity of the BY strain, measured by both microcolony counting (P≤0.05 at days 10, 13, 18 and 24) and colony formation (P≤0.05 at days 18 and 24). The BY *bul2Δ* strain exhibited CLS identical to the BY parental strain. (D) The RM parental strain had greater CLS than either the *BUL2BY* allele replacement (microcolony: P≤0.05 at days 18, 24, 31 and 38; CFU: P≤0.05 at days 24, 31 and 38) or *BUL2* deletion strain (P≤0.05 at days 13, 18, 24, 31 and 38). For longevity curves in C and D, triplicate cultures were aged in buffered SC media.

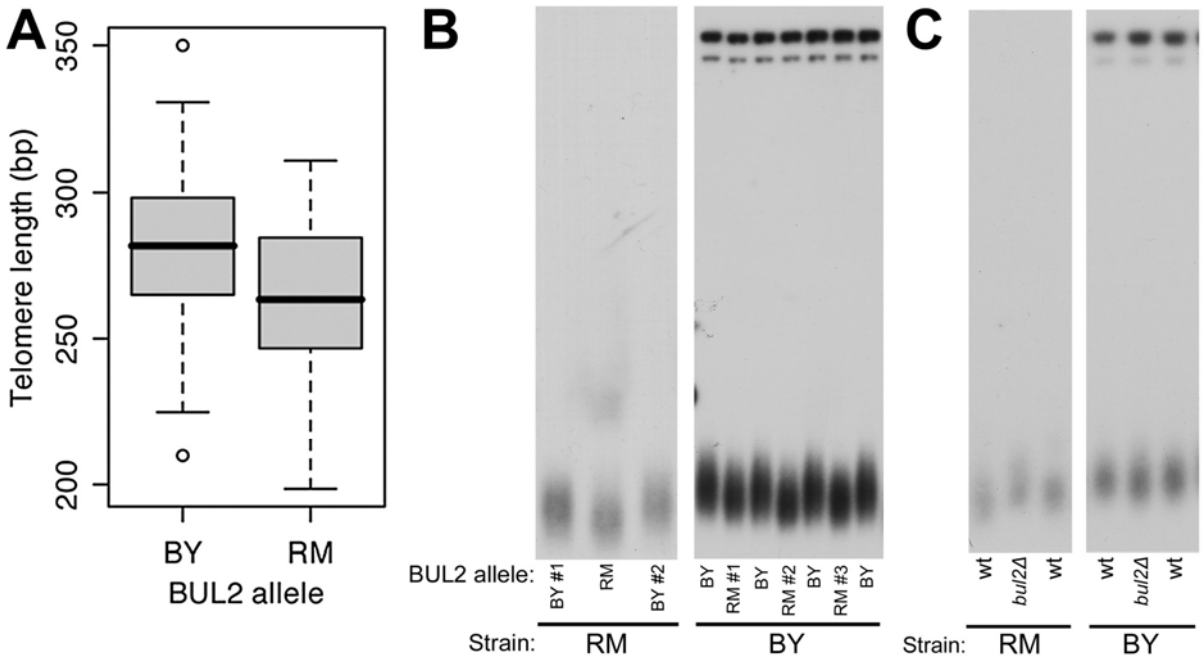

Figure 2.4. The *BUL2* polymorphism is responsible for segregant telomere length phenotypes.

142. Segregant telomere lengths, separated by *BUL2* inheritance. Mean telomere lengths of segregants with *BUL2BY* and *BUL2RM* are 286 basepairs and 261 basepairs respectively (P=3.0x10^{-4}). (B) Southern blot analysis comparing telomere length in multiple independent *BUL2* allele replacement transformants and wildtype parental strains. Strains with the BY allele of *BUL2* have longer telomeres in both parental backgrounds. (C) In the RM background, deletion of *BUL2* increases telomere length. *BUL2* deletion in the BY background has no effect on telomere length.

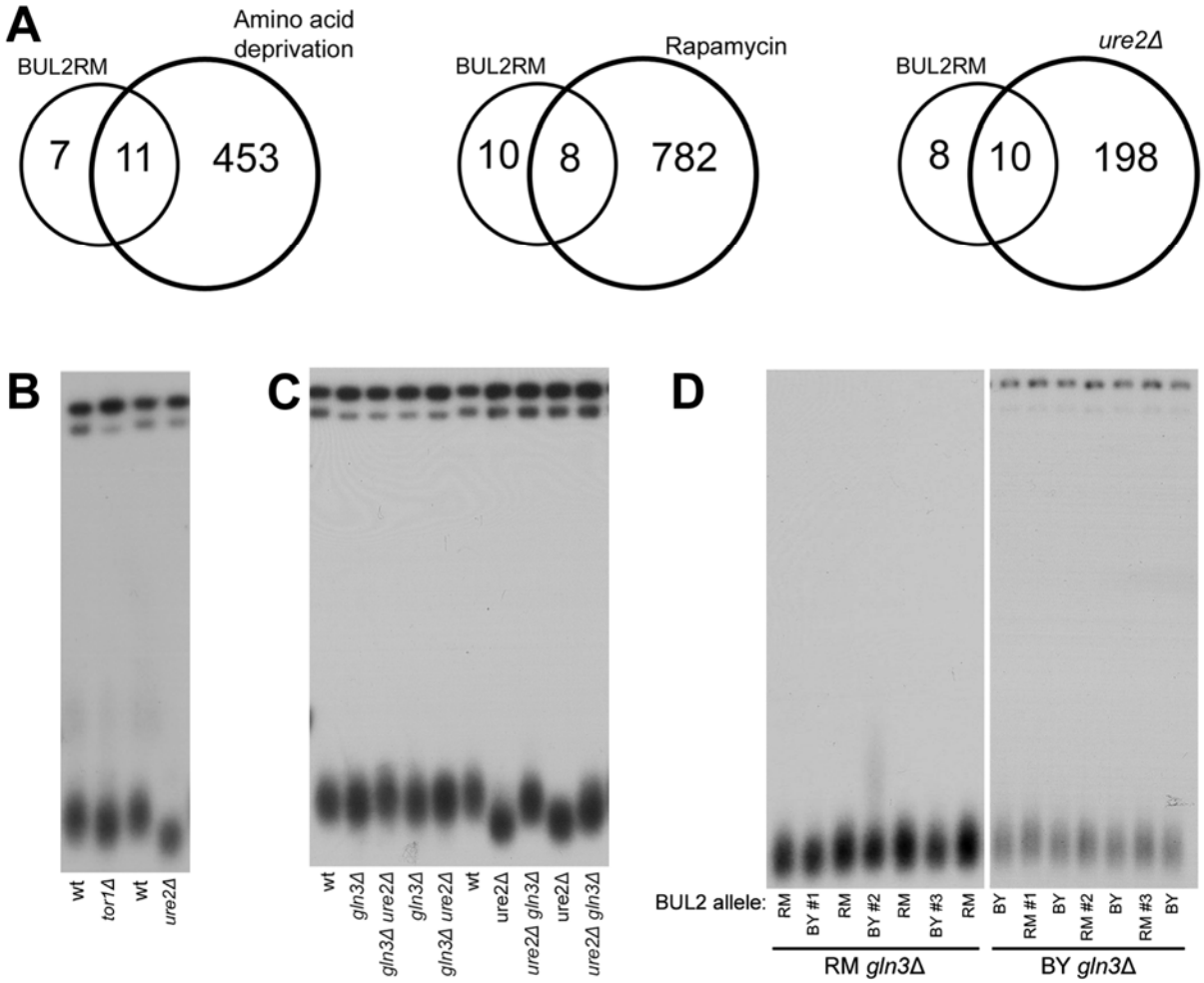

Figure 2.5. Transcriptional activator Gln3 mediates *BUL2* allele-induced telomere length alterations. (A) Overlap between transcripts upregulated by the RM allele of *BUL2* among the segregants and those which are upregulated by amino acid deprivation, rapamycin treatment, or the deletion of *URE2* in the BY background. 11 of the 464 genes upregulated by amino acid deprivation (1 hour), 8 of the 796 genes upregulated by rapamycin treatment (1 hour), and 10 of the 208 genes that are upregulated in *ure2Δ* cells are among the18 genes that are upregulated by the RM *BUL2* allele (P=1.1x10^{-8}, P=1.2x10^{-3}, and P=8.5x10^{-11} respectively for the probability of overlap occurring by chance). (18 of the 19 *BUL2RM* upregulated transcripts are represented in the amino acid deprivation, rapamycin, and *ure2Δ* transcript data). (B) *tor1Δ* and *ure2Δ* mutants in the BY background have shorter telomeres than wildtype cells. (C) Deletion of *URE2* in the BY background shortens telomere length through a *GLN3*-dependent mechanism. *Ure2Δ* mutant telomere length shortening is rescued by the deletion of *GLN3*. (D) Southern blot analysis comparing telomere length of multiple independent *BUL2* allele replacement transformants and parental strains lacking *GLN3*. *BUL2* allele replacement does not alter telomere length in parental strains lacking *GLN3*.

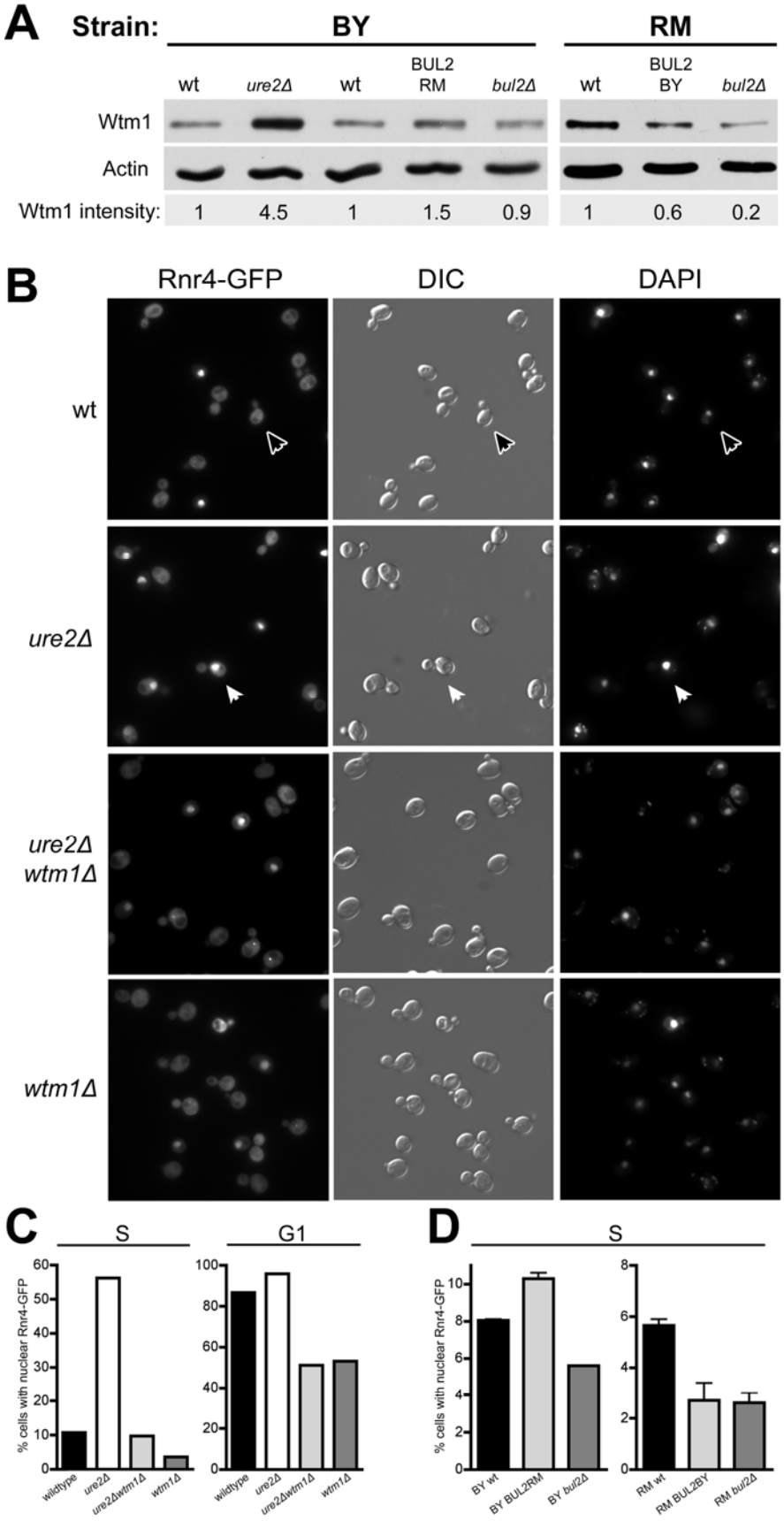
A
Strain:
BY
RM
wt
ure2Δ
wt
BUL2 RM
bul2Δ
wt
BUL2 BY
bul2Δ
Wtm1
Actin
Wtm1 intensity:
1
4.5
1
1.5
0.9
1
0.6
0.2
B
Rnr4-GFP
DIC
DAPI
wt
ure2Δ
ure2Δ wtm1Δ
wtm1Δ
C
S
G1
% cells with nuclear Rnr4-GFP
wildtype
ure2Δ
ure2Δwtm1Δ
wtm1Δ
D
S
% cells with nuclear Rnr4-GFP
BY wt
BY BUL2RM
BY bul2Δ
RM wt
RM BUL2BY
RM bul2Δ

Figure 2.6. *ure2Δ* mutants and cells with *BUL2RM* have increased Wtm1 expression and activity. (A) Immunoblotting confirms that *ureΔ* mutants and strains with *BUL2RM* have increased expression of Wtm1, an inhibitor of ribonucleotide reductase. Wtm1 expression was normalized to actin and Wtm1 intensity is listed as relative to wildtype expression. (B,C) Wildtype budded (S-phase) cells have largely cytoplasmic Rnr4-GFP localization (black arrowhead), with nuclear exclusion of Rnr4-GFP, while *ure2Δ* mutants exhibit high fractions of budded S-phase cells with nuclear localization of Rnr4-GFP (white arrowhead). Increased nuclear retention of Rnr4-GFP in *ure2Δ* mutant is rescued by deletion of *WTM1*. Unbudded (G1) wildtype and *ure2Δ* cells both have primarily nuclear Rnr4-GFP localization, which is reduced by the deletion of *WTM1*. (D) Restoration of Bul2 function with the *BUL2RM* allele in the BY strain increases the number of cells with nuclear S-phase Rnr4-GFP (P=0.02), while replacement with the hypomorphic *BUL2BY* allele in the RM strain results in fewer cells with S-phase nuclear Rnr4-GFP (P=0.05). Deletion of *BUL2* reduced the amount of cells with nuclear S-phase Rnr4-GFP in both the BY strain (P=0.0002) and RM strain (P=0.03).

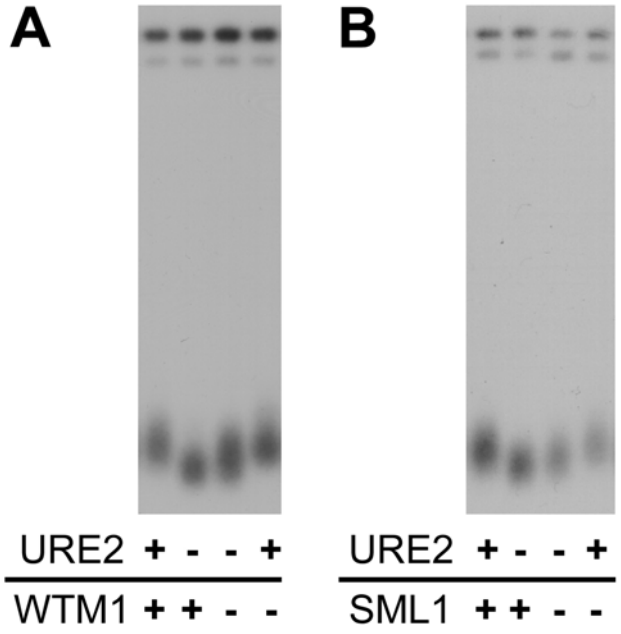

Figure 2.7. Removal of ribonucleotide reductase inhibition alleviates the short telomere phenotype in strains lacking *URE2*. Deletion of genes encoding ribonucleotide reductase inhibitors (A) *WTM1* and (B) *SML1* partially rescues telomere shortening conferred by deletion of *URE2*.

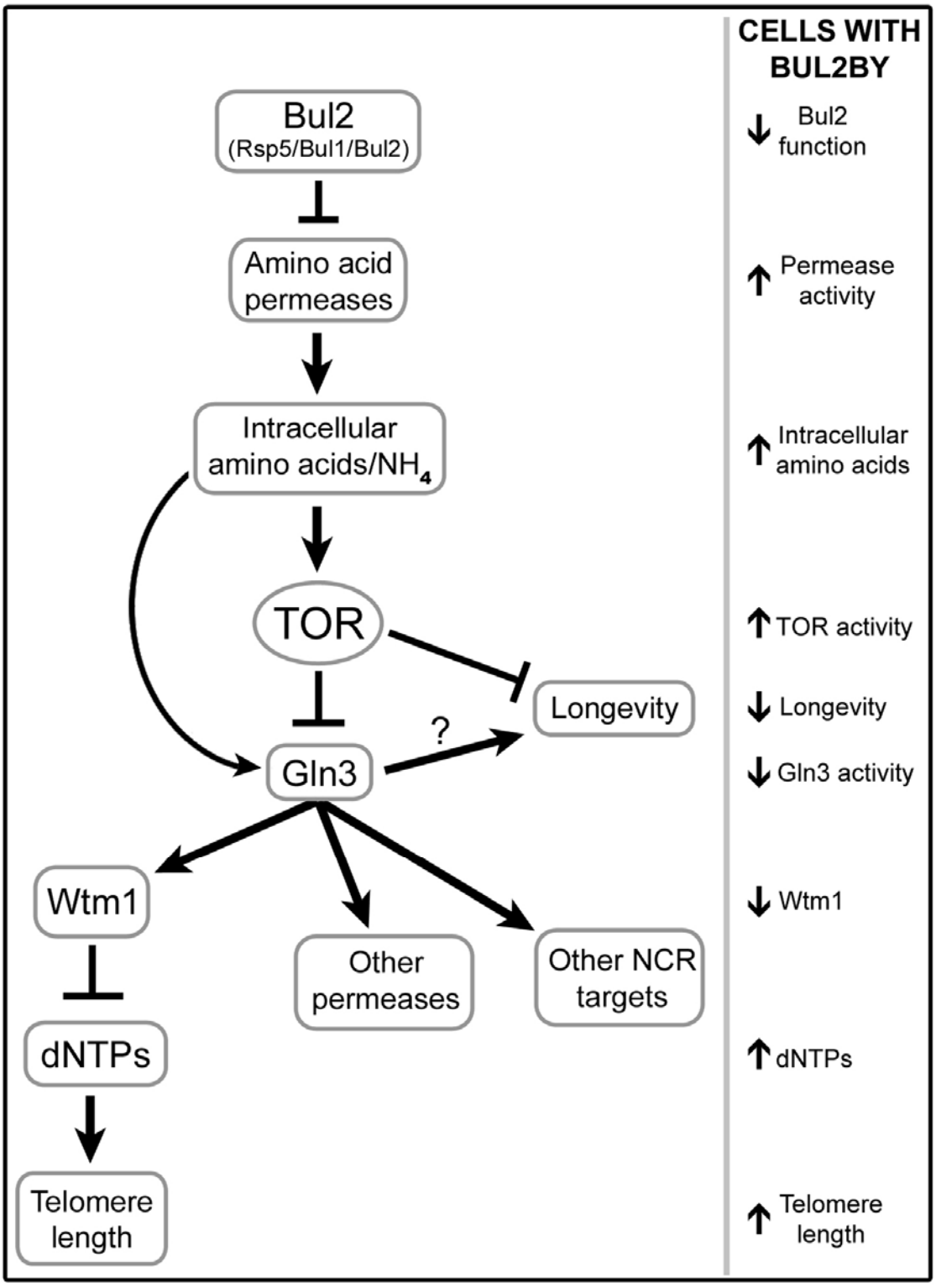

Figure 2.8: Model for *BUL2*-mediated alteration of telomere length and chronological lifespan.

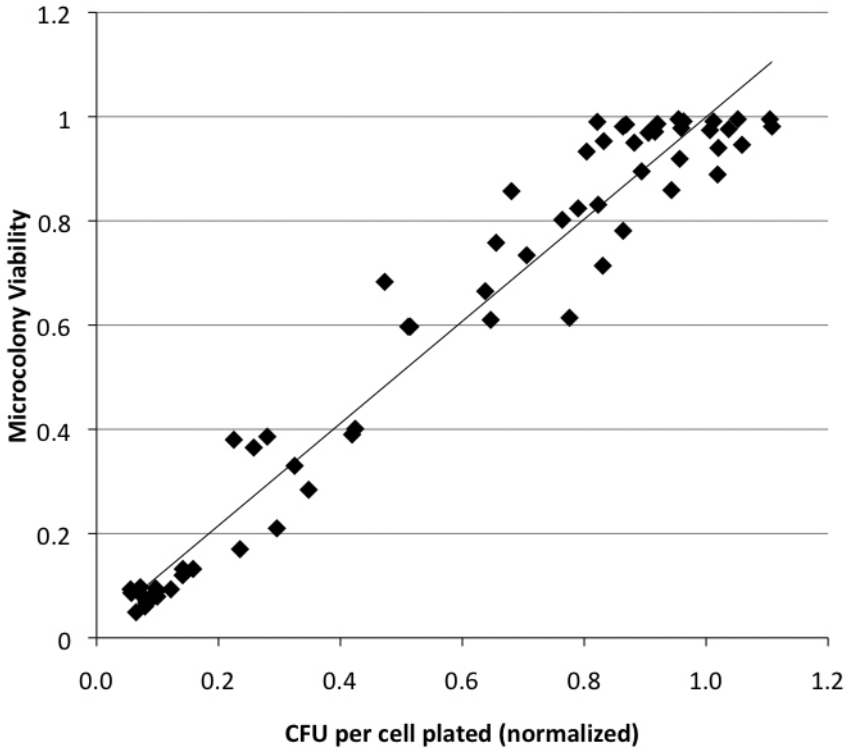

Figure 2.9: Comparison of viability values obtained via the CFU assay vs. the microcolony assay.

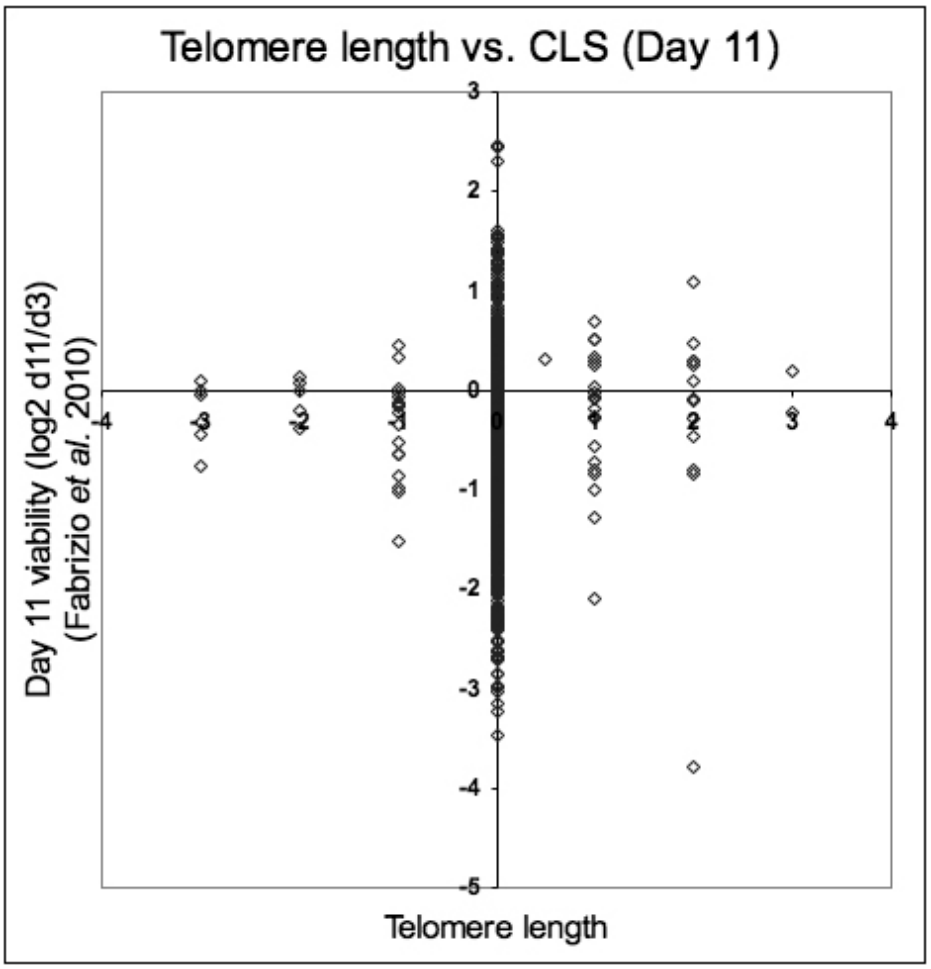

Figure 2.10: Comparison of phenotypes from telomere length and chronological aging genome-wide deletion screens. Telomere lengths of BY deletion strains from Gatbonton *et al.* [23] were plotted against their corresponding CLS from Fabrizio *et al.* [20]. Telomere length is indicated on the x-axis as -1,-2,-3 for mutants with shorter telomeres (shortened by ≤50bp, 50-200bp, and ≥200bp respectively) and as +1,+2,+3 for mutants with longer telomeres (longer by ≤50bp, 50-200bp, and ≥200bp respectively). In this study, 72 mutants were identified as having short telomeres and 80 mutants with long telomeres. On the y-axis, we have plotted the fitness at day 11 of each deletion strain relative to the rest of the pool of ~5000 strains from the deletion collection. (Strains were grown as pools and viability of each deletion strain is assessed at different time points as a ratio to the rest of the pool. Relative abundance of each strain at day 11 compared with their relative abundance at day 3 (t=0) is taken as a measure of their relative fitness at day 11. For instance, a strain with a score of 1 has doubled its ratio of viable cells when compared to its ratio to the rest of the pool at day 3.) Of the roughly 600 strains identified as having putative altered longevity, either increased or decreased CLS, only a few also exhibit a telomere length defect. Conversely, most of the telomere length mutants have unremarkable CLS (most of the strains fall between -1 and 1 on the y-axis). Even the strains exhibiting altered telomere length and altered CLS did not fall into a set pattern: strains with telomere length defects, for both longer and shorter telomeres, were equally likely exhibit have increased or decreased viability.

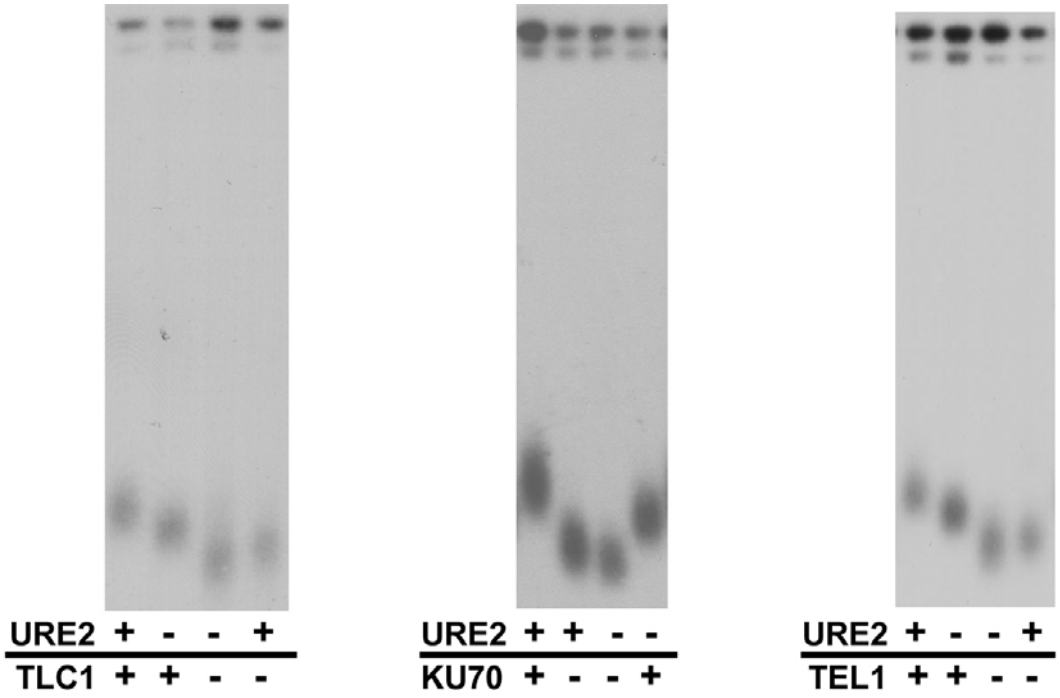

Figure 2.11: Short telomeres conferred by deletion of URE2 are not epistatic with *TLC1*, *YKU70* or *TEL1*. Southern blots show telomere length of single *ure2Δ* and double *ure2Δ tlc1Δ/yku70Δ/tel1Δ* mutants 25 doublings after germination of *URE2*/*ure2Δ* heterozygous diploids which are also *TLC1*/*tlc1Δ, YKU70*/y*ku70Δ,* or *TEL1*/*tel1Δ*. Telomere lengths of the double *ure2Δtlc1Δ, ure2Δyku70,* and *ure2Δtel1Δ* mutants are shorter than the telomere lengths of single *ure2Δ, tlc1Δ, yku70Δ,* or *tel1Δ* mutants.

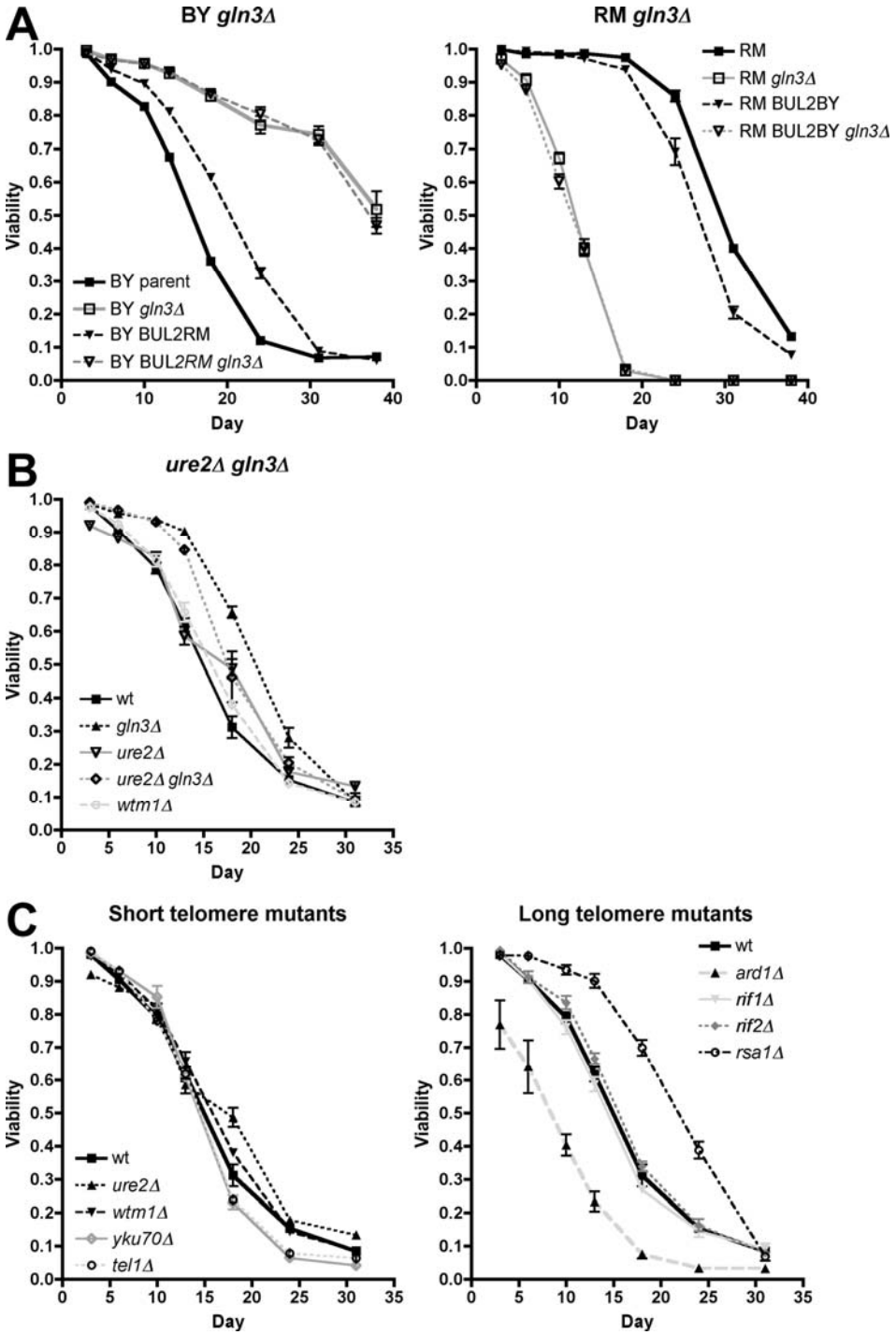

Figure 2.12: CLS curves for *gln3Δ* and telomere length mutants. (A) Deletion of *GLN3* extends lifespan in the BY parental strain, yet *GLN3* deletion decreases lifespan in the RM parental background. Changes to Bul2 function, from either *BUL2* allele replacement or *BUL2* deletion, have no effect on lifespan in *gln3Δ* mutants. (B) CLS analysis of *gln3Δ, ure2Δ* and *ure2Δgln3Δ* mutants in the BY background. (C) CLS analysis of mutants with long telomeres and short telomeres, from which we find no correlation between telomere length and chronological longevity.

Table 2.1: List of *S. cerevisiae* strains used in Chapter 2.

Lab Number	Background	MAT	Genotype	Figures
in plate	RmxBY		Segregant library (amn1::NAT)	2-1, 2-2B, 2-3B, 2-A, 52-A
15212	RM11-1a	a	*leu2d0 ura3d0 HO::KanMX amn1::NAT*	2-2A, 2-2D, 2-3A, 2-3D, 2-4B, 2-4C
15213	BY4716	α	*lys2d0 amn1::NAT*	2-2A
15214	BY4716	α	*lys2d0 amn1::NAT ura3::KanMX*	2-2D, 2-3A, 2-3C, 2-4B, 2-4C
15222	BY4716	α	*lys2d0 amn1::NAT ura3::KanMX BUL2RM #1*	2-2D, 2-3A, 2-3C, 2-4B, 2-4C
15224	BY4716	α	*lys2d0 amn1::NAT ura3::KanMX BUL2RM #2*	2-2D, 2-3A, 2-3C, 2-4B, 2-4C
15226	BY4716	α	*lys2d0 amn1::NAT ura3::KanMX BUL2(L883F) #3*	2-2D, 2-3A, 2-3C, 2-4B, 2-4C
15254	BY4716	α	*lys2d0 amn1::NAT ura3::KanMX bul2::HYG*	2-3C, 2-4C
15181	RM11-1a	a	*leu2d0 ura3d0 HO::KanMX amn1::NAT BUL2BY #1*	2-2A, 2-2D, 2-3A, 2-3D, 2-4B, 2-4C
15182	RM11-1a	a	*leu2d0 ura3d0 HO::KanMX amn1::NAT BUL2BY #2*	2-2A, 2-2D, 2-3A, 2-3D, 2-4B, 2-4C
15253	RM11-1a	a	*leu2d0 ura3d0 HO::KanMX amn1::NAT bul2::HYG*	2-2D, 2-3D, 2-4C
14141	BY4741	a	*leu2d0 ura3d0 met15d0 his3d0*	2-5B, 2-5C, 2-11, 2-12
15272	BY4742	a	*leu2d0 ura3d0 met15d0 his3d0 ure2::KanMX*	2-5B
15361	BY4742	α	*leu2d0 ura3d0 lys2d0 his3d0 yku70::KanMX*	2-11
in plate	BY4742	α	*leu2d0 ura3d0 lys2d0 his3d0 tel1::KanMX*	2-11
in plate	BY4741	a	*leu2d0 ura3d0 met15d0 his3d0 tel1::KanMX*	2-11
15351	BY4741	diploid	*leu2d0/leu2d0 ura3d0/ura3d0 met15d0/+ his3d0/his3d0 lys2/+ ure2::NAT/+ tlc1::KanMX/+*	2-11
in plate	BY4741	a	*leu2d0 ura3d0 met15d0 his3d0 tor1::KanMX*	2-5B, 2-12C
in plate	BY4741	a	*leu2d0 ura3d0 met15d0 his3d0 wtm1::KanMX*	2-12
in plate	BY4741	a	*leu2d0 ura3d0 met15d0 his3d0 rif11::KanMX*	2-12
in plate	BY4741	a	*leu2d0 ura3d0 met15d0 his3d0 rif21::KanMX*	2-12
in plate	BY4741	a	*leu2d0 ura3d0 met15d0 his3d0 ard1::KanMX*	2-12
in plate	BY4741	a	*leu2d0 ura3d0 met15d0 his3d0 rsa1::KanMX*	2-12
15271	BY4741	a	*leu2d0 ura3d0 met15d0 his3d0 gln3::KanMX*	5C
15335	BY4741	a	*leu2d0 ura3d0 met15d0 his3d0 ure2::NAT*	5C, 7B, 2-11
15276	BY4741	a	*leu2d0 ura3d0 met15d0 his3d0 ure2::KanMX gln3::NAT*	2-5C
15277	BY4741	a	*leu2d0 ura3d0 met15d0 his3d0 ure2::KanMX gln3::NAT*	2-5C
15285	BY4741	a	*leu2d0 ura3d0 met15d0 his3d0 gln3::KanMX ure2::NAT*	2-5C
15286	BY4741	a	*leu2d0 ura3d0 met15d0 his3d0 gln3::KanMX ure2::NAT*	2-5C
15395	BY4716	α	*lys2d0 amn1::NAT ura3::KanMX gln3::URA3*	2-5D
15398	BY4716	α	*lys2d0 amn1::NAT ura3::KanMX BUL2RM gln3::URA3*	2-5D

15399	BY4716	α	*lys2d0 amn1::NAT ura3::KanMX BUL2RM gln3::URA3*	2-5D
15400	BY4716	α	*lys2d0 amn1::NAT ura3::KanMX BUL2(L883F) gln3::URA3*	2-5D
15287	RM11-1a	a	*leu2d0 ura3d0 HO::KanMX amn1::NAT gln3::URA3*	2-5D
15379	RM11-1a	a	*leu2d0 ura3d0 HO::KanMX amn1::NAT BUL2BY gln3::URA3*	2-5D
15380	RM11-1a	a	*leu2d0 ura3d0 HO::KanMX amn1::NAT BUL2BY gln3::URA3*	2-5D
15965	RM11-1a	a	*leu2d0 ura3d0 HO::HYG amn1::NAT WTM1-3HA-KanMX*	2-6A
15966	RM11-1a	a	*leu2d0 ura3d0 HO::HYG amn1::NAT BUL2BY WTM1-3HA-KanMX*	2-6A
15983	RM11-1a	a	*leu2d0 ura3d0 HO::HYG amn1::NAT bul2::URA3 WTM1-3HA-KanMX*	2-6A
15967	BY4716	α	*lys2d0 amn1::NAT ura3::HYG WTM1-3HA-KanMX*	2-6A
15968	BY4716	α	*lys2d0 amn1::NAT ura3::HYG BUL2(L883F) WTM1-3HA-KanMX*	2-6A
15969	BY4716	α	*lys2d0 amn1::NAT ura3::HYG BUL2::HYG WTM1-3HA-KanMX*	2-6A
15970	BY4741	a	*leu2d0 ura3d0 met15d0 his3d0 WTM1-3HA-KanMX*	2-6A
15971	BY4741	a	*leu2d0 ura3d0 met15d0 his3d0 ure2::NAT WTM1-3HA-KanMX*	2-6A
15728	BY	a	*from BY4712xBY4716, auxotroph free spore*	
15729	BY	α	*from BY4712xBY4716, auxotroph free spore*	
15878	BY4741	a	*RNR4-GFP (UCSF/Invitrogen)*	2-6B, 2-6C
15890	BY4741	a	*RNR4-GFP ure2::HYG*	2-6B, 2-6C
15902	BY4741	a	*RNR4-GFP ure2::HYG wtm1::KanMX*	2-6B, 2-6C
15894	BY4741	a	*RNR4-GFP wtm1::HYG*	6B, 6C
15957	RM11-1a	a	*leu2d0 ura3d0 HO::HYG amn1::NAT RNR4-GFP-KanMX*	2-6B, 2-6C
15959	RM11-1a	a	*leu2d0 ura3d0 HO::HYG amn1::NAT RNR4-GFP-KanMX BUL2BY#1*	2-6B, 2-6C
15980	RM11-1a	a	*leu2d0 ura3d0 HO::HYG amn1::NAT RNR4-GFP-KanMX bul2::URA3*	2-6B, 2-6C
15961	BY4716	α	*lys2d0 amn1::NAT ura3::HYG RNR4-GFP-KanMX*	2-6B, 2-6C
15962	BY4716	α	*lys2d0 amn1::NAT ura3::HYG BUL2(L883F) wtm1-3HA-KanMX*	2-6B, 2-6C
15963	BY4716	α	*lys2d0 amn1::NAT ura3::HYG BUL2(L883F) wtm1-3HA-KanMX*	2-6B, 2-6C
15964	BY4716	α	*lys2d0 amn1::NAT ura3::HYG bul2::HYG RNR4-GFP-KanMX*	2-6B, 2-6C
15853	BY	α	*wtm1::HYG*	2-7A
15743	BY	a	*ure2::Nat*	2-7A
14606	BY4741	a	*leu2d0 ura3d0 met15d0 his3d0 sml1::NAT*	
in plate	BY4742	α	*leu2d0 ura3d0 lys2d0 his3d0 sml1::KanMX*	2-7B

Table 2.2: Genomic loci linked to chronological lifespan.

Day	Chromosome	Region	Viability RM	Viability BY	LOD Score
31	9	YIL066C-YILO34W	0.57	0.64	2.6
31	13	YML118W-YML083C	0.65	0.56	3.5
59	2	YBR072W-YBR092C	0.33	0.39	2.8
59	13	YML118W-YML077W	0.40	0.33	3.5
59	14	YNL093W-YNL066W	0.33	0.42	3.9
100	2	YBR045C-YBR092C	0.18	0.24	2.3
100	11	YKL010C-YKR015C	0.19	0.23	2.7
100	14	YNL093W-YNL066W	0.18	0.25	3.9

Table 2.3: *BUL2RM*-upregulated transcripts overlap with those upregulated by amino acid deprivation, rapamycin treatment and loss of *URE2*. (Can be accessed from Kwan *et al* PloS Genet 2011 [29].) Transcripts upregulated in the segregants with the RM *BUL2* allele and their corresponding expression level in cells undergoing amino acid deprivation, rapamycin treatment, or in *ure2Δ* mutant cells.

Table 2.4: *ure2Δ* transcript dataset. (Can be accessed from Kwan *et al* PloS Genet 2011 [29].) Transcripts which were upregulated 1.5-fold or more in *ure2Δ* cells relative to wildtype cells. The abundance of each transcript is presented as a $\log_2$ ratio relative to wildtype expression.

MATERIALS AND METHODS:

Yeast strains and media

Experiments were carried out using standard YPD media (2% glucose, 1% yeast extract, 2% peptone) unless otherwise noted (ie. ADCB assays). The strains used in this study are listed in Table 2.1and are from either the S288c (BY) or RM11-1A (RM) *S. cerevisiae* backgrounds. The segregant library has been previously described [28], except that *AMN1* has been deleted in each of the segregants to facilitate single cell viability analysis. (The RM allele of *AMN1* confers clumpiness, which precludes single cell analysis, whereas the S288c allele of *AMN1* was previously shown to create a loss of *AMN1* function [67]). Gene deletion mutants were either from yeast ORF deletion collection or were created using standard PCR transformation methods.

For allele replacement, we PCR-cloned a fragment containing 1kb of the 3' end of *BUL2* and 1kb *BUL2* downstream sequence from either the BY or RM strain using a 5' primer with an XhoI site (5'- GGCTCGAGGATTGATGATACCGCCAGCCAATCACC) and a 3' primer with a HindIII site (3'-GGCCAAGCTTGCGGGAAAAAGGCCAAACTCTACG). These fragments were inserted between the XhoI and HindIII sites in pRS406, a vector containing *URA3*. We used site-directed mutagenesis (QuikChange II kit, Stratagene) to introduce the L883F polymorphism into the BY *BUL2* plasmid. Allele replacement strains were generated using the "pop-in/pop-out" gene replacement method with the linearized *BUL2* plasmid [80]. *BUL2* allele replacement strains were first screened by sensitivity to ADCB and then PCR-sequenced to confirm the desired *BUL2* polymorphisms.

Microcolony assay for chronological aging

For each strain, 1μL of saturated culture was inoculated into 150μL of YPD (2% glucose) or buffered synthetic complete media [36] in 96-well plates. Plates were then incubated for 2 days at 30°C, at which point they were foil-sealed to prevent evaporation and kept at 30°C for the remaining time. Strains were examined in triplicate. To assay viability, 1μl of each resuspended culture was harvested, diluted in water, spotted onto solid YPD media, and incubated for 24 hours at 30°C. Microcolonies and cells that had not divided were counted using a microscope, with the total number of events ($n > 200$ for each culture) used as the denominator to determine viability percentage. Additionally, colony formation unit (CFU) assays was used to determine viability in select RM and BY strains. Comparison between CFU and microcolony values obtained show that the two assays are highly correlative ($R=0.98$) (Figure 2.9).

QTL mapping/genome-wide linkage analysis

Genome-wide linkage analysis of segregant data was performed using the publicly available R/qtl software. Effects of RM/BY allele inheritance in the segregants were examined using R (box plots) and Excel (student's t-test).

ADCB toxicity assays

Initial ADCB toxicity assays were carried out using 25μg/mL ADCB (L-Azetidine-2-Carboxylic Acid, Sigma-Aldrich) dissolved in SD media (1.9g YNB, 0.5% $(NH_4)_2SO_4$, 2% dextrose) supplemented with leucine (80μg/mL), lysine (60μg/mL), and uracil (20μg/mL) to

compensate for the auxotrophies present in the segregant library. Cells were inoculated into 150μL media in 96-well plate and incubated at 30°C. Segregant growth in ADCB was quantified using absorbance at OD660 after 17 hours in 30°C. *BUL2* allele replacement spot assays were carried out on solid SD media of the same composition with 25μg/mL ADCB.

Telomere length analysis

Genomic DNA was harvested from saturated 3mL cultures using a phenol:chloroform DNA extraction. Telomere lengths were evaluated as described in Gatbonton *et al.* [23]: genomic DNA was digested overnight with XhoI, resolved by gel electrophoresis (0.5% TBE, 0.9% agarose gel, run for 360V•hr) and transferred to Hybond-N membrane. Terminal restriction fragments containing telomeres were visualized using ^{32}P-labeled probes amplified from the Y' subtelomeric sequence.

Microarrays

Total RNA was harvested from 20mL logarithmic phase cultures in biological triplicate using the hot phenol method previously described by Schmitt *et al*. [81]. Three competitive hybridizations for each experimental group (*ure2Δ* versus wildtype) were performed using three separate cultures, and the $\log_2$ of the expression ratio was calculated for every ORF. To assess the intrinsic variation of expression levels for different ORFs, wildtype versus pooled wildtype hybridizations were performed using three separate cultures. Arrays used were spotted oligo probe arrays generated by the Fred Hutchinson Cancer Research Center Genomics Resource. Probability of overlap with *BUL2RM*-upregulated transcripts was calculated using the binomial probability formula.

Western blot analysis

Yeast whole cell extracts from 5mL logarithmic phase cultures were harvested using the NaOH protein extraction method previously used by Thaminy *et al.* [82] and Kushnirov [83]. Proteins were resolved using SDS-PAGE (10% polyacrylamide gel, 120V for 90 minutes) and transferred to a nitrocellulose membrane. Proteins of interest were probed with antibodies against actin (1:1000 dilution, Neomarkers) or HA (1:5000 dilution, Covance) and visualized using HRP-conjugated IgG antibodies (1:1000, Vector Laboratories). Wtm1 blot intensity was quantified using ImageJ and normalized to actin intensity.

Fluorescence microscopy

The Rnr4-GFP strain was obtained from the commercially available Invitrogen/UCSF GFP-tagged collection and genes were deleted using standard PCR transformation protocols. Cells from logarithmic phase cultures were harvested and fixed using paraformaldehyde, as previously described by Biggins *et al.* [84]. To visualize nuclei, fixed cells were incubated with 1μg/mL DAPI for 1 hour, washed once and resuspended in sorbitol. Cells were sonicated before visualization and scoring. At least 200 events for both S-phase and G1 cells were scored for wildtype, *ure2Δ*, *wtm1Δ* and *ure2Δwtm1Δ* strains. At least 500 S-phase cells were scored for RM and BY *BUL2* allele strains. Images were captured using a Nikon E800 fluorescence microscope.

CHAPTER 3

Origin activation at rDNA locus regulates lifespan

INTRODUCTION

The budding yeast *S. cerevisiae* has become a favorite model for studying the genetic and molecular basis for variation in lifespan. In particular, the unequal division of mother and daughter cells in this species makes it especially amenable to analysis of replicative lifespan (RLS), the number of "daughter" cells that a "mother" cell can produce before it senesces, which is approximately 20-30 on average, and is thought to be analogous to aging of mitotic cells such stem cells and epithelia. Genetic screens for genes which can alter RLS have identified many whose deletion confers lifespan extension, such as those in growth and metabolism pathways, and many more genes whose absence reduces yeast longevity. Of the previously identified lifespan regulators, a considerable body of evidence already exists linking metabolic events that occur in the yeast rDNA locus with replicative aging, including involvement of the protein deacetylase, Sir2, and the replication fork blocking protein, Fob1.

The discovery of *SIR2* and *FOB1* as regulators of yeast lifespan first implicated rDNA stability as limiting RLS. The rDNA locus is highly repetitive region of the genome, 1MB in size, and consists of 150 tandem repeats of a 9.1kb sequence encoding highly transcribed rRNA transcripts (18S, 5.8S, 25S, 5S) as well as non-transcribed regions with features to allow it to maintain its chromosome-like size, such as origins of replication. The rDNA locus is also highly transcribed: 60% of all transcription in a yeast cell is dedicated to the production of rRNA [85] and can only be accomplished with the concurrent transcription

of rRNA from multiple rDNA repeats [86]. Sir2p is a NAD-dependent histone deacetylase which silences the rDNA locus and promotes equal sister chromatid exchange by inhibiting the RNA polymerase II (RNA PolII) transcription that disrupts rDNA-bound cohesion [87]. Unequal sister chromatid exchange in the absence of *SIR2* results in rDNA expansion/contraction, resulting in formation of extrachromosomal rDNA circles (ERCs) [88], and this instability has been proposed to be responsible for the decreased lifespan seen in *sir2Δ* mutants [89]. Conversely, an extra copy of genomic *SIR2* extends the lifespan of laboratory yeast by 30% and promotes equal sister chromatid exchange. The Fob1 protein binds to the rDNA replication fork barrier (RFB), creating a unidirectional replication block thought to prevent the collision between the rRNA PolI transcription machinery and the DNA replication machinery. However, Fob1 binding also promotes rDNA recombination by increasing the probability of double strand breaks. While the collision between transcription machinery and replication forks is anticipated to be detrimental, the longer lifespan of a *fob1Δ* mutant suggested that cells are more sensitive to the damage from Fob1-induced recombination. In addition, the lifespan of a *sir2Δ* mutant is restored to wildtype length in the absence of *FOB1*, perhaps because unequal chromatid exchange may be less problematic when double strand break-induced recombination is decreased [90].

Calorie restriction is a universal regulator of longevity between species. Restriction of dietary intake to 70% *ad libitum* was first reported to extend the lifespans of mice and rats [1,91,92]. Since then, this calorie restriction-mediated lifespan extension has been also documented in worms, flies, and yeast [4,6,93]. Additionally, single gene changes that reduce activity of conserved nutrient-signaling pathways such as TOR and IGF-1 have been

shown to mimic calorie restriction's benefit to longevity, though the exact mechanisms governing lifespan extension remains unclear. There is no evidence, however, that the known yeast lifespan regulators *SIR2* and *FOB1* are affected by calorie restriction. Furthermore, calorie restriction is able to extend lifespan of *sirΔ2 fob1Δ* double mutants [94], indicating that *SIR2* and *FOB1* are dispensable in calorie restriction's regulation of yeast longevity. Though independent from *SIR2* and *FOB1* function, the mechanisms of calorie restriction must still overcome the events at the rDNA locus that limit yeast lifespan.

We used an outbred yeast model, consisting of strains generated between a cross between the laboratory strain S288c (BY) and the vineyard strain RM11-1a (RM), to identify naturally occurring polymorphisms that regulate replicative lifespan and found that the rDNA locus is the major regulator of lifespan. Among the rDNA sequences that differ between RM and BY, we identified a polymorphism in the RM rDNA that leads to a marked reduction in rDNA origin activity in a plasmid maintenance assay. The less active RM rDNA origins confer a reduced size of the rDNA array and extend lifespan independent from *SIR2* and *FOB1*. Paradoxically, the origin activity at the endogenous rDNA origin is the same between both strains, underlining the importance of chromosomal context in the regulation of origin firing. We hypothesize that the increased activity of the inherently weaker RM rDNA origin in the chromosomal context is generated by the high rate of rRNA transcription. Because rRNA transcription is heavily influenced by nutrient availability, our observation provides a link between calorie restriction, rDNA origin activation, and lifespan.

RESULTS

Replicative lifespan analysis of outbred segregant library

We measured the replicative life span (RLS) of 90 meiotic segregants previously derived from a cross between the laboratory strain s288C (BY parent) and the vineyard yeast strain RM11-1a (RM parent) [28]. By following 20 individual cells for each segregant strain, we found continuous variation in lifespan, with mean RLS ranging from 12 to more than 40 generations (Figure 3.1A), suggesting that multiple loci are involved in controlling longevity. This wide variation of RLS among the segregants is derived from parents with similar lifespans (26.5 and 28.6 generations for BY and RM respectively) and indicates the presence of multiple loci that have compensating effects in the parental strains, i.e. transgressive segregation. In order to determine to what extent was the observed lifespan variation genetically determined, we repeated lifespan analysis of 40 segregant strains. We found that heritability was 82%, indicating that a large fraction of lifespan variation in this cross is determined genetically.

Genome-wide linkage analysis revealed overwhelming linkage to a locus on chromosome XII (LOD score of 8) (Figure 3.1B). Further investigation refined this linkage to the rDNA locus, with significant LOD scores on both sides of this 1.2Mbp region. Only one meiotic crossover event between the markers flanking the rDNA region was found within segregants, consistent with the previous observation that rDNA is inherited as one locus [95]. We determined that 38% of total lifespan variation (46% of heritable variation) between the segregants is controlled by the rDNA locus, indicating that rDNA is the major

regulator of lifespan in the RM and BY cross. Several other minor loci were identified in our genome-wide analysis and the residual lifespan variation not explained by the rDNA locus is most likely due to the combination of their smaller but significant contributions (Table 3.1). We quantified the influence of rDNA on longevity by separating segregants into populations based on rDNA allele inheritance (Figure 3.1B). The segregant population inheriting BY rDNA had an average RLS of 23.5±4.6, comparable to lifespans previously seen from laboratory strains such as s288c and W303. Segregants inheriting RM rDNA, however, had an average RLS of 33.1±7.0 cell divisions, a 41% increase in longevity (P=9.5x10^{-12}, ν=88).

In order to isolate the effects of the rDNA allele from other genomic polymorphisms, we carried out eight sequential backcrosses to the BY laboratory strain while maintaining the RM vineyard rDNA. This backcrossed strain had a mean lifespan of 38.6, a 46% increase compared to mean of 26.5 for parental BY strain (P=10^{-4}, ν=2, Figure 3.1C). Conversely, when we used eight backcrosses to transfer the laboratory rDNA in the RM background, we found that the BY rDNA backcrossed strain had a lifespan of 20.9, a drop of 26% compared to vineyard parental lifespan of 28.5 (P=5x10^{-4}, ν=2, Figure 3.1D). Thus, consistent with mapping results, the backcross analysis confirmed that vineyard rDNA confers increased lifespan.

While a link between the rDNA locus and yeast longevity is a well established one [96,97], it is still unclear how exactly the rDNA locus influences replicative lifespan. It has been previously proposed that mitotic intrachromosomal recombination at the rDNA locus, concomitant with the production of extrachromosomal rDNA circles (ERCs) [97],

contributes to the decrease in replicative lifespan potential. Although the recombination model has been established, there is still debate as to whether this shortening of lifespan is due to accumulation of ERCs, genomic instability generated by rDNA recombination, or another yet unidentified cellular process. Armed with our findings, we hope to shed some light on how rDNA regulates lifespan.

rDNA affects lifespan independently of *SIR2* and *FOB1*

To investigate whether the effect of RM rDNA required *SIR2*, we deleted *SIR2* in 28 randomly selected segregant strains and analyzed their replicative lifespan. While the average lifespan dramatically decreased upon *SIR2* deletion, *sir2Δ* segregant strains with RM rDNA had significantly longer RLS (17.0±2.1) compared to their BY rDNA counterparts (10.8±1.7, P=6.1x10^{-9}, ν=2) (Figure 3.2A), which demonstrates that *SIR2* function is not required for RM rDNA induced increase in RLS. The *SIR2*-independence of the RM rDNA allele benefit was recapitulated in our backcross strains: BY *sir2Δ* strains with RM rDNA fared better than the parental strain, with lifespan means of 18.0 and 12.0 (p=1.7x10^{-3}, ν=2, Figure 3.2B). The RM *sir2Δ* strain also lived longer (17.0) than the BY rDNA *sir2Δ* strain (10.1) (P=9.0x10^{-4}, ν=2, Figure 3.2E). Additionally, we generated segregant strains in which an extra copy of SIR2 was inserted in the genome and found that longevity benefit of the RM rDNA allele was still maintained in the presence of *SIR2* overexpression (35.40±3.4 vs. 28.08±3.0 divisions, P=2.0x10^{-2}, ν=9, Figure 3.2D). These results demonstrate the RM rDNA lifespan extension is independent of *SIR2*.

To determine whether *FOB1* is required for vineyard rDNA mediated lifespan extension, we deleted *FOB1* in parental strains and strains with the replaced rDNA loci. In the BY background, *FOB1* deletion led to increased lifespan in strains with both native rDNA (38.9) and vineyard rDNA (44.3) (P=6.7x10^{-3}, ν=2, Figure 3.2C). Since the RM rDNA allele still increased lifespan in the absence of FOB1, we concluded that the longevity benefit of the RM rDNA was not dependent on the presence of *FOB1*. Unexpectedly, in the vineyard background (RM), loss of *FOB1* reduced lifespan by half, an effect that occurred in both the RM parental strain (17.2 generations) and the strain with BY rDNA (10.3 generations; Figure 3.2F). Thus it appears that in the RM strain, unlike most of the laboratory strains, *FOB1* deletion decreases lifespan through unknown mechanisms. However, the longevity effects of the RM rDNA allele persisted (P=10^{-4}, ν=2) and are therefore separable from Fob1 function.

BY and RM rDNA differ in ERCs, copy number, and intergenic sequence polymorphisms

The rDNA array size was first determined in the parental vineyard (RM) and laboratory (BY) strains using Southern blot analysis (Figure 3.3A), which revealed that the number of rDNA repeats in the vineyard strain was approximately 60% of that in the laboratory strain (~90 vs. ~150 copies [98]). We confirmed that RM rDNA is shorter than BY rDNA using contour-clamped homogeneous electric field (CHEF) gel electrophoresis. Remarkably, the reduced size of the vineyard rDNA locus, measured by the size of chromosome XII by CHEF gel electrophoresis (Figure 3.3B), was preserved after 10 successive backcrosses to the laboratory strain (~ 500 population doublings). This

observation suggest that cis-elements in the vineyard rDNA sequence are responsible for maintaining reduced steady-state copy number relative to rDNA of the laboratory strain.

Intrachromosomal recombination between the tandem rDNA repeats generates extrachromosomal rDNA circles (ERCs), whose preferential accumulation in mother cells has been proposed as one of the mechanisms that limits replicative potential [97,99]. To determine whether vineyard and laboratory rDNA loci differ in their ability to generate/maintain ERCs, we measured ERC levels in logarithmically growing cultures of the parental strains and their respective rDNA replacement backcross strains. Using 2D gels to resolve uncut genomic DNA from ERCs, we find ERCs were reduced by 90% in the BY strain with the RM rDNA allele (Figure 3.3D). This large reduction in ERC level in logarithmically growing cultures, which consist primarily of young cells, suggests that having RM rDNA leads to decreased ERC accumulation. However, we determined that the RM parental strain had more ERCs than both the shorter-lived BY parent strain and the RM strain with BY rDNA allele, indicating no correlation between rDNA and lifespan. These results do not follow the previously proposed recombination model and, at least in logarithmically growing cultures, suggest dissociation between lifespan and ERC accumulation.

Since our results suggest that the rDNA sequence itself is important for longevity as well as for copy number, we checked for polymorphisms between RM and BY rDNA. We found no sequence polymorphisms in the 37S and 5S regions encoding rRNA transcripts, consistent with their conservation. However, we found that the non-transcribed spacer (NTS)

region is highly divergent between these two strains (Figure 3.4A). Within the NTS are several elements that have been found to play an important role in the maintenance of the rDNA locus: NTS2 contains the rDNA origin of replication (rARS) [100] and the cohesin associating region (CAR) [101], and NTS1 contains the replication fork barrier (RFB) [102], which binds Fob1, and the E-pro RNA PolII promoter silenced by Sir2 [87]. While many of the NTS polymorphisms do not alter these landmarks, we identified sequence changes in the rDNA origin of replication and in the replication fork barrier involved in mitotic recombination. Using high-throughput sequencing and examination of the total number of reads from the rDNA array of both the RM and BY parent strains, we found that the identified RFB and rARS variants are homogenous within a strain: all 150 copies of rDNA in the BY strain have the same BY origin and RFB sequences, all 90 RM rDNA copies have the RM sequences. This homogeneity within the rDNA array allows us to investigate the effects of an rDNA array as a single sequence rather than a complex hodgepodge of heterogeneous repeats.

To assess how the rARS and RFB polymorphisms affect lifespan, we examined rDNA sequences from a diverse collection of wild yeast. The majority of the 37 *S. cerevisiae* isolates sequenced by the Saccharomyces Genome Resequencing Project (SGRP) [103,104] possessed the RM rDNA sequence, with only a handful with polymorphisms seen in the BY strain. More fortuitously, we found a handful of strains that have hybrid rDNA sequences: strains whose rDNA is mostly the RM sequence but contains either the BY rARS or BY RFB polymorphism. In order to parse out the importance of the RFB and rARS alterations, we generated outcrossed rDNA from 3 *S. cerevisiae* isolates with hybrid rDNA sequences into

the BY background. The rDNA sequences from DBVPG6765 and L_1374 look like RM rDNA but have the BY RFB. Backcross strains with either of these rDNA sequences had significant lifespan extension (P=10^{-4}, ν=2) on par with RM rDNA (Figure 3.4B), suggesting that the BY RFB does not decrease the benefit of the RM rDNA allele. However, when we examined rDNA from the sake strain Y12, which has the RM sequence with the BY rARS polymorphism, we found that the Y12 rDNA allele does not extend lifespan of the BY strain (P=0.1404, ν=2). The Y12 rDNA results indicate that it is the RM rARS sequence, and not the RFB sequence, which is responsible for conferring the RM rDNA-dependent lifespan extension.

RM rDNA ARS polymorphisms greatly reduces ARS activity

While we have not yet examined the effects of each rDNA polymorphism, we have confirmed that polymorphism in the rDNA origin of replication affects its activity. The RM rDNA origin of replication has a cytosine polymorphism at a highly conserved thymidine residue in the A/T-rich rDNA ACS1 sequence, suggesting that it may impair origin function and DNA replication (Figure 3.4A) [100,105,106]. To measure and compare origin activity of the different rDNA sequences, we cloned the rARS sequences from RM and BY rDNA into an origin-free vector containing a KanMX marker and tested the ability to these sequences to promote plasmid maintenance. We found that the BY rARS is highly active while the RM rARS is much less active, as evidenced by the lack of growth on G418 plates (Figure 3.5). Use of the whole 2.2kb RM rDNA NTS still resulted in greatly decreased origin activity, refuting the possibility of replication from a cryptic origin in the larger rDNA

sequence. An origin-free plasmid (no ARS) and a plasmid with a highly active yeast origin (ARS1) served respectively as a negative and positive control.

Plasmid maintenance is influenced by a strain's rDNA sequence

In the course of our studies of RM rDNA origin usage, we noticed that the RM parental strain exhibited robust growth on G418 while maintaining the RM NTS plasmid (Figure 3.5). Further investigation revealed that increased capacity to maintain these weak origin plasmids is linked to the RM rDNA allele: the BY with RM rDNA grew better on G418 while the RM strain with BY rDNA strain exhibited poorer growth. In fact, the increased capacity to maintain a plasmid with a weak origin depends on a strain's rDNA origin sequence. BY strains with rDNA from DBVPG6765 and L_1374 (BY RFB) were able to maintain plasmids with RM NTS and RM rARS sequences, visible by growth on G418 (Figure 3.6C). The BY strain with Y12 rDNA (BY rARS), however, resembled the BY parent strain and was unable to maintain the RM NTS and RM rARS plasmids, illustrating that increased use of weak plasmid origins relies on having the RM rDNA origin sequence. We wanted to address the possibility that our observations were an artifact of the plasmid containing an rDNA sequence, which could associate them with the nucleolus where they would be directly affected by the same replication forces governing the endogenous rDNA. We therefore examined a plasmid containing a weak origin sequence from *Lachancea waltii*, a non-rDNA sequence from different yeast species, and found that the *L. waltii* plasmid was also better maintained in the BY strain with RM rDNA, suggesting that increased plasmid maintenance is not specific to a plasmid containing an rDNA sequence.

RM rDNA allele confers increased activity of weak genomic origins and suppresses orc2-1 mutation

Why would having an impaired rARS sequence lead to increased plasmid origin activity and extended lifespan? Our results led us to hypothesize that decreased activity at rDNA origins reduces the competition for replication factors and therefore allows for greater replication of the weak origin plasmids (Figure 3.7A). If the rDNA sequence can promote usage of weak origins on a plasmid through increased availability of replication factors, it is therefore possible that the rDNA locus alters origin activity across the genome. We then examined activity at several genomic origins in strains with RM and BY rDNA using 2D gel electrophoresis. While not all origins were affected, we found that activity at the inefficient ARS605 origin was increased with the RM rDNA allele (Figure 3.7B). This ARS605 origin was previously noted to have different efficiencies between two different strains, A364A[107] and DKD-5D-HD [108], which could be due to rDNA sequence differences. Our results suggest that the RM rDNA allele increases efficiency at a subset of genomic origins.

While we only examined a handful of genomic origins, we wanted to know if the RM rDNA allele can globally compensate for a limiting replication factor. Since we do not yet know which replication factors are limited by rDNA, we decided to engineer a situation where we restrict formation of replication complexes using a temperature-sensitive *orc2-1* mutant [109,110]. Orc2 is a subunit of the origin recognition complex (ORC) which recruits replication factors to *S. cerevisiae* origin sequences. The *orc2-1* mutant allele generates an unstable ORC: wildtype *orc2-1* mutants, with BY rDNA, are unable to grow at non-

permissive 26°C and also exhibit slower growth at room temperature. However, we found this *orc2-1* deficiency was rescued in strains with the RM rDNA allele (Figure 3.7C), suggesting that having weaker and fewer origins at the rDNA locus facilitates genome-wide replication when ORC function would be otherwise insufficient.

RM rARS maintains comparable replication function and timing at the endogenous rDNA locus

The extreme differences in origin activity from our plasmid maintenance assay suggest that the replication of the RM rDNA locus could be very different from that of BY rDNA. To examine origin activity at the endogenous rDNA locus, we used 2D-gel electrophoresis to compare the quantity of replication bubbles, which are generated by active origins, from the passively-replicating Y-shaped intermediates. The relative origin activity can then be estimated as the ratio of bubble arc intensity to that of the Y-arc. Although plasmid transformation assays suggested that the RM rARS is crippled, we found that activity of the endogenous RM rARS was as strong as the BY rARS (Figure 3.8B). We then wanted to know if RM rDNA is perhaps replicated slower than BY rDNA. To do so, we examined rDNA replication kinetics using a density transfer experiment [111], in which cells cultured in "dense" media consisting of ^{13}C and ^{15}N isotopes, are released into isotopically light media, where newly the synthesized DNA will be labeled with less dense ^{12}C and ^{14}N. We found that the rDNA locus replicates late when compared to the rest of the genome and that the rates of replication of BY and RM rDNA are strikingly similar (Figure 3.8C). The paradoxical difference we find between origin activity on a plasmid versus genomic origin activity illustrates the importance of chromosomal context in origin regulation, as

demonstrated by the dramatic increase in RM rARS origin activity when at the genomic rDNA locus.

Calorie restriction reduces rDNA origin activity

Our finding that yeast lifespan is extended by a vineyard polymorphism at rDNA which decreases rARS activity led us to hypothesize that calorie restriction could also be reducing rDNA origin activity. Calorie restriction was previously known affect rDNA through the reduction of ribosome biogenesis [30] and downregulation of rRNA transcription [112], but its effects on rDNA replication have not been examined. To investigate calorie restrictions effects on rDNA origin efficiency, we compared rDNA replication intermediates from cells grown in 2% glucose (normal media) and 0.05% glucose (calorie-restricted media [94]). Quantitative Southern blotting verified that the there was no difference in rDNA copy number between normal and calorie-restricted cultures (data not shown). We found that calorie restriction reduced BY rDNA origin activity by 58% when compared to cells grown in normal 2% glucose (Figure 3.9A). Calorie restriction had an even more dramatic effect in cells with RM rDNA, where rDNA origin activity was reduced by 84% in 0.05% glucose. In fact, the reduced origin activity of the RM rDNA compared to the BY rDNA is evident in calorie-restricted cells, in which the promotion of origin activity via rRNA transcription is presumably reduced. The magnitude of inhibition of rDNA origin activity by calorie restriction suggests that it may also have profound effects on genome-wide replication.

We then wanted to determine if calorie restriction could phenocopy other traits of RM rDNA, particularly if calorie restriction could also increase genomic origin usage. To

examine the effects of calorie restriction on genome-wide replication, we examined *orc2-1* sensitivity in the absence of *GPA2*, encoding a signaling component of the G-protein coupled receptor, *RPL6B* or *RPL31A*, components of the large ribosome subunit. Loss of any of these three genes extends replicative lifespan through effects that are epistatic with calorie restriction [94,113]. We found that *orc2-1* temperature sensitivity was partially rescued by all three deletions (Figure 3.9B), suggesting that calorie restriction mimetics can promote usage of genomic origins of replication. While further calorie restriction studies of genome-wide replication are needed, the rescue of *orc2-1* sensitivity by *gpa2Δ, rpl6bΔ,* or *rpl31aΔ* suggests that calorie restriction could also affect global replication though the same mechanism as RM rDNA.

DISCUSSION

Our replicative lifespan studies of genetically diverse strains revealed that the rDNA locus is the key determinant of yeast longevity between the laboratory S288c strain and the vineyard RM11-1a strain and that the RM rDNA allele provides robust lifespan extension. The modulation of lifespan by the RM rDNA allele was found to be independent of SIR2 and FOB1, two previously established regulators of yeast longevity which also interact with the rDNA locus [89,114], suggesting that the rDNA locus itself contains intrinsic properties important for lifespan manipulation. While the intergenic rDNA sequence is highly divergent between *S. cerevisiae* isolates, our studies pinpoint a polymorphism which reduces the activity of the RM rDNA origin of replication (rARS) as being responsible for lifespan extension. Further characterization indicates that the RM rARS polymorphism, when propogated across the endogenous rDNA array, alters global DNA replication.

How does rDNA affect lifespan?

We propose that fewer active origins at the rDNA locus would promote genome stability and longevity via two possible mechanisms. The first possibility is that reduction of rDNA origin firing promotes the stability of the rDNA locus, contributing to overall genome stability. The rDNA locus is an incredibly difficult region of the genome to replicate and full of potential pitfalls: replication forks have to dodge transcription at the 5S locus and the densely populated 37S rRNA region. Replication forks are halted unidirectionally at the Fob1-bound RFB in order to prevent collision between replication and transcription machinery, but the RFB function also guarantees that most rDNA origins that fire will generate a stalled replication fork [102,115] and increase the probability of rDNA recombination[116]. Evidence for the rDNA's greater vulnerability comes from loss-of-heterozygosity studies of regions on chromosome VI and the rDNA-containing chromosome XII. Loss-of-heterozygosity events on chromosome XII increased significantly as cells aged, while loss-of-heterozygosity on chromosome VI remain unaffected, indicating sequences proximal to the rDNA locus are more prone to age-associated instability [117]. While the origin activity is the same between RM and BY rDNA (30% of rDNA origins are estimated to be active), the smaller RM rDNA array (90 vs. 150 copies) would have fewer active origins (30 vs. 50) and therefore less recombination, leading to greater overall stability of the rDNA array.

Our second model proposes that a reduction in the number of actively replicating origins at the rDNA locus would decrease the competition for replication factors and

therefore increase usage of more genomic origins, ensuring the complete replication of the genome. We found that strains with a less active rDNA origin sequence had more activity at a genomic origin and partially rescues lethality in *orc2-1* mutants. A similar rescue was reported by Ide *et al*. [109] when they characterized clones that were able to suppress the *orc1-4* and *orc2-1* temperature sensitive phenotype. A majority of the rescued strains possessed a dramatically smaller chromosome XII, a result of severe reductions to the rDNA array. This flexibility in rDNA size suggests that it is a dynamic structure which can respond to and compensate for replication constraints. Our model proposes rDNA can affect normal genome-wide replication through decreased competition for a putative limiting replication factor, artificially emulated using the *orc2-1* mutant. Future experiments include a screen for the putative replication factor(s) limited by rDNA and determining if lifespan can be extended by the increased availability of said factors.

Could a reduction in rDNA origin firing make a difference in yeast genome replication?

In addition to 300-400 genomic origins, *S. cerevisiae* has another 150 potential origins of replication contributed by the laboratory strain's rDNA locus. Therefore, a third of available origins of replication reside in the rDNA locus, reported previously with ORC ChIP-seq data. As rDNA origin efficiency is estimated to be approximately 20-30%, the initiation of 50 active rDNA origins [102,118] would comprise 15% of total origins used during replication. Although we found rDNA origin efficiency to be the same between the RM and BY rDNA alleles, the shorter RM rDNA array would utilize 20 less rDNA origins, approximately 5% of the total origins used. While a 5% decrease may not appear significant, this modest reduction in origin firing may be enough to reduce the chances of having a large

region of DNA without origin firing, the "random replication gap problem [119] (Figure 3.10)," previously observed in fission yeast [120]. Large gaps between active origins may lead to stretches of incomplete DNA replication, which is undesirable and can induce genomic instability. Strains deficient in origin initiation, such as an *orc2* mutant or a *sic1* initiation mutant, arrest at the end of S-phase with large stretches of unreplicated DNA and cells which recover from this checkpoint arrest do so through massive genome destabilization, seen as gross chromosomal rearrangements and chromosome loss [121]. Due to the stochastic nature of origins, each origin has only a probability of being active, with late firing origins used to synthesize any remaining stretches of unreplicated DNA. Since rDNA is a late replicating region of the genome and most likely consists of late-firing origins, having the shorter RM rDNA array would facilitate replication from 20 more late-firing origins, which may be crucial in the completion of any remaining unreplicated genomic gaps. The resultant increase in the probability of completing genomic replication would therefore be beneficial to overall genomic stability.

***SIR2* mutants and rDNA origin efficiency**

rDNA biology has long been proposed to govern yeast longevity. However, the canonical model proposed is that the stability of the rDNA locus determines lifespan. Examination of *sir2Δ* mutants revealed a correlation with increased mitotic recombination between rDNA repeats [88] and decreased longevity [89]. Conversely, manipulations which decrease rDNA recombination, namely *SIR2* overexpression and *FOB1* deletion [122], extend yeast lifespan [89]. Along with the increased accumulation of recombination-generated ERCS seen in old cells [97,117], this correlation between rDNA instability and

lifespan culminated in the hypothesis that increased rates of rDNA recombination could destabilize the genome and reduce replicative potential. Our model, however, proposes that decreasing the number and efficiency of rDNA origins increases genome stability and replicative lifespan though decreased competition for replication factors. While we propose that lifespan may also be regulated through rDNA replication, it does not necessarily preclude the effects of *SIR2* on longevity. The loss of *SIR2* deacetylase activity opens up rDNA chromatin to increased transcription [87] and doubles the number of rDNA origins utilized [123], which would reduce replicative lifespan as per our model.

Transcription at the rDNA locus promotes replication

The comparable activity of the RM and BY rARS genomic sequences was indeed puzzling. More perplexingly, most plasmid-genome disparities from identified ARS sequences are opposite to what we have found with the rDNA origin of replication: many origins sequences have activity on a plasmid, but are dormant in their endogenous sites. However, the unique biology of the rDNA region may account for this paradox. Firstly, rDNA replication initiation is associated with rRNA transcription. The rDNA locus is a heavily transcribed region of the genome [86] and two-thirds of all transcription is devoted to the generation of rRNA [85] for ribosome biogenesis required for cell growth. This constant transcription of rDNA repeats may be responsible for keeping this region in a nucleosome-poor open chromatin state [124], which could allow for increased replication factor accessibility. Previous studies have found that rDNA replication is primarily induced downstream of transcribed rRNA sequences [125]. Secondly, cells with shorter rDNA arrays have increased percentage of transcribed repeats [86] and increased rARS activity [109].

French *et al.* [86] demonstrated that a strain with 150 repeats will have transcription at 50% of rDNA array, while a strain with 42 repeats will transcribe all repeats, each with an increased polymerase load, suggesting that cells require a certain rate of rRNA synthesis regardless of rDNA size. Ide *et al*. [109] additionally found increased rDNA origin efficiency in strains with severely reduced rDNA repeat numbers.

We therefore propose that the RM rDNA with its reduced rDNA repeat number would have increased transcription, leading to increased rARS efficiency (Figure 3.11). Since our plasmid maintenance assay used plasmids without heavily transcribed rRNA sequences, the RM rARS sequences remain poorly utilized. We anticipate that a plasmid with a complete RM rDNA repeat would show more origin activity than just the limited rARS sequence due to rRNA transcription. If true, if we were then to disable plasmid transcription by removing the rRNA-transcribing PolI promoter, the RM rDNA plasmid would revert back to being a weakly maintained plasmid. We also predict that if we were to disable PolI transcription, expressing rRNA instead through a GAL-driven plasmid sequence, we would find a dramatic decrease in the RM rDNA origin activity.

This permission of origin activity by transcription solves the puzzle of how the chromosome-sized rDNA locus is able to replicate itself with the apparently crippled RM rARS sequence and may help to explain the smaller size of the RM rDNA array. The similarity between RM and BY rDNA origin activities suggests that there may be a preferred origin efficiency required to maintain rDNA. And expansion of the RM rDNA array to 150 repeats would be predicted to decrease the density of rRNA transcription, corresponding with

decrease in origin efficiency. This would lead to longer gaps between active rDNA origins and result in stretches of unreplicated DNA by the end of S-phase. Confronted with this situation, a cell would likely have to contract its rDNA locus in order to complete replication in a timely fashion or die. We predict that strains with BY rDNA would behave similarly if their rDNA array ever doubled in size.

Could calorie restriction mediate lifespan extension through rDNA origin efficiency?

The coupling of rRNA transcription to rDNA replication could provide the yet-elusive mechanism behind the lifespan extension mediated by calorie restriction, which also extends lifespan independent of *SIR2* and *FOB1* [94]. The promotion of longevity by calorie restriction is well documented in wide range of species [6] and suggests the involvement of a highly conserved mechanism. Since all organisms require ribosomes for protein synthesis, a region encoding ribosomal components is attractive as a universal regulator of lifespan. Abnormal nucleolar phenotypes have been reported in aging mammalian cells and reduction in rRNA production is seen with age [126,127], suggesting that the nucleolus/rDNA may be responding to age-related cues. Indeed, rDNA stability was initially hailed as potential explanation for the conservation of calorie restriction's influence on longevity, though the exact mechanism of lifespan regulation has remained unclear.

Use of calorie restriction mimetics, either through genetic and pharmaceutical manipulation of conserved pathways such as the TOR nutrient-signaling pathway, have illustrated the tight regulation of ribosome biogenesis by nutrient availability. Cellular growth requires a high level of protein synthesis and therefore transcription of rRNA and

ribosomal subunits must be coordinated to the demand for ribosomes. In situations when growth is reduced, such as with calorie restriction or TOR pathway inhibition, there is a dramatic downregulation of genes involved in ribosome biogenesis. rRNA transcription is particularly attuned to growth conditions and the number of repeats transcribed decreases when cells are shifted from rich complete media to nutrient-poor minimal media [112]. Coincidently, the rDNA locus has a dramatic increase in nucleosome occupancy when cells are shifted to a nutrient-deprivation situation [124], and the rDNA origin itself becomes populated by a nucleosome in low nutrient situations, presumably obstructing ORC binding and replication initiation. Supported by our finding that calorie restriction reduces rDNA origin activity by 60-80%, we propose that the decrease in rRNA transcription decreases rDNA origin efficiency and therefore regulates replicative lifespan in response to nutrient availability.

While we acknowledge that our findings are not congruent with those of previous *S. cerevisiae* rDNA studies, we note that differences exist which may help explain the discrepancies between our results. Previous studies of rDNA size found that strains with shortened rDNA arrays, rather than granting lifespan extension, exhibit either shortening of [128] or little change to replicative lifespan [129]. The shorter-lived strains have extremely reduced rDNA arrays, decreased down to approximately 20 repeats in size, which is much shorter than the 90 repeats in an RM rDNA array. No obvious growth defects were found between strains with long or short rDNA arrays. A strain with a mere 20 repeats must heavily transcribed each repeat to maintain production of rRNA. Combined with the dramatic increase in origin efficiency, collisions between replication and transcription machinery in

20-repeat strains may become unavoidable and detrimental to cells. The RM rDNA has a less dramatic but significant reduction in repeat number and retains similar rDNA origin efficiency to BY rDNA, suggesting that the difficulty of coordinating rDNA transcription and replication are not as extreme as with a 20 repeat rDNA array. While no difference in sensitivity to the DNA damaging agent MMS was found between strains with RM and BY rDNA (unpublished), cells with a 20 repeat rDNA array were much more sensitive to MMS exposure, suggesting the incredibly short rDNA may be more prone to or unable to repair replication lesions due to constant interference of rRNA transcription. The genetic instability generated at such a short rDNA array could result in the lost of replicative lifespan. The similarity of lifespans of strains with long (200 copies) and short (~135 copies) rDNA arrays seen by Michel *et al.* [129] may be due to size-dependent regulation of rDNA origin efficiency, resulting in the same number of origins firing regardless of rDNA size.

Also in direct contrast to our findings, a previous study by Ganley *et al.* [130] reported that a decrease in rDNA origin activity was correlated with loss of replicative potential. In this study, Ganley et al. reduced origin activity by replacing the non-essential rARS ACS3 sequence with the *URA3* marker (*rARSΔ-3*). While *rARSΔ-3* did show decreased origin efficiency by 2D gel electrophoresis, we noted two differences between the *rARSΔ-3* array and our RM rDNA allele. Firstly, the *rARSΔ-3* allele allowed the integration of a foreign open reading frame, *URA3*, into the NTS2 sequence. In addition to possibly disrupting rRNA transcription with a foreign ORF, the proximity to the *URA3* sequence was previously reported to alter timing of origin firing [131], shifting origin activity to earlier in replication. Since the rDNA locus is a late replicating sequence, this disruption of replication

timing may dramatically change the role of the rDNA locus. Second, in direct contrast to the RM rDNA array, which maintains its reduced copy number after 10 backcrosses (~500 generations), the size of the *rARSΔ-3* array achieved the wildtype size of 150 copies after 500 divisions. These discrepancies suggest that, even though they both exhibit loss of origin efficiency, the RM rARS and *rARSΔ-3* sequences may have other fundamentally different behaviors that could affect rDNA mediated lifespan.

Does replication become more problematic with age? Our studies focus on rDNA's mediation of genomic replication in young cells, but do not yet address replication in old yeast cells. Young cells are adept at responding to replication stress. However, as they age, it is possible that DNA damage responses decline and any replication stress may be exacerbated in old cells. There are hints in the literature that replication may become problematic for an old cell. Experiments by McMurray *et al.* showed that old mother cells had more loss-of-heterozygosity events than young cells, indicating the increase of genomic instability with age [132]. Kobayashi *et al.* also report that old mother cells exhibit more difficulty in replicating chromosome XII, almost certainly due to the rDNA locus [130]. Though needing further study, our preliminary study of old mother *S. cerevisiae* cells has found that older cells have decreased plasmid maintenance when compared with young cells (data not shown). Additionally, though not surprisingly, defects in genes involved in DNA replication lead to a decrease in lifespan [133]. The importance of DNA replication may become more important with age and, if so, faithful maintenance of DNA replication programs may prolong cellular longevity.

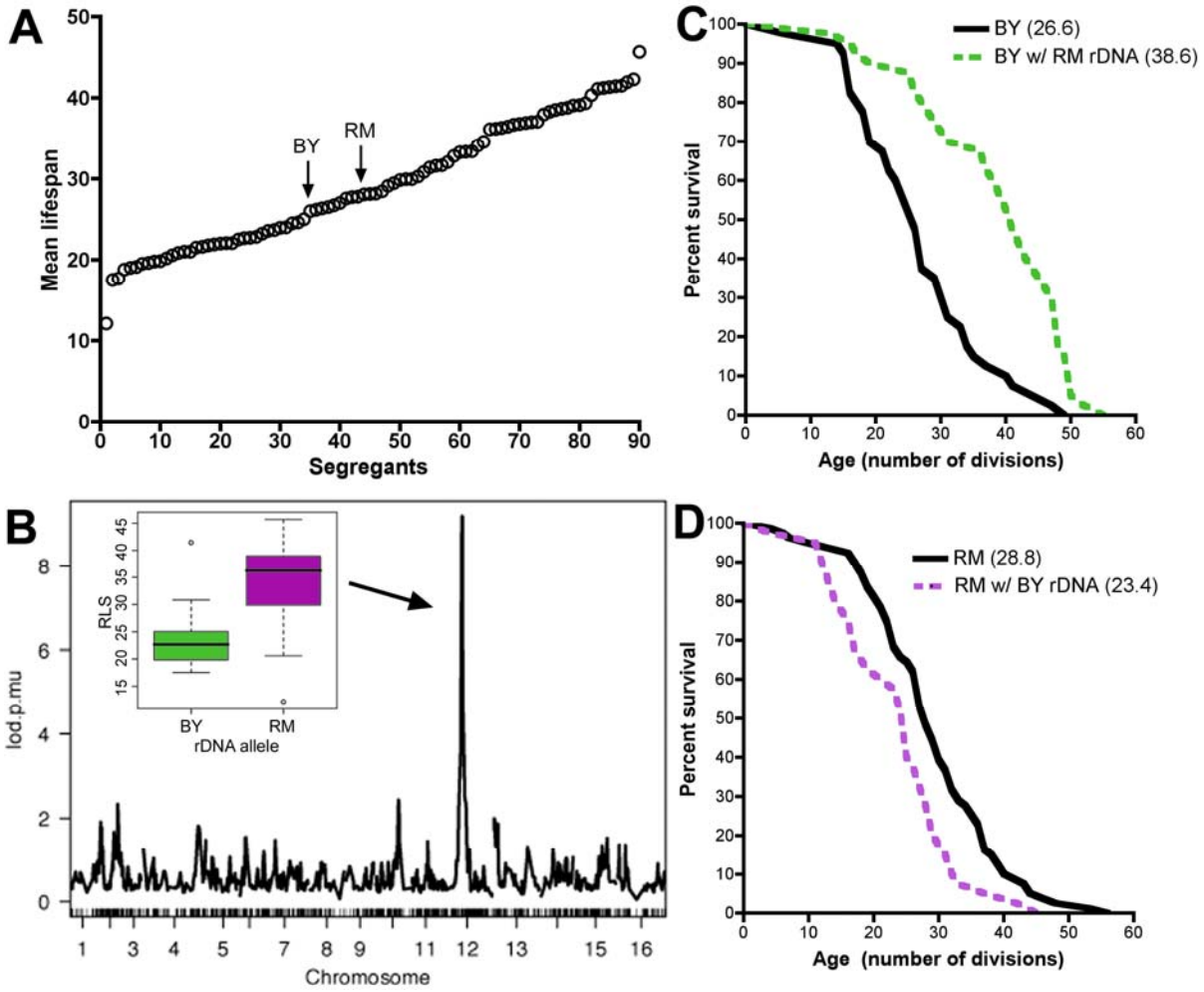

Figure 3.1. rDNA is the major regulator of replicative lifespan in the RM/BY cross.

142. Mean replicative lifespans (RLS) of 90 segregants and parental strains (indicated by arrows). (B) Genome-wide linkage analysis of RLS. rDNA linkage on chromosome XII is indicated by arrow. RLS distribution of strains inheriting the BY or RM rDNA allele (inset). Average RLS for strains with BY rDNA was 23.5±4.6 and average RLS for strains with RM rDNA was of 33.1±7.0 (P=9.5x10^{-12}, ν=88). (C) Replicative lifespan curves for the BY parent and the significantly longer-lived backcrossed BY strain with RM rDNA (P=1x10^{-3}, ν=2). (D) RLS curves for the RM parent and RM strain with BY rDNA (P=5.0x10^{-3}, ν=2). Mean RLS for backcross strains are indicated in parentheses (C,D).

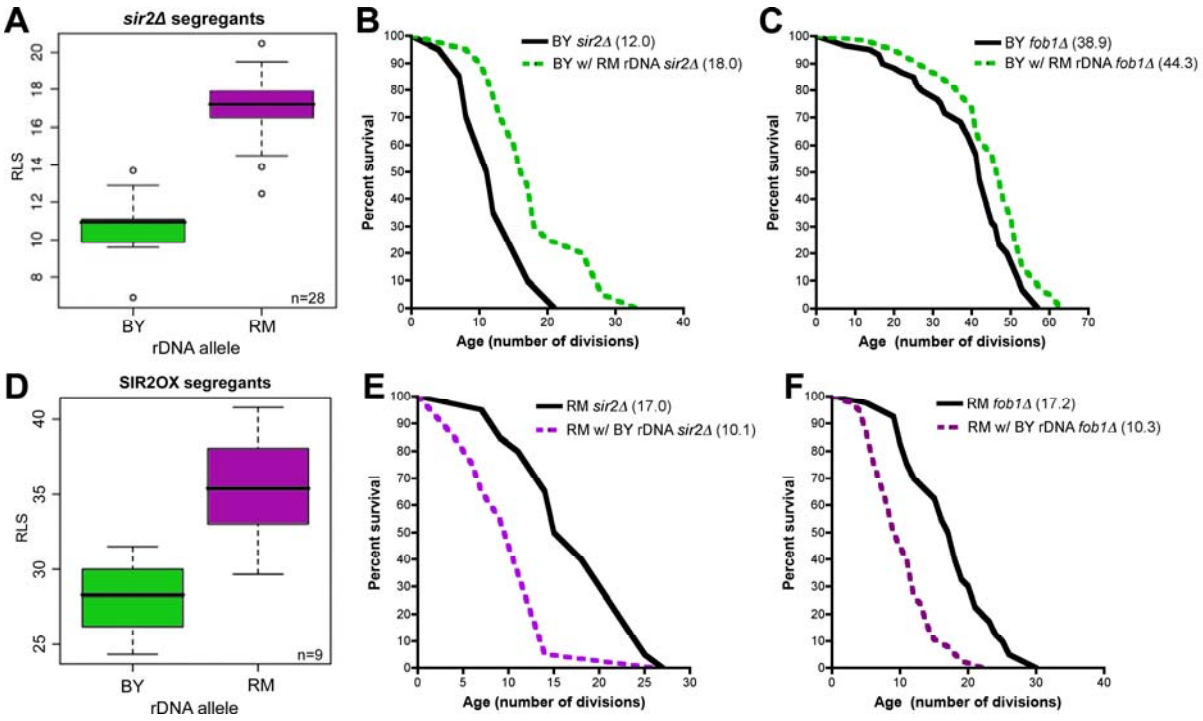

Figure 3.2. rDNA inheritance regulates lifespan independently of *SIR2* and *FOB1*.
Mean RLS distribution of (A) 28 segregants with SIR2 deleted or (D) 9 segregants overexpressing *SIR2*. Segregants with the RM rDNA allele remained longer-lived than those inheriting the BY allele even in the absence of *SIR2* (17.0±2.1 vs. 10.8±1.7, P=6.1x10^{-9}, ν=2) or with *SIR2* overexpression (35.4±3.4 vs. 28.1±3.0, P=2.0x10^{-2}, ν=2). Examination of the BY backcross strain found that RM rDNA still granted lifespan extension in both (B) *sir2Δ* and (C) *fob1Δ* backgrounds. (E) Even in the absence of *SIR2,* the RM parental strain lives longer than the RM strain with BY rDNA. (F) Deletion of *FOB1* decreased lifespan in the RM background, but the RM *fob1Δ* strain remained longer-lived than the RM *fob1Δ* strain with BY rDNA.

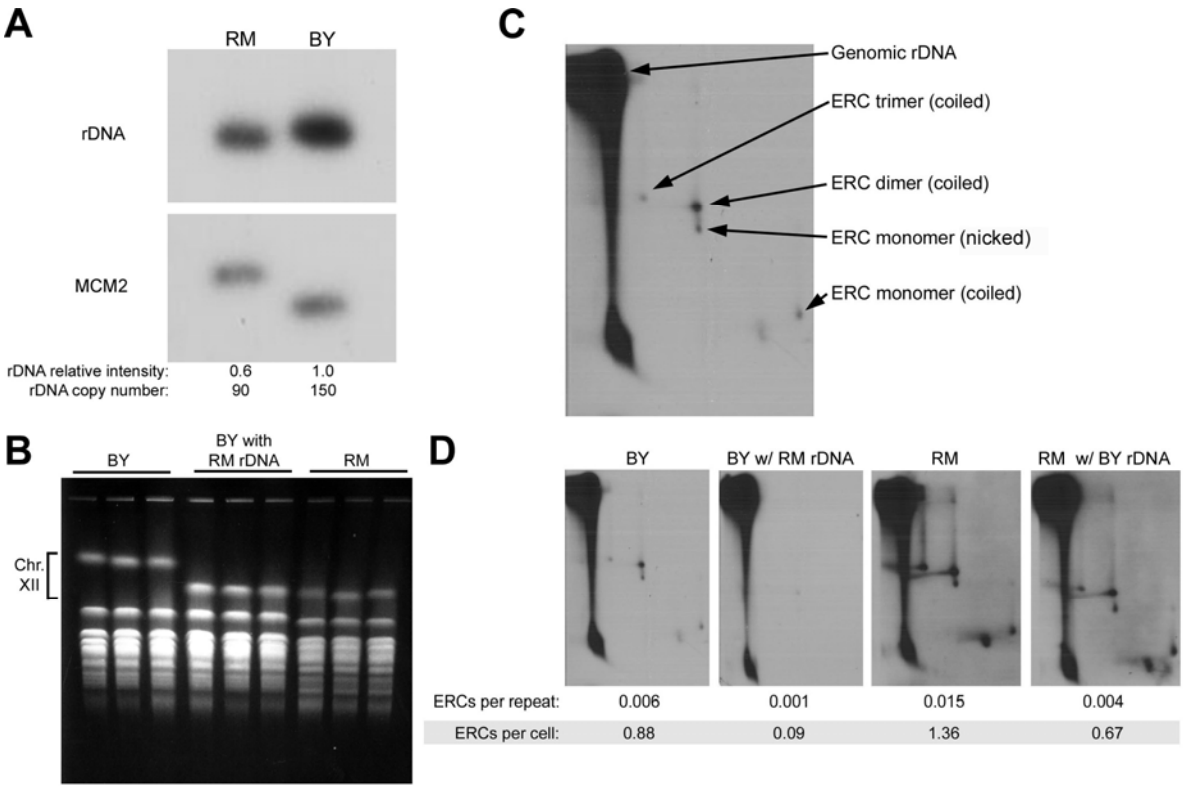

Figure 3.3. Examination of rDNA copy number and ERCs in the RM and BY strains.

142. Southern blot comparing intensity of the rDNA signal from the RM and BY parent strains. Single-copy *MCM2* was used to normalize amount of input. (B) CHEF gel electrophoresis analysis of chromosome XII size reveals that RM rDNA size is the same in the RM parent and BY backcross, indicating that the regulation of rDNA array size is determined in cis. (C) Diagram of rDNA and ERC positions on 2D-gel run from an undigested genomic DNA sample. (D) ERC quantification in RM and BY strains using 2D-gel electrophoresis.

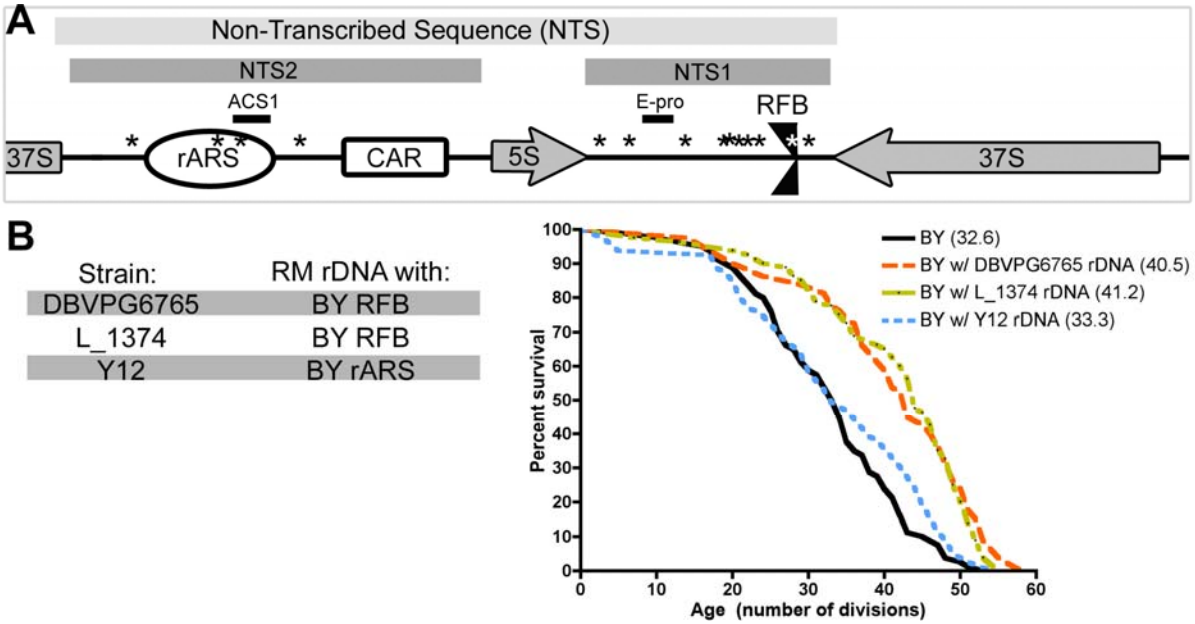

Figure 3.4. Polymorphism in the rDNA origin of replication mediates replicative lifespan. (A) Schematic of rDNA landmarks and identified polymorphisms, not drawn to scale. Location of differences between the RM and BY rDNA sequences are noted with asterisks (*). (B) Wild yeast isolates DBVPG6765, L_1374, and Y12 have RM rDNA sequences with the single BY RFB or BY rARS polymorphisms. When backcrossed into the BY background, rDNA alleles from DBVPG6765 and L_1374 confer significant lifespan extension (P=10^{-4}, ν=2) while the Y12 rDNA allele does not (P=$1.4x10^{-1}$, ν=2). Mean replicative lifespan is indicated in parentheses.

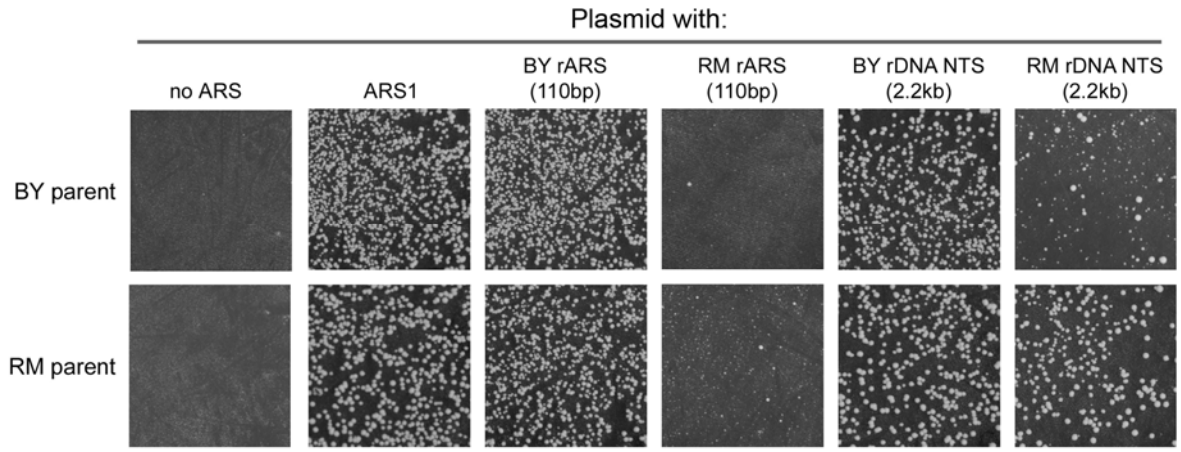

Figure 3.5. The RM rDNA origin (rARS) has a loss of function polymorphism.
Various replication origin sequences were cloned into a vector containing the KanMX6 gene. With a strong origin of replication such as ARS1, cells are able to replicate the KanMX6 plasmid and grow on media containing the antibiotic G418. Cells transformed with plasmids containing the 110bp BY rARS sequence and the 2.2kb NTS region from BY rDNA also grow on G418, indicating the robust activity of the BY rDNA origin. Plasmids containing the RM rARS and RM NTS sequences, however, conferred much lower G418 resistance, suggesting that they are poorly maintained due to poor replication. Interestingly, the RM parental strain was able to better replicate the plasmids containing RM rDNA origin sequences, suggesting the presence of a strain-specific mechanism that increases initiation of RM rDNA origins.

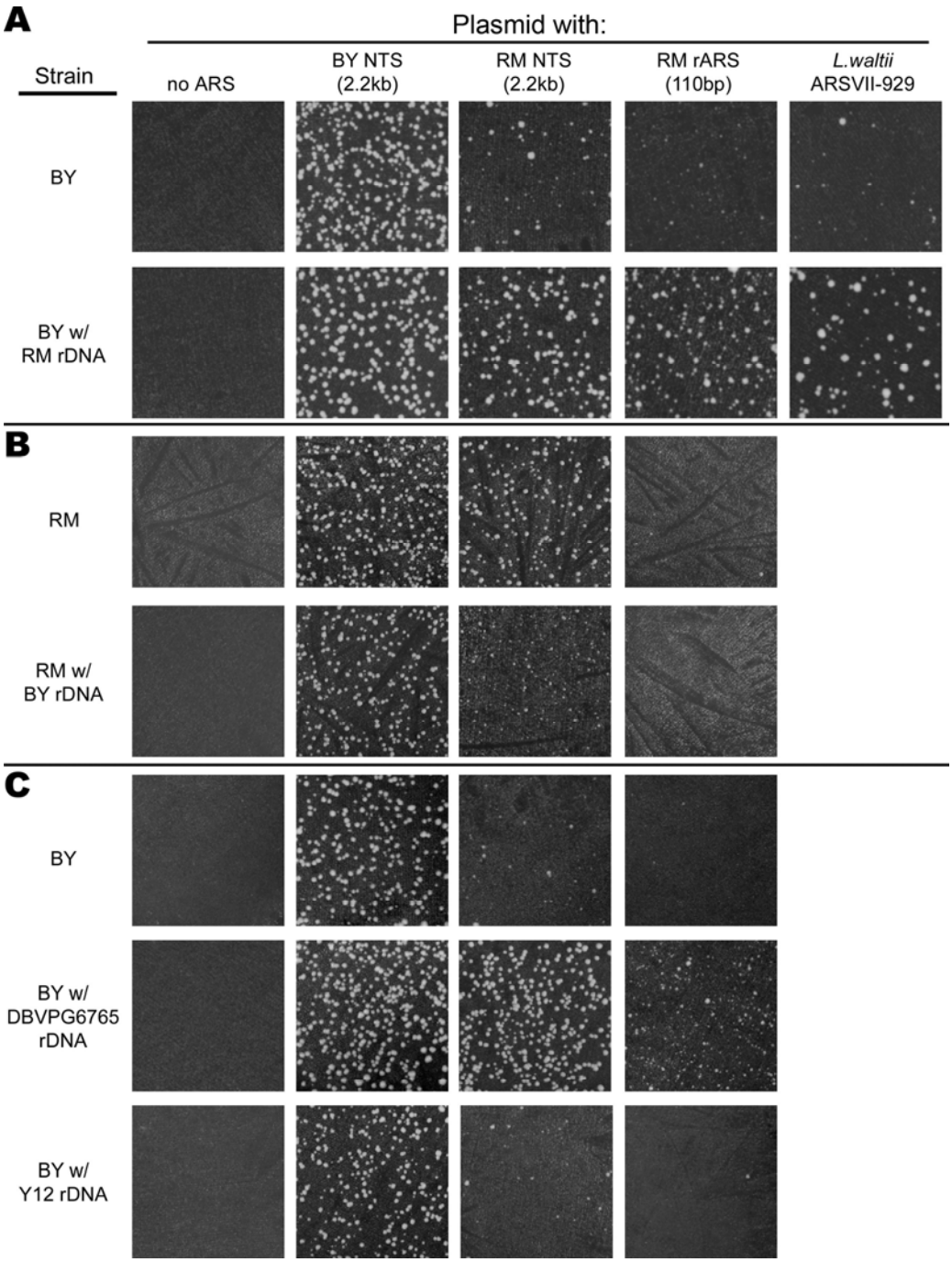

Figure 3.6. Strains with the RM rARS array can utilize weaker origins.

142. The BY strain with RM rDNA can better maintain plasmids using the weak origin sequences from the RM NTS, RM rARS, and *L. waltii* ARSVII-929. (B) When the BY rDNA allele is backcrossed into the RM strain, it loses capacity to utilize weak plasmid origins. (C) Strains with rDNA inherited from DBVPG6765 (RM rDNA w/ BY RFB) are able to maintain weak origin plasmids better than strains inheriting rDNA with BY rARS sequence (BY parent or Y12 rDNA).

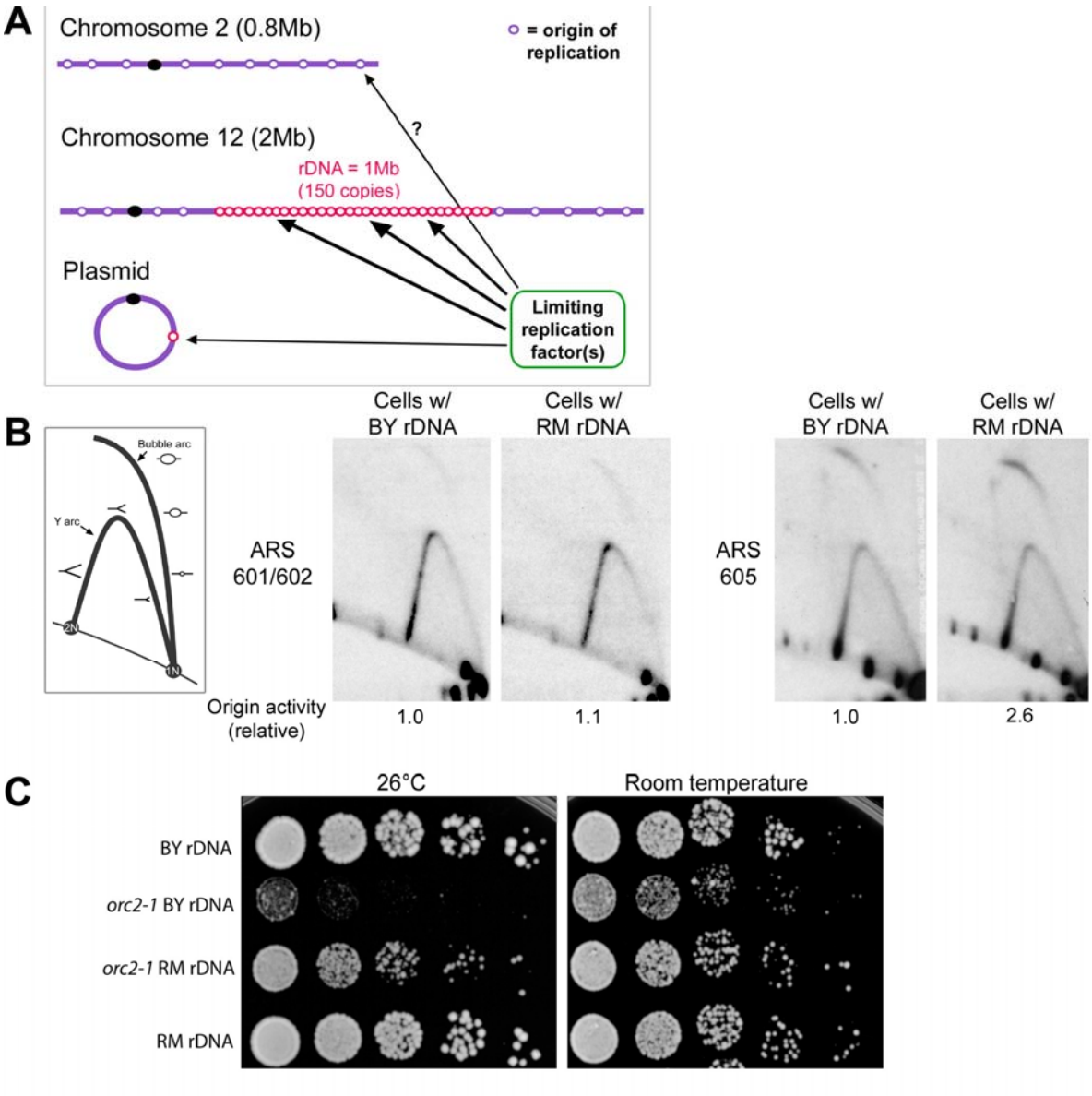

Figure 3.7. RM rDNA allele may promote genome replication through decreased competition for replication factors. (A) Proposed model in which the rDNA locus titrates putative limiting replication factors away from initiating plasmid and genomic origins of replication. (B) Analysis of activity at genomic origins ARS601/602 and ARS605 on chromosome VI. There was no difference in ARS601/602 activity between the two strains, but ARS605 activity was doubled in the BY strain with RM rDNA. (C) Partial rescue of *orc2-1* temperature sensitivity by RM rDNA.

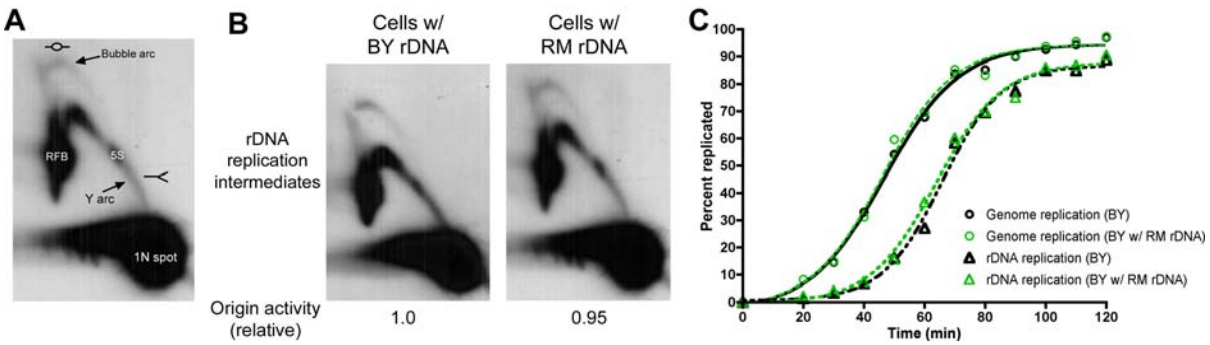

Figure 3.8. Replication of RM rDNA and BY rDNA is unexpectedly similar.

142. Diagram of rDNA replication intermediates seen by 2D gel electrophoresis. Stalling of replication forks at the RFB and 5S rRNA transcript can be seen as spots of increased intensity on the Y arc. (B) No difference was found between origin activity in the BY rDNA versus the RM rDNA, which had a surprisingly strong bubble arc. (C) Replication kinetics of strains with BY rDNA (black) or RM rDNA (green). rDNA synthesis occurs late in S-phase, but the rates of both total genomic replication (circles) and rDNA replication (triangles) are identical between the BY parental strain and the BY strain with RM rDNA.

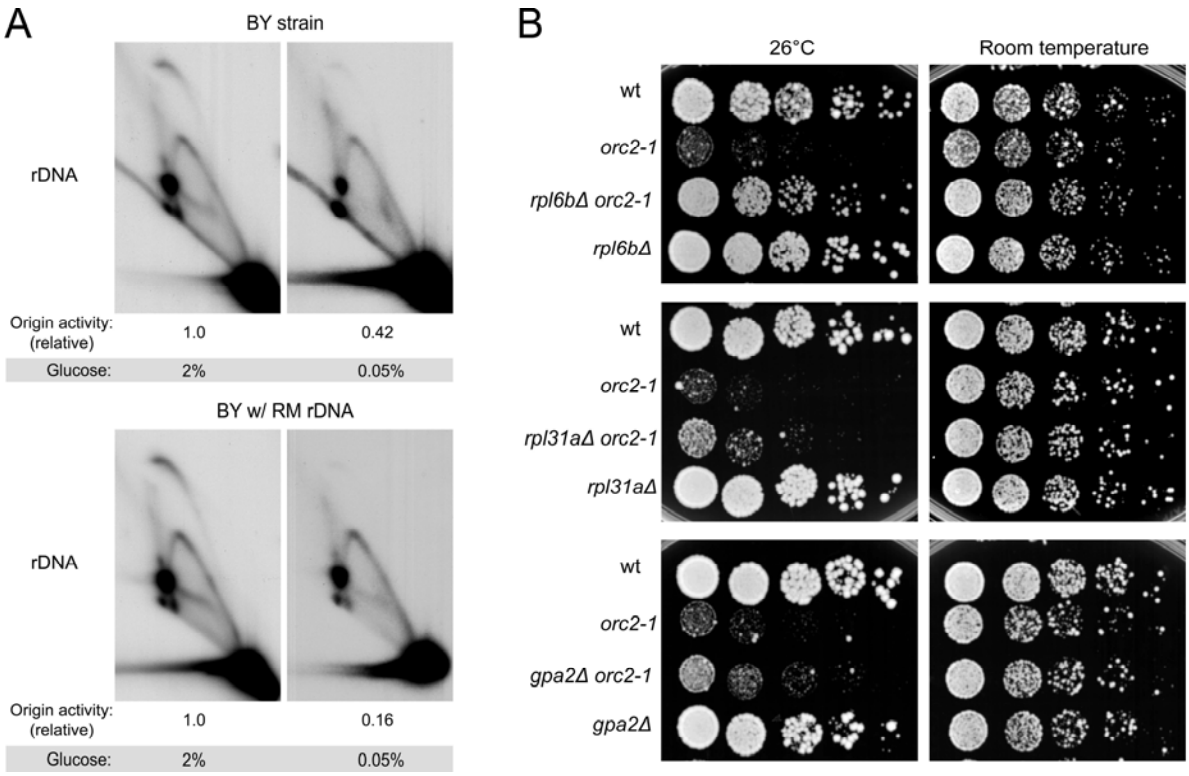

Figure 3.9. Calorie restriction (CR) reduces rDNA origin activity and CR mimetic mutants can partially rescue *orc2-1*. (A) 2D gel analysis of rDNA replication intermediates reveals that both BY and RM rDNA have dramatic reductions to origin activity in response to calorie restriction (0.05% glucose). Additionally, in 0.05% glucose, RM rDNA has much less origin activity than the BY rDNA, reflective of origin plasmid transformation assays. (B) Similar to strains with RM rDNA, strains that are *rpl6bΔ, rpl31aΔ,* or *gpa2Δ* can partially rescue *orc2-1* temperature sensitivity.

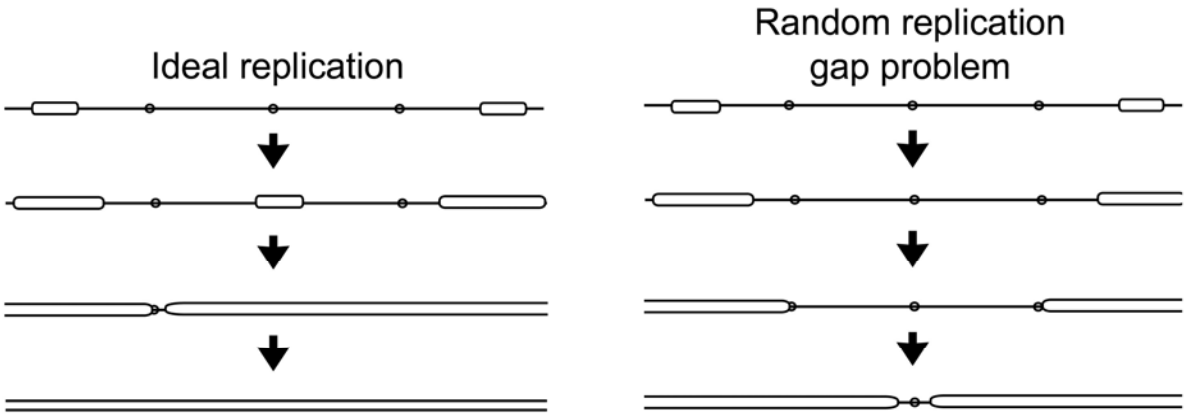

Figure 3.10. The random replication gap problem. (Left) Genome replication is initiated at early firing origins of replication during early S-phase. If a stretch of unreplicated DNA persists later in S-phase, replication can initiate at a later firing origin to ensure timely completion of replication. Due to the stochastic nature of origins, however, there is only a probability of initiation at a late firing origin of replication. The resultant stretch of unreplicated DNA remaining at the end of S-phase is detrimental to cell fitness and is known as the "random replication gap" problem (right).

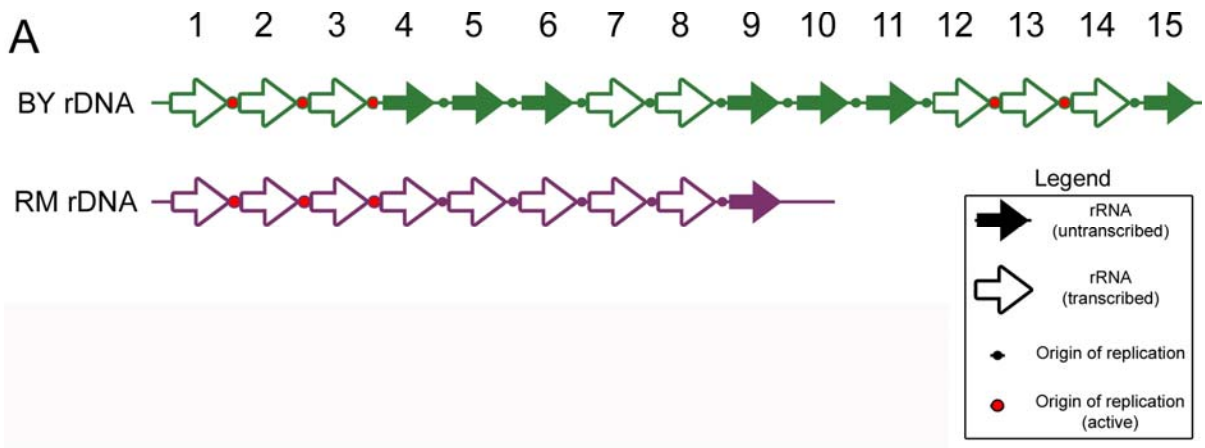

B

	BY rDNA	RM rDNA
Actively transcribed copies:	8/15 = 53%	8/9 = 89%
Transcribed copies with active origins:	5/8 = 63%	3/8 = 38%
Active origins per total rDNA copy:	5/15 = 33%	3/9 = 33%

Figure 3.11. Hypothetical model of how the similar origin efficiency between BY and RM rDNA may be achieved through transcription's influence on origin firing. (A) BY rDNA's 150 copies is represented by 15 arrows, RM rDNA's 90 copies is represented by 9 arrows. The amount of rRNA transcription remains static regardless of the number of rDNA copies, indicated here by open arrows. Active rDNA origins of replication are found downstream from actively transcribed repeats. (B) Since BY rDNA origin activity is estimated at 30%, this would mean that 5 of the 15 copies would have active origins, found with the 8 actively transcribed BY rDNA repeats. Fewer active RM rDNA origins would be found in the 8 actively transcribed RM rDNA repeats, but 3 active origins in 9 RM rDNA copies would maintain the same origin efficiency as the BY rDNA. The difference between RM and BY rDNA origin activity is therefore lost in the "active origins" to "total rDNA copies" ratio, but can be seen in the ratio between the "active origins" to the "transcribed repeats."

Table 3.1: List of *S. cerevisiae* strains used in Chapter 3.

Lab Number	Background	MAT	Genotype	Figures
in plate	RmxBY		Segregant library (amn1::NAT)	3-1A
15212	RM11-1a	a	*leu2d0 ura3d0 HO::KanMX amn1::NAT*	3-1D, 3-3A-D, 3-5, 3-6B
15213	BY4716	α	*lys2d0 amn1::NAT*	
15691	BY4715	a	*lys2d0 amn1::NAT*	3-1C, 3-3A, 3-3D, 3-5, 3-6A, 3-7B, 3-8B
15695	BY4715	a	*lys2d0 amn1::NAT*; RM rDNA	3-1C, 3-3A, 3-3D, 3-5, 3-6A, 3-7B, 3-8B
15859	RM11-1a	a	*leu2d0 ura3d0 HO::KanMX amn1::NAT*; BY rDNA	3-1D, 3-3A-D, 3-6B
in plate	RmxBY		Segregant library (*amn1::NAT*) *sir2::HYG*	3-2A
in plate	RmxBY		Segregant library (*amn1::NAT*) (with integrated BglII-digested pRS305-*SIR2*)	3-2B
in plate	RM11-1a	a	*leu2d0 ura3d0 HO::KanMX amn1::NAT sir2::HYG*	3-2C
in plate	BY4715	a	*lys2d0 amn1::NAT sir2::HYG*	3-2B
in plate	RM11-1a	a	*leu2d0 ura3d0 HO::KanMX amn1::NAT sir2::HYG*; BY rDNA	3-2C
in plate	BY4715	a	*lys2d0 amn1::NAT sir2::HYG*; RM rDNA	3-2B
in plate	RM11-1a	a	*leu2d0 ura3d0 HO::KanMX amn1::NAT fob1::HYG*	3-2F
in plate	BY4715	a	*lys2d0 amn1::NAT fob1::KanMX*	3-2E
in plate	RM11-1a	a	*leu2d0 ura3d0 HO::KanMX amn1::NAT fob1:HYG*; BY rDNA	3-2F
in plate	BY4715	a	*lys2d0 amn1::NAT fob1::KanMX*; RM rDNA	3-2E
15728	BY	a		3-3B, 3-4B, 3-6C, 3-8C
16075	BY	a	RM rDNA	3-3B, 3-8C
in plate	BY	a	DBVPG6765 rDNA	3-4B, 3-6C
in plate	BY	a	L_1374 rDNA	3-4B, 3-6C
in plate	BY	a	Y12 rDNA	3-4B, 3-6C
JRY7459	BY4741	α	*his3 leu2 lys2 ura3 can1 mfa1::MFA1-pr-HIS3 orc2-1::NAT* (has another NAT allele segregating)	
16099	BY4741		*leu2 lys2 his3 (ura3?)*	3-7C
16102	BY4741		*leu2 lys2 his3 (ura3?) orc2-1::NAT*	3-7C
16100	BY4741		*leu2 lys2 his3 (ura3?) orc2-1::NAT*; RM rDNA (marked w/ HYG)	3-7C
16101	BY4741		*leu2 lys2 his3 (ura3?);* RM rDNA (marked w/ HYG)	3-7C
in plate	BY4742	a	*leu2d0 ura3d0 met15d0 his3d0 rpl6b::KanMX*	3-9B
in plate	BY4742	a	*leu2d0 ura3d0 met15d0 his3d0 rpl31a::KanMX*	3-9B
in plate	BY4742	a	*leu2d0 ura3d0 met15d0 his3d0 gpa2::KanMX*	3-9B

Table 3.2. Genomic loci linked to replicative lifespan.

Chromosome	Region	RLS RM	RLS BY	LOD Score
2	YBR218-YBR231C	32.0	26.9	2.3
4	YDR475C-YDR481C	31.4	27.1	2.1
10	YJR066W-YJR080C	27.3	32.0	2.4
12	YLR139C-YLR182W	33.0	23.4	9.0
13	YML121W-YML101C	26.7	31.8	2.3

MATERIALS AND METHODS

Yeast strains and media

Experiments were carried out using standard YPD media (2% glucose, 1% yeast extract, 2% peptone) unless otherwise noted (ie. Density transfer, calorie restriction.) The segregant library has been previously described [28], except that *AMN1* has been deleted in each of the segregants to facilitate single cell viability analysis. (The RM allele of *AMN1* confers clumpiness which precludes single cell analysis whereas the S288c allele of *AMN1* was previously shown to create a loss of *AMN1* function [67]). The Saccharomyces Genome Resequencing Project (SGRP) strains were provided by the National Collection of Yeast Cultures (NCYC) [104,134]. The S288c *orc2-1* mutant strain was generously provided by the Rine lab. Gene deletion mutants were either from yeast ORF deletion collection or were created using standard PCR transformation methods.

Replicative lifespan analysis

Replicative lifespan studies were conducted as previously described by Kaeberlein *et al.* [18]. All lifespan studies were conducted on YPD plates (2% glucose) and 40 individual cells (virgin mothers) were analyzed for each strain, except for the segregant strain studies in which 20 cells were analyzed. Statistical significance between strain lifespans was determined using Mantel-Haenszel logrank test (the PRIZM program's survival curve comparison function).

QTL mapping

Genome-wide linkage analysis of segregant data was performed using the publicly available R/qtl software. Effects of RM/BY rDNA allele inheritance were examined using R (box plots) and Excel (student's t-test).

Analysis of rDNA size by quantitative Southern blot and CHEF gel

For quantification by Southern blot, genomic rDNA was harvested from saturated 3mL cultures. Sample DNA was then digested overnight with BglII, resolved by gel electrophoresis (0.5X TBE, 0.9% agarose gel, run for 360•Vhr), and transferred to Hybond-N membrane. Abundance of single-copy MCM2 was visualized using ^{32}P-labeled probes amplified from the MCM2 sequence; rDNA was similarly visualized using ^{32}P-labeled probes amplified from the BY rDNA NTS sequence. Relative rDNA copy number was determined by normalizing rDNA band intensity to the intensity of single-copy MCM2 [135].

DNA sample preparation for CHEF (clamped homogeneous electric field) gel electrophoresis (also known as "pulse field gel electrophoresis") has been previously described. For each strain, genomic DNA from saturated cultures from 3 individual colonies was harvested in 1% agarose plugs, each plug containing approximately 10^8 cells. Chromosome XII size was resolved by CHEF electrophoresis as previously described by Ganley *et al.* [130]: 300–900 s pulse time and 100V for 68 hours at 14°C in a 1% agarose gel in 0.5X TBE. Chromosomes were visualized by ethidium bromide staining.

2D gel electrophoresis

For ERC and rDNA replication intermediate analysis, DNA from logarithmically growing cultures was harvested in 0.5% agarose plugs. The agarose-embedded DNA was either digested with NheI (for rDNA replication intermediates) or run undigested (for ERC analysis). DNA for genomic origin (ARS605) analysis was harvested from logarithmically-growing cultures, grown in synthetic complete media, using Huberman preparation[136,137]. Genomic origin samples were then digested with HincII and NcoI.

Two dimensional (2D) gel electrophoresis was performed as described previously [138]. Samples were resolved in the first dimension using 0.5% agarose at 1V/cm for approximately 20-22 hours; second dimension was run at 7V/cm for 4-6 hours using 1% agarose and 0.3ug/mL ethidium bromide. The 2D gel was then transferred to Hybond-N member and probed using ^{32}P-labeled probes amplified from either the RM NTS2 or ARS605 sequence.

rDNA sequence analysis

The BY rDNA sequence was obtained from the Saccharomyces Genome Database[139] and the RM11-1a rDNA sequence was obtained from the Broad Institute Saccharomyces cerevisiae RM11-1a Database [140]. To examine wild yeast rDNA, BLAST searches using rDNA sequences were performed using the SGRP database. rDNA sequence comparison was performed with DNA Strider. To verify polymorphisms found in RM and BY rDNA, the 2.2kb NTS sequence (NTS1/5S/NTS2) was amplified from genomic DNA, cloned into pRS416, and sequenced from the plasmid. In order to assess the potential heterogeneity within an rDNA array, genomic DNA from parental strains was further

analyzed using Illumina sequencing and read abundance from each sequence was used to estimate rDNA repeat variation.

Plasmid maintenance assay

S. cerevisiae origin sequences were amplified from genomic DNA and cloned into the ARS-free pU18-KanMX-LwCEN vector previously used by Di Rienzi *et al.* [141]. 50ng of each plasmid was transformed into 10^8 cells of logarithmically growing culture. Transformation cultures were allowed to recover 24 hours on YPD plates before being replica-plated onto selective YPD+G418 media. Colony formation was visualized after 48 hours at 30°C, 72 hours for plasmids with RM rARS or *L. waltii* ARSVII-929.

Density transfer

Density transfer experiments were performed as previously described by the protocol by Raghuraman *et al.* [142]. Cells were grown at 26°C to permit finer resolution of replication. 30 minutes prior to release from α-factor, G1-arrested cells were transferred from dense isotope media (minimal media with 0.01% 15N ammonium sulfate, 0.1% 13C glucose) to isotopically light synthetic complete media with α-factor. A-factor release was induced by addition of pronase to culture. Genomic DNA was harvested at the indicated time points, digested with EcoRI, separated by density using ultracentrifugation in a CsCl gradient, and drip-fractionated to preserve the density gradient. Samples were then slot-blotted and probed, first with ^{32}P-labeled ρ^0 genomic DNA (low rDNA) and then with ^{32}P-labeled rDNA. Abundance of dense replicated (HL) and lighter unreplicated (HL) DNA was determined by plotting slot blot intensity and quantified using ImageJ.

ACKNOWLEDGMENTS

I have had the great fortune to have collaborations with the Kennedy lab and the Brewer/Raghuraman lab during my thesis work. The Kennedy lab, especially Dr. Brian Kennedy, Scott Tsuchiyama, and Soumya K., ran all of the replicative lifespan analyses and Chapter 3 would not have been possible without them. Gina Alvino, Dr. Bonny Brewer, and Raghu from the Brewer/Raghuraman lab taught me how to perform 2D gel electrophoresis, CHEF gel electrophoresis, and density transfer experiments. A big thank you to Dr. Brewer for running the calorie restriction 2D gel experiment in Figure 3.9 and to Dr. Sara di Rienzi for the pUC18-KanMX-LwCEN vector. Thank you to Dr. Leonid Kruglyak for providing us with the segregant library and Dr. Jasper Rine for the *orc2-1* strain. Thank you to my graduate committee members (Sue Biggins, Bonny Brewer, Brian Kennedy, and Katie Peichel) for being a great source of support, feedback throughout my graduate career. A big thank you to Dr. Bonny Brewer and Dr. Katie Peichel for reading and critiquing my dissertation.

The Bedalov lab and the Simon lab were full of wonderful people to work with over the last 6 years. I am grate for the help from Dr. Eric Foss with the lifespan heritability calculations, Tonibelle Gatbonton for teaching me yeast techniques, Benjamin Newcomb for his western blot expertise, Gemma Park and Uyen Lao for their occasional help with experiments, and Jessica Kim for help with telomere length analysis. Thank you to Dr. Julian Simon, Vid Leko, Sumit Mahajan, Eli Ocheltree, Sarwat Chowdhury, Aaron Schuler, and Sean Kelly for their support and advice. And thank you to Dr. Toni Bedalov for the fantastic high-throughput graduate research experience.

I am also grateful to my friends, family, and my husband for their continuous support, both near and far, in my pursuit of new scientific frontiers.

REFERENCES

1. McCay CM, Crowell MF, Maynard LA (1935) The effect of retarded growth upon the length of life span and upon the ultimate body size. 1935. Nutrition 5: 155-171; discussion 172.
2. Klass MR (1977) Aging in the nematode Caenorhabditis elegans: major biological and environmental factors influencing life span. Mech Ageing Dev 6: 413-429.
3. Mair W, Sgro CM, Johnson AP, Chapman T, Partridge L (2004) Lifespan extension by dietary restriction in female Drosophila melanogaster is not caused by a reduction in vitellogenesis or ovarian activity. Exp Gerontol 39: 1011-1019.
4. Lin SJ, Defossez PA, Guarente L (2000) Requirement of NAD and SIR2 for life-span extension by calorie restriction in Saccharomyces cerevisiae. Science 289: 2126-2128.
5. Colman RJ, Anderson RM (2011) Nonhuman primate calorie restriction. Antioxid Redox Signal 14: 229-239.
6. Guarente L, Kenyon C (2000) Genetic pathways that regulate ageing in model organisms. Nature 408: 255-262.
7. Holzenberger M, Dupont J, Ducos B, Leneuve P, Geloen A, et al. (2003) IGF-1 receptor regulates lifespan and resistance to oxidative stress in mice. Nature 421: 182-187.
8. Tatar M, Kopelman A, Epstein D, Tu MP, Yin CM, et al. (2001) A mutant Drosophila insulin receptor homolog that extends life-span and impairs neuroendocrine function. [see comments]. Science 292: 107-110.
9. Kenyon C, Chang J, Gensch E, Rudner A, Tabtiang R (1993) A C. elegans mutant that lives twice as long as wild type. Nature 366: 461-464.
10. Miller RA, Harper JM, Galecki A, Burke DT (2002) Big mice die young: early life body weight predicts longevity in genetically heterogeneous mice. Aging Cell 1: 22-29.
11. Harrison DE, Strong R, Sharp ZD, Nelson JF, Astle CM, et al. (2009) Rapamycin fed late in life extends lifespan in genetically heterogeneous mice. Nature 460: 392-395.
12. Watson JD (1972) Origin of concatemeric T7 DNA. Nat New Biol 239: 197-201.
13. Olovnikov AM (1973) A theory of marginotomy. The incomplete copying of template margin in enzymic synthesis of polynucleotides and biological significance of the phenomenon. J Theor Biol 41: 181-190.
14. Cervantes RB, Lundblad V (2002) Mechanisms of chromosome-end protection. Curr Opin Cell Biol 14: 351-356.
15. Cawthon RM, Smith KR, O'Brien E, Sivatchenko A, Kerber RA (2003) Association between telomere length in blood and mortality in people aged 60 years or older. Lancet 361: 393-395.
16. Fabrizio P, Longo VD (2003) The chronological life span of Saccharomyces cerevisiae. Aging Cell 2: 73-81.
17. Kaeberlein M, Kennedy BK (2005) Large-scale identification in yeast of conserved ageing genes. Mech Ageing Dev 126: 17-21.
18. Kaeberlein M, Powers RW, 3rd, Steffen KK, Westman EA, Hu D, et al. (2005) Regulation of yeast replicative life span by TOR and Sch9 in response to nutrients. Science 310: 1193-1196.

19. Powers RW, 3rd, Kaeberlein M, Caldwell SD, Kennedy BK, Fields S (2006) Extension of chronological life span in yeast by decreased TOR pathway signaling. Genes Dev 20: 174-184.
20. Fabrizio P, Hoon S, Shamalnasab M, Galbani A, Wei M, et al. (2010) Genome-wide screen in Saccharomyces cerevisiae identifies vacuolar protein sorting, autophagy, biosynthetic, and tRNA methylation genes involved in life span regulation. PLoS Genet 6: e1001024.
21. Lundblad V, Szostak JW (1989) A mutant with a defect in telomere elongation leads to senescence in yeast. Cell 57: 633-643.
22. Askree SH, Yehuda T, Smolikov S, Gurevich R, Hawk J, et al. (2004) A genome-wide screen for Saccharomyces cerevisiae deletion mutants that affect telomere length. Proc Natl Acad Sci U S A 101: 8658-8663.
23. Gatbonton T, Imbesi M, Nelson M, Akey JM, Ruderfer DM, et al. (2006) Telomere length as a quantitative trait: genome-wide survey and genetic mapping of telomere length-control genes in yeast. PLoS Genet 2: e35.
24. Ungar L, Yosef N, Sela Y, Sharan R, Ruppin E, et al. (2009) A genome-wide screen for essential yeast genes that affect telomere length maintenance. Nucleic Acids Res 37: 3840-3849.
25. Martin GM, Oshima J (2000) Lessons from human progeroid syndromes. Nature 408: 263-266.
26. Yu CE, Oshima J, Fu YH, Wijsman EM, Hisama F, et al. (1996) Positional cloning of the Werner's syndrome gene. Science 272: 258-262.
27. Hjelmborg Jv, Iachine I, Skytthe A, Vaupel JW, McGue M, et al. (2006) Genetic influence on human lifespan and longevity. Hum Genet 119: 312-321.
28. Brem RB, Yvert G, Clinton R, Kruglyak L (2002) Genetic dissection of transcriptional regulation in budding yeast. Science 296: 752-755.
29. Kwan EX, Foss E, Kruglyak L, Bedalov A (2011) Natural polymorphism in BUL2 links cellular amino acid availability with chronological aging and telomere maintenance in yeast. PLoS Genet 7: e1002250.
30. Kapahi P, Chen D, Rogers AN, Katewa SD, Li PW, et al. (2010) With TOR, less is more: a key role for the conserved nutrient-sensing TOR pathway in aging. Cell Metab 11: 453-465.
31. Barbieri M, Bonafe M, Franceschi C, Paolisso G (2003) Insulin/IGF-I-signaling pathway: an evolutionarily conserved mechanism of longevity from yeast to humans. Am J Physiol Endocrinol Metab 285: E1064-1071.
32. Fabrizio P, Longo VD (2007) The chronological life span of Saccharomyces cerevisiae. Methods Mol Biol 371: 89-95.
33. Bodnar AG, Ouellette M, Frolkis M, Holt SE, Chiu CP, et al. (1998) Extension of life-span by introduction of telomerase into normal human cells. Science 279: 349-352.
34. Epel ES, Blackburn EH, Lin J, Dhabhar FS, Adler NE, et al. (2004) Accelerated telomere shortening in response to life stress. Proc Natl Acad Sci U S A 101: 17312-17315.
35. Bakaysa SL, Mucci LA, Slagboom PE, Boomsma DI, McClearn GE, et al. (2007) Telomere length predicts survival independent of genetic influences. Aging Cell 6: 769-774.
36. Burtner CR, Murakami CJ, Kennedy BK, Kaeberlein M (2009) A molecular mechanism of chronological aging in yeast. Cell Cycle 8: 1256-1270.

37. Helliwell SB, Losko S, Kaiser CA (2001) Components of a ubiquitin ligase complex specify polyubiquitination and intracellular trafficking of the general amino acid permease. J Cell Biol 153: 649-662.
38. Soetens O, De Craene JO, Andre B (2001) Ubiquitin is required for sorting to the vacuole of the yeast general amino acid permease, Gap1. J Biol Chem 276: 43949-43957.
39. Andreasson C, Neve EP, Ljungdahl PO (2004) Four permeases import proline and the toxic proline analogue azetidine-2-carboxylate into yeast. Yeast 21: 193-199.
40. Durbin R, Louis E Saccharomyces Genome Resequencing Project.
41. Foss EJ, Radulovic D, Shaffer SA, Ruderfer DM, Bedalov A, et al. (2007) Genetic basis of proteome variation in yeast. Nat Genet 39: 1369-1375.
42. De Virgilio C, Loewith R (2006) The TOR signalling network from yeast to man. Int J Biochem Cell Biol 38: 1476-1481.
43. Binda M, Peli-Gulli MP, Bonfils G, Panchaud N, Urban J, et al. (2009) The Vam6 GEF controls TORC1 by activating the EGO complex. Mol Cell 35: 563-573.
44. Wei M, Fabrizio P, Hu J, Ge H, Cheng C, et al. (2008) Life span extension by calorie restriction depends on Rim15 and transcription factors downstream of Ras/PKA, Tor, and Sch9. PLoS Genet 4: e13.
45. Cox KH, Rai R, Distler M, Daugherty JR, Coffman JA, et al. (2000) Saccharomyces cerevisiae GATA sequences function as TATA elements during nitrogen catabolite repression and when Gln3p is excluded from the nucleus by overproduction of Ure2p. J Biol Chem 275: 17611-17618.
46. Zaman S, Lippman SI, Zhao X, Broach JR (2008) How Saccharomyces responds to nutrients. Annu Rev Genet 42: 27-81.
47. Bertram PG, Choi JH, Carvalho J, Ai W, Zeng C, et al. (2000) Tripartite regulation of Gln3p by TOR, Ure2p, and phosphatases. J Biol Chem 275: 35727-35733.
48. Scherens B, Feller A, Vierendeels F, Messenguy F, Dubois E (2006) Identification of direct and indirect targets of the Gln3 and Gat1 activators by transcriptional profiling in response to nitrogen availability in the short and long term. FEMS Yeast Res 6: 777-791.
49. Crespo JL, Helliwell SB, Wiederkehr C, Demougin P, Fowler B, et al. (2004) NPR1 kinase and RSP5-BUL1/2 ubiquitin ligase control GLN3-dependent transcription in Saccharomyces cerevisiae. J Biol Chem 279: 37512-37517.
50. Yao R, Zhang Z, An X, Bucci B, Perlstein DL, et al. (2003) Subcellular localization of yeast ribonucleotide reductase regulated by the DNA replication and damage checkpoint pathways. Proc Natl Acad Sci U S A 100: 6628-6633.
51. Lee YD, Wang J, Stubbe J, Elledge SJ (2008) Dif1 is a DNA-damage-regulated facilitator of nuclear import for ribonucleotide reductase. Mol Cell 32: 70-80.
52. Lee YD, Elledge SJ (2006) Control of ribonucleotide reductase localization through an anchoring mechanism involving Wtm1. Genes Dev 20: 334-344.
53. Chabes A, Domkin V, Thelander L (1999) Yeast Sml1, a protein inhibitor of ribonucleotide reductase. J Biol Chem 274: 36679-36683.
54. Zhang H, Stallock JP, Ng JC, Reinhard C, Neufeld TP (2000) Regulation of cellular growth by the Drosophila target of rapamycin dTOR. Genes Dev 14: 2712-2724.
55. Meissner B, Boll M, Daniel H, Baumeister R (2004) Deletion of the intestinal peptide transporter affects insulin and TOR signaling in Caenorhabditis elegans. J Biol Chem 279: 36739-36745.

56. Grandison RC, Piper MD, Partridge L (2009) Amino-acid imbalance explains extension of lifespan by dietary restriction in Drosophila. Nature 462: 1061-1064.
57. Orentreich N, Matias JR, DeFelice A, Zimmerman JA (1993) Low methionine ingestion by rats extends life span. J Nutr 123: 269-274.
58. Zimmerman JA, Malloy V, Krajcik R, Orentreich N (2003) Nutritional control of aging. Exp Gerontol 38: 47-52.
59. Miller RA, Buehner G, Chang Y, Harper JM, Sigler R, et al. (2005) Methionine-deficient diet extends mouse lifespan, slows immune and lens aging, alters glucose, T4, IGF-I and insulin levels, and increases hepatocyte MIF levels and stress resistance. Aging Cell 4: 119-125.
60. Sengupta S, Peterson TR, Sabatini DM (2010) Regulation of the mTOR complex 1 pathway by nutrients, growth factors, and stress. Mol Cell 40: 310-322.
61. Cybulski N, Hall MN (2009) TOR complex 2: a signaling pathway of its own. Trends Biochem Sci 34: 620-627.
62. Sancak Y, Peterson TR, Shaul YD, Lindquist RA, Thoreen CC, et al. (2008) The Rag GTPases bind raptor and mediate amino acid signaling to mTORC1. Science 320: 1496-1501.
63. Gao M, Kaiser CA (2006) A conserved GTPase-containing complex is required for intracellular sorting of the general amino-acid permease in yeast. Nat Cell Biol 8: 657-667.
64. Courchesne WE, Magasanik B (1983) Ammonia regulation of amino acid permeases in Saccharomyces cerevisiae. Mol Cell Biol 3: 672-683.
65. Magasanik B, Kaiser CA (2002) Nitrogen regulation in Saccharomyces cerevisiae. Gene 290: 1-18.
66. Rubio-Texeira M, Kaiser CA (2006) Amino acids regulate retrieval of the yeast general amino acid permease from the vacuolar targeting pathway. Mol Biol Cell 17: 3031-3050.
67. Yvert G, Brem RB, Whittle J, Akey JM, Foss E, et al. (2003) Trans-acting regulatory variation in Saccharomyces cerevisiae and the role of transcription factors. Nat Genet 35: 57-64.
68. Deutschbauer AM, Davis RW (2005) Quantitative trait loci mapped to single-nucleotide resolution in yeast. Nat Genet 37: 1333-1340.
69. Yang B, Kumar S (2010) Nedd4 and Nedd4-2: closely related ubiquitin-protein ligases with distinct physiological functions. Cell Death Differ 17: 68-77.
70. Cao XR, Lill NL, Boase N, Shi PP, Croucher DR, et al. (2008) Nedd4 controls animal growth by regulating IGF-1 signaling. Sci Signal 1: ra5.
71. Kapahi P, Zid BM, Harper T, Koslover D, Sapin V, et al. (2004) Regulation of lifespan in Drosophila by modulation of genes in the TOR signaling pathway. Curr Biol 14: 885-890.
72. Jia K, Chen D, Riddle DL (2004) The TOR pathway interacts with the insulin signaling pathway to regulate C. elegans larval development, metabolism and life span. Development 131: 3897-3906.
73. Bonawitz ND, Chatenay-Lapointe M, Pan Y, Shadel GS (2007) Reduced TOR signaling extends chronological life span via increased respiration and upregulation of mitochondrial gene expression. Cell Metab 5: 265-277.

74. Matecic M, Smith DL, Pan X, Maqani N, Bekiranov S, et al. (2010) A microarray-based genetic screen for yeast chronological aging factors. PLoS Genet 6: e1000921.
75. Pedruzzi I, Dubouloz F, Cameroni E, Wanke V, Roosen J, et al. (2003) TOR and PKA signaling pathways converge on the protein kinase Rim15 to control entry into G0. Mol Cell 12: 1607-1613.
76. Pedruzzi I, Burckert N, Egger P, De Virgilio C (2000) Saccharomyces cerevisiae Ras/cAMP pathway controls post-diauxic shift element-dependent transcription through the zinc finger protein Gis1. EMBO J 19: 2569-2579.
77. Martinez-Pastor MT, Marchler G, Schuller C, Marchler-Bauer A, Ruis H, et al. (1996) The Saccharomyces cerevisiae zinc finger proteins Msn2p and Msn4p are required for transcriptional induction through the stress response element (STRE). EMBO J 15: 2227-2235.
78. Schmitt AP, McEntee K (1996) Msn2p, a zinc finger DNA-binding protein, is the transcriptional activator of the multistress response in Saccharomyces cerevisiae. Proc Natl Acad Sci U S A 93: 5777-5782.
79. Shen C, Lancaster CS, Shi B, Guo H, Thimmaiah P, et al. (2007) TOR signaling is a determinant of cell survival in response to DNA damage. Mol Cell Biol 27: 7007-7017.
80. Rothstein R (1991) Targeting, disruption, replacement, and allele rescue: integrative DNA transformation in yeast. Methods Enzymol 194: 281-301.
81. Schmitt ME, Brown TA, Trumpower BL (1990) A rapid and simple method for preparation of RNA from Saccharomyces cerevisiae. Nucleic Acids Res 18: 3091-3092.
82. Thaminy S, Newcomb B, Kim J, Gatbonton T, Foss E, et al. (2007) Hst3 is regulated by Mec1-dependent proteolysis and controls the S phase checkpoint and sister chromatid cohesion by deacetylating histone H3 at lysine 56. J Biol Chem 282: 37805-37814.
83. Kushnirov VV (2000) Rapid and reliable protein extraction from yeast. Yeast 16: 857-860.
84. Biggins S, Severin FF, Bhalla N, Sassoon I, Hyman AA, et al. (1999) The conserved protein kinase Ipl1 regulates microtubule binding to kinetochores in budding yeast. Genes Dev 13: 532-544.
85. Warner JR (1999) The economics of ribosome biosynthesis in yeast. Trends Biochem Sci 24: 437-440.
86. French SL, Osheim YN, Cioci F, Nomura M, Beyer AL (2003) In exponentially growing Saccharomyces cerevisiae cells, rRNA synthesis is determined by the summed RNA polymerase I loading rate rather than by the number of active genes. Mol Cell Biol 23: 1558-1568.
87. Kobayashi T, Ganley AR (2005) Recombination regulation by transcription-induced cohesin dissociation in rDNA repeats. Science 309: 1581-1584.
88. Gottlieb S, Esposito RE (1989) A new role for a yeast transcriptional silencer gene, SIR2, in regulation of recombination in ribosomal DNA. Cell 56: 771-776.
89. Kaeberlein M, McVey M, Guarente L (1999) The SIR2/3/4 complex and SIR2 alone promote longevity in Saccharomyces cerevisiae by two different mechanisms. Genes & Development 13: 2570-2580.
90. Delaney JR, Sutphin GL, Dulken B, Sim S, Kim JR, et al. (2011) Sir2 deletion prevents lifespan extension in 32 long-lived mutants. Aging Cell 10: 1089-1091.

91. Tucker MJ (1979) The effect of long-term food restriction on tumours in rodents. Int J Cancer 23: 803-807.
92. Segall P (1977) Long-term tryptophan restriction and aging in the rat. Aktuelle Gerontol 7: 535-538.
93. Lakowski B, Hekimi S (1998) The genetics of caloric restriction in Caenorhabditis elegans. Proc Natl Acad Sci U S A 95: 13091-13096.
94. Kaeberlein M, Kirkland KT, Fields S, Kennedy BK (2004) Sir2-independent life span extension by calorie restriction in yeast. PLoS Biol 2: E296.
95. Petes TD, Botstein D (1977) Simple Mendelian inheritance of the reiterated ribosomal DNA of yeast. Proc Natl Acad Sci U S A 74: 5091-5095.
96. Kennedy BK, Gotta M, Sinclair DA, Mills K, McNabb DS, et al. (1997) Redistribution of silencing proteins from telomeres to the nucleolus is associated with extension of life span in S. cerevisiae. Cell 89: 381-391.
97. Sinclair DA, Guarente L (1997) Extrachromosomal rDNA circles--a cause of aging in yeast. Cell 91: 1033-1042.
98. Ide S, Miyazaki T, Maki H, Kobayashi T (2010) Abundance of ribosomal RNA gene copies maintains genome integrity. Science 327: 693-696.
99. Falcon AA, Aris JP (2003) Plasmid accumulation reduces life span in Saccharomyces cerevisiae. J Biol Chem 278: 41607-41617.
100. Miller CA, Kowalski D (1993) cis-acting components in the replication origin from ribosomal DNA of Saccharomyces cerevisiae. Mol Cell Biol 13: 5360-5369.
101. Kobayashi T, Horiuchi T, Tongaonkar P, Vu L, Nomura M (2004) SIR2 regulates recombination between different rDNA repeats, but not recombination within individual rRNA genes in yeast. Cell 117: 441-453.
102. Brewer BJ, Fangman WL (1988) A replication fork barrier at the 3' end of yeast ribosomal RNA genes. Cell 55: 637-643.
103. Louis E Saccharomyces Genome Resequencing.
104. Liti G, Carter DM, Moses AM, Warringer J, Parts L, et al. (2009) Population genomics of domestic and wild yeasts. Nature 458: 337-341.
105. Bouton AH, Smith MM (1986) Fine-structure analysis of the DNA sequence requirements for autonomous replication of Saccharomyces cerevisiae plasmids. Mol Cell Biol 6: 2354-2363.
106. Eaton ML, Galani K, Kang S, Bell SP, MacAlpine DM (2010) Conserved nucleosome positioning defines replication origins. Genes Dev 24: 748-753.
107. Friedman KL, Brewer BJ, Fangman WL (1997) Replication profile of Saccharomyces cerevisiae chromosome VI. Genes Cells 2: 667-678.
108. Shirahige K, Iwasaki T, Rashid MB, Ogasawara N, Yoshikawa H (1993) Location and characterization of autonomously replicating sequences from chromosome VI of Saccharomyces cerevisiae. Mol Cell Biol 13: 5043-5056.
109. Ide S, Watanabe K, Watanabe H, Shirahige K, Kobayashi T, et al. (2007) Abnormality in initiation program of DNA replication is monitored by the highly repetitive rRNA gene array on chromosome XII in budding yeast. Mol Cell Biol 27: 568-578.
110. Ehrenhofer-Murray AE, Rivier DH, Rine J (1997) The role of Sas2, an acetyltransferase homologue of Saccharomyces cerevisiae, in silencing and ORC function. Genetics 145: 923-934.

111. McCarroll RM, Fangman WL (1988) Time of replication of yeast centromeres and telomeres. Cell 54: 505-513.
112. Dammann R, Lucchini R, Koller T, Sogo JM (1993) Chromatin structures and transcription of rDNA in yeast Saccharomyces cerevisiae. Nucleic Acids Res 21: 2331-2338.
113. Steffen KK, MacKay VL, Kerr EO, Tsuchiya M, Hu D, et al. (2008) Yeast life span extension by depletion of 60s ribosomal subunits is mediated by Gcn4. Cell 133: 292-302.
114. Defossez PA, Prusty R, Kaeberlein M, Lin SJ, Ferrigno P, et al. (1999) Elimination of replication block protein Fob1 extends the life span of yeast mother cells. Mol Cell 3: 447-455.
115. Kobayashi T (2003) The replication fork barrier site forms a unique structure with Fob1p and inhibits the replication fork. Mol Cell Biol 23: 9178-9188.
116. Ward TR, Hoang ML, Prusty R, Lau CK, Keil RL, et al. (2000) Ribosomal DNA replication fork barrier and HOT1 recombination hot spot: shared sequences but independent activities. Mol Cell Biol 20: 4948-4957.
117. Lindstrom DL, Leverich CK, Henderson KA, Gottschling DE Replicative age induces mitotic recombination in the ribosomal RNA gene cluster of Saccharomyces cerevisiae. PLoS Genet 7: e1002015.
118. Saffer LD, Miller OL, Jr. (1986) Electron microscopic study of Saccharomyces cerevisiae rDNA chromatin replication. Mol Cell Biol 6: 1148-1157.
119. Rhind N (2006) DNA replication timing: random thoughts about origin firing. Nat Cell Biol 8: 1313-1316.
120. Patel PK, Arcangioli B, Baker SP, Bensimon A, Rhind N (2006) DNA replication origins fire stochastically in fission yeast. Mol Biol Cell 17: 308-316.
121. Bielinsky AK (2003) Replication origins: why do we need so many? Cell Cycle 2: 307-309.
122. Kobayashi T, Horiuchi T (1996) A yeast gene product, Fob1 protein, required for both replication fork blocking and recombinational hotspot activities. Genes Cells 1: 465-474.
123. Pasero P, Bensimon A, Schwob E (2002) Single-molecule analysis reveals clustering and epigenetic regulation of replication origins at the yeast rDNA locus. Genes Dev 16: 2479-2484.
124. Zhang L, Ma H, Pugh BF (2011) Stable and dynamic nucleosome states during a meiotic developmental process. Genome Res 21: 875-884.
125. Muller M, Lucchini R, Sogo JM (2000) Replication of yeast rDNA initiates downstream of transcriptionally active genes. Mol Cell 5: 767-777.
126. Buys CH, Osinga J, Anders GJ (1979) Age-dependent variability of ribosomal RNA-gene activity in man as determined from frequencies of silver staining nucleolus organizing regions on metaphase chromosomes of lymphocytes and fibroblasts. Mech Ageing Dev 11: 55-75.
127. Thomas S, Mukherjee AB (1996) A longitudinal study of human age-related ribosomal RNA gene activity as detected by silver-stained NORs. Mech Ageing Dev 92: 101-109.
128. Takeuchi Y, Horiuchi T, Kobayashi T (2003) Transcription-dependent recombination and the role of fork collision in yeast rDNA. Genes Dev 17: 1497-1506.

129. Michel AH, Kornmann B, Dubrana K, Shore D (2005) Spontaneous rDNA copy number variation modulates Sir2 levels and epigenetic gene silencing. Genes Dev 19: 1199-1210.
130. Ganley AR, Ide S, Saka K, Kobayashi T (2009) The effect of replication initiation on gene amplification in the rDNA and its relationship to aging. Mol Cell 35: 683-693.
131. Brewer BJ, Fangman WL (1994) Initiation preference at a yeast origin of replication. Proc Natl Acad Sci U S A 91: 3418-3422.
132. McMurray MA, Gottschling DE (2003) An age-induced switch to a hyper-recombinational state. Science 301: 1908-1911.
133. Hoopes LL, Budd M, Choe W, Weitao T, Campbell JL (2002) Mutations in DNA replication genes reduce yeast life span. Mol Cell Biol 22: 4136-4146.
134. Cubillos FA, Louis EJ, Liti G (2009) Generation of a large set of genetically tractable haploid and diploid Saccharomyces strains. FEMS Yeast Res 9: 1217-1225.
135. Kobayashi T, Heck DJ, Nomura M, Horiuchi T (1998) Expansion and contraction of ribosomal DNA repeats in Saccharomyces cerevisiae: requirement of replication fork blocking (Fob1) protein and the role of RNA polymerase I. Genes Dev 12: 3821-3830.
136. Huberman JA, Spotila LD, Nawotka KA, el-Assouli SM, Davis LR (1987) The in vivo replication origin of the yeast 2 microns plasmid. Cell 51: 473-481.
137. Brewer BJ, Lockshon D, Fangman WL (1992) The arrest of replication forks in the rDNA of yeast occurs independently of transcription. Cell 71: 267-276.
138. Brewer BJ, Fangman WL (1987) The localization of replication origins on ARS plasmids in S. cerevisiae. Cell 51: 463-471.
139. Saccharomyces Genome Database. http://www.yeastgenome.org/.
140. Saccharoymyces cerevisiae RM11-1a Database. http://www.broadinstitute.org/annotation/genome/saccharomyces_cerevisiae/.
141. Di Rienzi SC, Lindstrom KC, Lancaster R, Rolczynski L, Raghuraman MK, et al. (2011) Genetic, genomic, and molecular tools for studying the protoploid yeast, L. waltii. Yeast.
142. Raghuraman MK, Winzeler EA, Collingwood D, Hunt S, Wodicka L, et al. (2001) Replication dynamics of the yeast genome. Science 294: 115-121.

CURRICULUM VITAE

Elizabeth Kwan

Education:

Ph.D. in Molecular Cell Biology, University of Washington, Seattle, WA. (February 2012).

Magna cum laude, B.A. in Biochemistry and Molecular Biology, Honors, Lewis & Clark College, Portland, OR (May 2005)

Publications:

Kwan EX, Foss E, Kruglyak L, Bedalov A. 2011. Natural polymorphism in BUL2 links cellular amino acid availability with chronological aging and telomere maintenance in yeast. PLoS Genet *7*, e1002250.

Rabbitts BM, Ciotti MK, Miller NE, Kramer M, Lawrenson AL, Levitte S, Kremer S, Kwan E, Weis AM, Hermann GJ. 2008. glo-3, a novel Caenorhabditis elegans gene, is required for lysosome-related organelle biogenesis. Genetics *180*, pp. 857-871.

Shroeder LK, Kremer S, Kramer MJ, Currie E, Kwan E, Watts JL, Lawrenson AL, Hermann GJ. 2007. Function of the Caenorhabditis elegans ABC transporter PGP-2 in the biogenesis of a lysosome-related fat storage organelle. Mol Biol Cell *18*, pp. 995-1008.

Research Experience:

Graduate Student, University of Washington Molecular Cell Biology Graduate Program, Fred Hutchinson Cancer Research Center, Seattle, WA.

(With Antonio Bedalov, M.D., Clinical Research), January 2006 to March 2006, Summer 2006 to 2012. Characterization of small molecular inhibitors of NAD-dependent histone deacetylases in *S. cerevisiae,* characterization of histone mutants, and genetic analysis of aging in diverse populations.

(With Cecilia Moens, Ph.D., Basic Sciences Division), April 2006 to June 2006. Zebrafish hindbrain development.

(With Steven Collins, M.D., Human Biology), September 2005 to December 2005. Retinoic acid-induced cell differentiation in myeloid leukemia cell lines

Research Student, John S. Rogers Science Research Program, Lewis & Clark College, Portland, OR.

(With Greg Hermann, Ph.D, Assistant Professor, Dept. of Biology), Summer 2002 to July 2005. *C. elegans* lysosome biogenesis, intestinal organogenesis pathways, the control of protein expression.
Research posters presented at the 2003 International *C. elegans* Conference and the 2004 West Coast *C. elegans* conference.

Student Researcher, Beckman Research Institute, City of Hope National Medical Center, Duarte, CA.

(With David Bleich, M.D., Dept. of Diabetes and Endocrinology), Summer 1999, Summer and Fall 2000, Summer 2001. Apoptosis pathways mechanisms in pancreatic tumor cell cultures.

Honors:

Barry M. Goldwater Scholar (2004)
Phi Beta Kappa (2005)